JAERI - M
83-115

EVALUATION REPORT ON CCTF CORE-I REFLOOD TESTS CI-18 (RUN 37) AND CI-8 (RUN 17)

—INVESTIGATION OF THE EFFECT OF WATER REMAINING IN THE LOOP SEAL SECTION ON REFLOOD BEHAVIOR—

July 1983

Takashi SUDOH* and Yoshio MURAO

日本原子力研究所
Japan Atomic Energy Research Institute

JAERI-M レポートは，日本原子力研究所が不定期に公刊している研究報告書です。

入手の問合わせは，日本原子力研究所技術情報部情報資料課（〒319—11 茨城県那珂郡東海村）あて，お申しこしください。なお，このほかに財団法人原子力弘済会資料センター（〒319—11 茨城県那珂郡東海村日本原子力研究所内）で複写による実費頒布をおこなっております。

JAERI-M reports are issued irregularly.

Inquiries about availabiljty of the reports should be addressed to Information Section, Division of Technical Information, Japan Atomic Energy Research Institute, Tokai-mura, Naka-gun, Ibaraki-ken 319-11, Japan.

編集兼発行　日本原子力研究所

印　　刷　㈱原子力資料サービス

JAERI-M 83-115

EVALUATION REPORT ON CCTF CORE-I REFLOOD TESTS C1-18 (RUN 37) AND C1-8 (RUN 17)

—— Investigation of the effect of water remaining in the loop seal section on reflood behavior ——

Takashi SUDOH* and Yoshio MURAO

Department of Nuclear Safety Research,
Tokai Research Establishment, JAERI

(Received July 1, 1983)

The loop seal experiments, C1-18 and C1-8, were conducted in the Cylindrical Core Test Facility (CCTF). For these experiments, the saturated water was filled in four loop seal sections to the elevation of 1.5 m from the bottom of them prior to the experiment initiation in order to simulate the remaining water in the loop at the initiation of a reflood phase during a loss-of-coolant accident (LOCA) in a pressurized water reactor (PWR).

The results of the loop seal experiment, C1-18, was mainly discussed in this report because, in the other loop seal experiment, C1-8, the core power was prematurely turned off during the transient of it.

The significant steam penetration through the broken loop seal section initiated at 32 seconds after flood, and most of the filled water was blown away until 65 seconds. Before that time, the core water accumulation was suppressed due to the water seal in the loop seal section. The turnaround temperature was higher than that for the C1-5 which was conducted under no filled water in the loop seal section. The driving force of the steam penetration is the difference of the differential pressures in the downcomer and the core. The driving force was equal to the pump-side water head at the initiation of the

---

The work was performed under the contract with the Atomic Energy Bureau of Science and Technology Agency of Japan.

* Nuclear Data Center

steam penetration. The ECC injection rate affected the water accumulation in the downcomer and controlled the timing of the initiation of the steam penetration.

Keywords: PWR-LOCA, ECCS, Reflood, Blocked-loop-seal, Turnaround, Core-heat-transfer, Reacter Safety

大型再冠水円筒第1次炉心試験 C1－18（RUN37），C1－8（RUN17）評価報告書 ― ループシール部留水の再冠水挙動への影響 ―

日本原子力研究所東海研究所安全工学部
須藤高史＊・村尾良夫

（１９８３年７月１日受理）

円筒炉心試験装置においてループシール部留水試験Ｃ１－18，Ｃ１－８が行なわれた。加圧水型原子炉の冷却材喪失事故時再冠水期の開始時に，１次系ループ部に水が留まり，ループを閉塞していることを想定し，この試験では，４ループのループシール部に底面より1.5 mの高さまで飽和水をあらかじめ貯え，試験を開始した。Ｃ１－８試験では，模擬炉心温度が設定温度を越えたために炉心供給電源を停止し，試験を中断したため，主に，Ｃ１－18 試験結果の検討を行なった。

炉心で発生した蒸気は，再冠水開始後32秒で留水で閉塞されたループシール部を貫流しはじめ，６５秒までに，留水を押し出してしまった。ループシールに留水が残っている間は炉心蓄水が抑えられ，ループシール部留水がなかったＣ１－５試験と比べターンアラウンド温度は高くなった。蒸気貫流のための駆動力はダウンカマ水頭と炉心水頭の差により得られ，蒸気貫流開始時のその水頭差は，ループシール部ポンプ側の水頭に等しかった。ダウンカマ水頭は冷却材注入流量に影響されるため，注入流量が蒸気貫流開始時期に大きな影響を及ぼしている。

本報告書は，電源開発促進対策特別会計法に基づき，科学技術庁からの受託によって行なった研究の成果である。

＊　原子力データセンター

CONTENTS

目　　次

Table and Figures List

1. Introductions

The Large Scale Reflood Test (LSRT) program has been conducted since 1977 to study the Emergency-Core-Cooling System (ECCS) behaviors during refill and reflood phases in a Loss-of-Coolant Accident (LOCA) of a Pressurized Water Reactor (PWR).

The series of tests have been performed in two experimental facilities. One is the Cylindrical Core Test Facility (CCTF) and the other is the Slab Core Test Facility (SCTF).

The objective of the CCTF program are:

a. Demonstration of ECCS behavior during refill and reflood period.

b. Verification of reflood analysis codes.

c. Collection of information to improve the thermo-hydrodynamics models in analysis codes, such as, (a) multi-dimensional core thermo-hydrodynamics including the radial power distribution effect, fallback effect and spatial oscillatory behavior, (b) flow behavior in the upper plenum and hot legs, (c) behavior of accumulated water at the bottom of the upper plenum including possible counter-current flow and sputtering effects, (d) hydrodynamic behavior of the injected ECC water and the water passing through the steam generator, (e) multidimensional thermo-hydrodynamics behavior in the hot annular downcomer, and (f) overall oscillatory behavior in the system.

The special objective of this work is to study the effect of the water remaining in the loop seal section on a reflood behavior. At the end of a refill phase in a PWR LOCA, there is a possibility that some amount of the injected Emergency Core Cooling (ECC) water is accumulated in the loop seal section and blocks the primary loop piping.

The reflood experiments C1-18 (RUN 37) and C1-8 (RUN 17) were performed in the CCTF with the filled water in the loop seal section pipings.

In the test, C1-8, the objective could not be achieved, because the heater rod surface temperature exceeded the maximum allowable temperature and the core power supply was turned off at first 134 s.

C1-18 was performed with nominally the same experimental condition as those for C1-8. The experiment C1-5[1)] has been completed under no filled water in the loop seal section.

This report presents the investigation of the effect of the loop

seal section blockage on the reflood behavior. The experimental facility and conditions are summarized in Chapter 2. Chapter 3 presents the results and discussions of C1-18 and C1-8, together with C1-5. The conclusions are described in Chapter 4.

For better understanding of the experimental results, selected data of C1-18 and C1-8 are given in Appendix B and C, respectively.

2. Experimental Conditions

2.1 Facility design

The facility design is detailed in the reference 2. It consists of a pressure vessel and four primary loops, as shown in Fig.2.1.

To simulate the system effect during refill and reflood phase of a PWR LOCA, the following items were considered as the design criteria:

(1) The elevations of the components are maintained to be as close to those of a PWR as possible.
(2) The lengthes of the flow pathes in the components are also preserved.
(3) The flow areas of the components are scaled down in proportion to the scaling factor of core flow area.
(4) The facility has three intact loops and one broken loop which simulates double-ended cold leg break.

The reference reactor is the Torjan reactor in the USA, and the Ohi reactor in Japan is also referred partly.

The pressure vessel contains a core, upper and lower plenum, and a downcomer. The core has thirty-two 8×8 bundles which simulate 15×15 fuel assembly of which unheated rods are included. The core configuration is shown in Fig.2.2.

The core is full height and has 1824 electrically heated rod, as shown in Fig.2.3. An axial power distribution is chopped cosign. There are high, medium and low power heaters in a bundle.

The downcomer is annulus as shown in Fig.2.2. The core baffle region area in a PWR is scaled and included in the simulated downcomer flow area to reduce a small gap effect in a downcomer. Then the gap size of the annulus is 61.5 mm.

The internals in the upper plenum consist of control rod guide tubes, support colums, short stubs, orifice plates and open holes, as shown in Fig.2.4 and Fig.2.5. These internals simulate those of a 17×17 type PWR. The radial dimensions of them are scaled down in proportion to the bundle array size.

The primary loop arrangement is shown in Fig.2.1. The loop consists of a hot leg and a cold leg piping, an active steam generator, and a pump simulator, as shown in Fig.2.6. U-tubes in the steam generator are about 5 m shorter than actuals and those of two loops are housed

in a single shell.

2.2 Experimental procedure

Prior to the experiment initiation, the primary system was heated to the saturation temperature except the downcomer wall which was heated to 471 K, and pressurized to a specified pressure (0.2 MPa) by the saturated steam. The saturated water was filled in the lower plenum to 0.9 m level. For the experiments C1-8 and C1-18, the saturated water was also filled in each loop seal section to 1.5 m level. This loop seal filling was not adapted for the reference experiment, C1-5.

The power was supplied to the core after establishing the initial condition. When the maximum temperature of the heated rod reached 775 K, the accumulator water directly injected into the lower plenum. The rod temperature was expected to reach 873 K at the core flooding initiation. At the expected flooding initiation, the core power was initiated to simulate a decay heat which was obtained by the equation of $1.2 \times$ ANS standard + ^{238}U capture.

The accumulator injection port was switched from the lower plenum to the intact cold leg ECC ports, when the assumed water level in the core reached 0.5 m. The simulated low pressure coolant injection (LPCI) took the place of the accumulator injection at 24 seconds after the initiation of the accumulator injection. The LPCI rate was maintained at the constant value of 8.33×10^{-3} m^3/s.

For C1-18, after confirming the total core quench, the power supply to the core and LPCI were turned off, and the experiment was turminated. For C1-8, since the maximum rod surface temperature exceeded the allowable rod temperature, 1173 K, the power supply to the core was turned off at 134 seconds after the experiment initiation.

2.3 Experimental conditions

The experimental conditions of the loop seal experiments, C1-18 and C1-8, and the reference test, C1-5, are given in Table 2.1, 2.2 and 2.3, respectively. For the loop seal experiments, the saturated water was filled in the four loop seal sections to 1.5 m elevation from the bottom of the loop seal section. The other conditions were nominally

the same as those of the reference test.

The chronology of the events for the three experiments are listed in Table 2.4, 2.5 and 2.6, respectively. The time was defined as the passed time from the initiation of the data recording. At the same time, the power supply to the core was also initiated.

For C1-8, the power to the core central region was reduced by 20%, since the maximum temperature exceeded 1133 K at 129.5 seconds, and all the core power was turned off at 134 seconds when the maximum core temperature reached the designed allowable temperature, 1173 K.

Table 2.1 Experiment condition for C1-18

1. TEST TYPE : LOOP SEAL WATER FILLING TEST
2. TEST NUMBER : RUN 037 3. DATE : March 10, 1981
4. POWER : A: TOTAL: 9.40 MW; B:LINEAR: 1.41 KW/M
5. RELATIVE RADIAL POWER SHAPE :

   A: ZONE: A B C

   B: RATIO: 1.153 : 1.079 : 0.885
6. AXIAL POWER SHAPE : CHOPPED COSINE
7. PRESSURE (KG/CM^2A) :

   A: SYSTEM: 1.96, B: CONTAINMENT 1.95,

   C: STEAM GENERATOR SECONDARY: 53.6
8. TEMPERATURE (DEG.C) :

   A: DOWNCOMER WALL 166, B: VESSEL INTERNALS 108,

   C: PRIMARY PIPING WALL 120, D: LOWER PELNUM LIQUID 114,

   E: ECC LIQUID 38.8, F: STEAM GENERATOR SECONDARY 263,

   G: CORE TEMPERATURE AT ECC INITIATION 597
9. ECC INJECTION TYPE: C

   A: COLD LEG, B: LOWER PLENUM, C: LOWER PLENUM + COLD LEG
10. PUMP K-FACTOR : $\sim$ 15
11. ECC FLOW RATES AND DURATION :

    A: ACCUMULATOR 285 M^3/HR FROM 0 TO 24 SECONDS

    B: LPCI 30.2 M^3/HR FROM 24 TO 805 SECONDS

    C: ECC INJECTION TO LOWER PLENUM : FROM 0 TO 17.5 SECONDS

    (VALVE OPENING AND CLOSING TIMES ARE INCLUDED IN THE INJECTION DURATION)
12. INITIAL WATER LEVEL IN LOWER PLENUM : 0.88 M.
13. POWER CONTROL : ANS x 1.2 + ACTINIDE (30 SEC AFTER SCRAM)
14. EXPECTED BOCREC TIME FROM ECC INITIATION 12 SEC
15. EXPECTED PEAK TEMPERATURE AT BOCREC 600 C

Table 2.2 Experiment condition for C1-8

1. TEST TYPE : LOOP SEAL WATER FILLING TEST
2. TEST NUMBER : RUN 017 3. DATE : Nov.29, 1979
4. POWER : A: TOTAL: 9.37 MW; B:LINEAR: 1.4 KW/M
5. RELATIVE RADIAL POWER SHAPE :

   A: ZONE: A B C

   B: RATIO: 1.07 : 1.0 : 0.82
6. AXIAL POWER SHAPE : CHOPPED COSINE
7. PRESSURE (KG/CM^2A) :

   A: SYSTEM: 2.08, B: CONTAINMENT 2.09,

   C: STEAM GENERATOR SECONDARY: 51
8. TEMPERATURE (DEG.C) :

   A: DOWNCOMER WALL 183, B: VESSEL INTERNALS 110,

   C: PRIMARY PIPING WALL 120, D: LOWER PELNUM LIQUID 111,

   E: ECC LIQUID 37, F: STEAM GENERATOR SECONDARY 264,

   G: CORE TEMPERATURE AT ECC INITIATION 516
9. ECC INJECTION TYPE: C

   A: COLD LEG, B: LOWER PLENUM, C: LOWER PLENUM + COLD LEG
10. PUMP K-FACTOR : ∿15
11. ECC FLOW RATES AND DURATION :

    A: ACCUMULATOR 279 M^3/HR FROM 0 TO 24 SECONDS

    B: LPCI 30.9 M^3/HR FROM 24 TO 355 SECONDS

    C: ECC INJECTION TO LOWER PLENUM : FROM 0 TO 17.5 SECONDS

    (VALVE OPENING AND CLOSING TIMES ARE INCLUDED IN THE INJECTION DURATION)
12. INITIAL WATER LEVEL IN LOWER PLENUM : 0.87 M.
13. POWER CONTROL : ANS x 1.2 + ACTINIDE (30 SEC AFTER SCRAM)
14. EXPECTED BOCREC TIME FROM ECC INITIATION 12 SEC
15. EXPECTED PEAK TEMPERATURE AT BOCREC 600 C

Table 2.3 Experiment condition for C1-5

1. TEST TYPE : TEST C1-5 (CCTF MAIN TEST NO.5)
2. TEST NUMBER : RUN 014 3. DATE : Oct.19, 1979
4. POWER : A: TOTAL: 9.36 MW; B:LINEAR: 1.40 KW/M
5. RELATIVE RADIAL POWER SHAPE :

   A: ZONE: A B C

   B: RATIO: 1.07 : 1.0 : 0.82
6. AXIAL POWER SHAPE : CHOPPED COSINE
7. PRESSURE (KG/CM^2A) :

   A: SYSTEM: 2.02, B: CONTAINMENT 1.99,

   C: STEAM GENERATOR SECONDARY: 50
8. TEMPERATURE (DEG.C) :

   A: DOWNCOMER WALL 182, B: VESSEL INTERNALS 115,

   C: PRIMARY PIPING WALL 120, D: LOWER PELNUM LIQUID 114,

   E: ECC LIQUID 39, F: STEAM GENERATOR SECONDARY 262,

   G: CORE TEMPERATURE AT ECC INITIATION 502
9. ECC INJECTION TYPE: C

   A: COLD LEG, B: LOWER PLENUM, C: LOWER PLENUM + COLD LEG
10. PUMP K-FACTOR : ∿ 15
11. ECC FLOW RATES AND DURATION :

    A: ACCUMULATOR 278 M^3/HR FROM 0 TO 23.5 SECONDS

    B: LPCI 30.2 M^3/HR FROM 23.5 TO 585.5 SECONDS

    C: ECC INJECTION TO LOWER PLENUM : FROM 0 TO 14.5 SECONDS

    (VALVE OPENING AND CLOSING TIMES ARE INCLUDED IN THE INJECTION DURATION)
12. INITIAL WATER LEVEL IN LOWER PLENUM : 0.87 M.
13. POWER CONTROL : ANS x 1.2 + ACTINIDE (30 SEC AFTER SCRAM)
14. EXPECTED BOCREC TIME FROM ECC INITIATION 12 SEC
15. EXPECTED PEAK TEMPERATURE AT BOCREC 600 C

Table 2.4 Chronology of events for C1-18

EVENT	TIME (sec)
Test Initiated (Heater Rods Power on) (Data Recording Initiated)	0
Accumulator Injection Initiated	55
Power Decay Initiated (Bottom of Core Recovery)	67.5 (67.5)
Accumulator Injection Switched from Lower Plenum to Cold Leg	72.5
Accumulator Injection Ended and LPCI Injection Initiated	79.0
All Heater Rods Quenched	626
Power Off	680
LPCI Injection Ended	860
Test Ended (Data Recording Ended)	1009

Table 2.5 Chronology of events for C1-8

EVENT	TIME (sec)
Test Initiated (Heater Rods Power on) (Data Recording Initiated)	0.0
Accumulator Injection Initiated	53
Power Decay Initiated (Bottom of Core Recovery)	65
Accumulator Injection Switched from Lower Plenum to Cold Leg	70.5
Accumulator Injection Ended and LPCI Injection Initiated	77
Power zone M5 reduced 20%	129.5
Power off	134
All heater rods quenched	287
LPCI injection ended	408
Test C1-8 ended (Data recording ended)	500

Table 2.6 Chronology of events for C1-5

EVENT	TIME (sec)
Test C1-5 initiated (Heater rods power on) (Data recording initiated)	0.0
Accumulator injection initiated	52.5
Power decay initiated (Bottom of core recovery)	63
Accumulator injection switched from lower plenum to cold leg	67
Accumulator injection ended and LPCI injection initiated	76
All heater rods quenched	598
Power off	648
LPCI injection ended	738
Test ended (Data recording ended)	1068

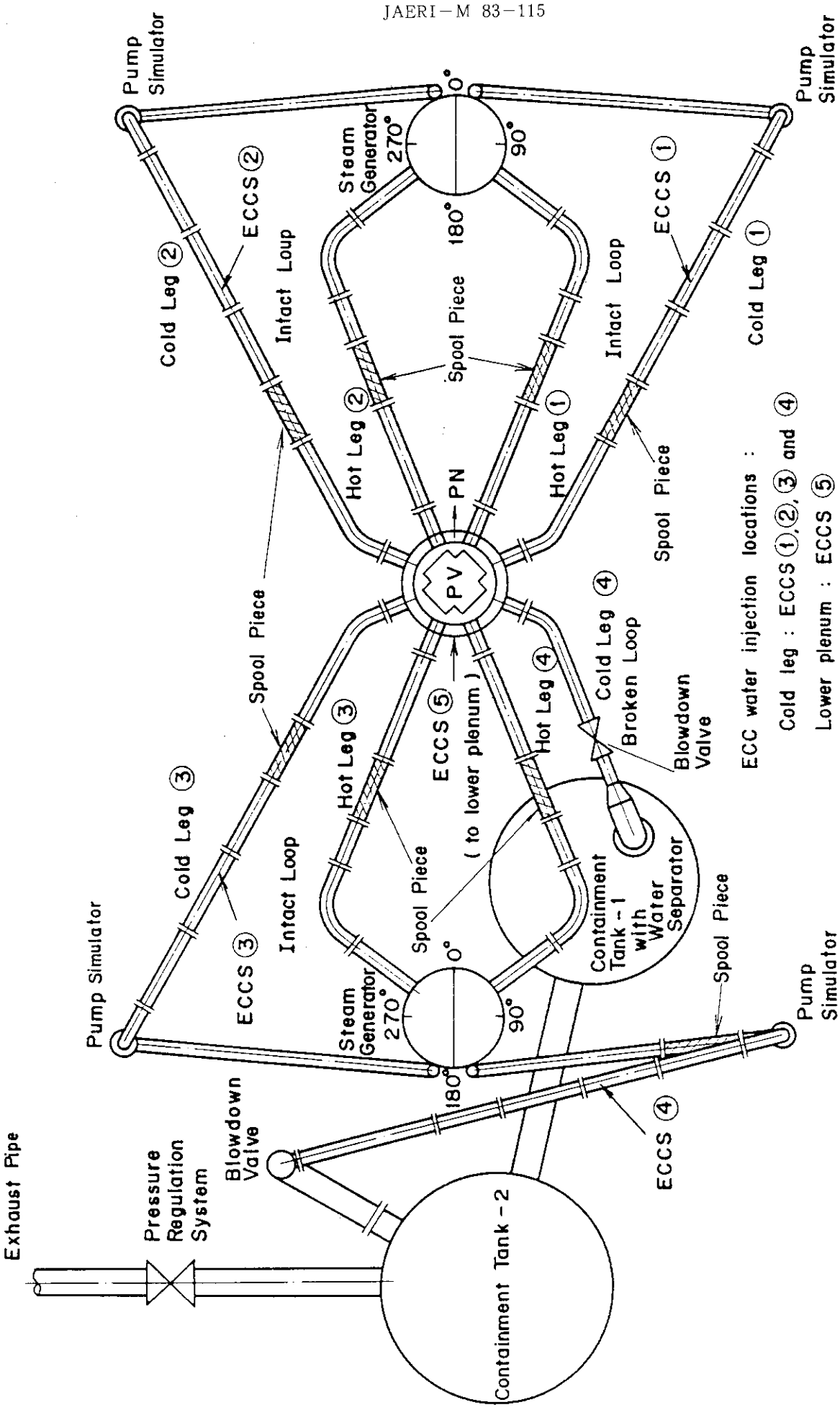

Fig.2.1 Primary loop piping

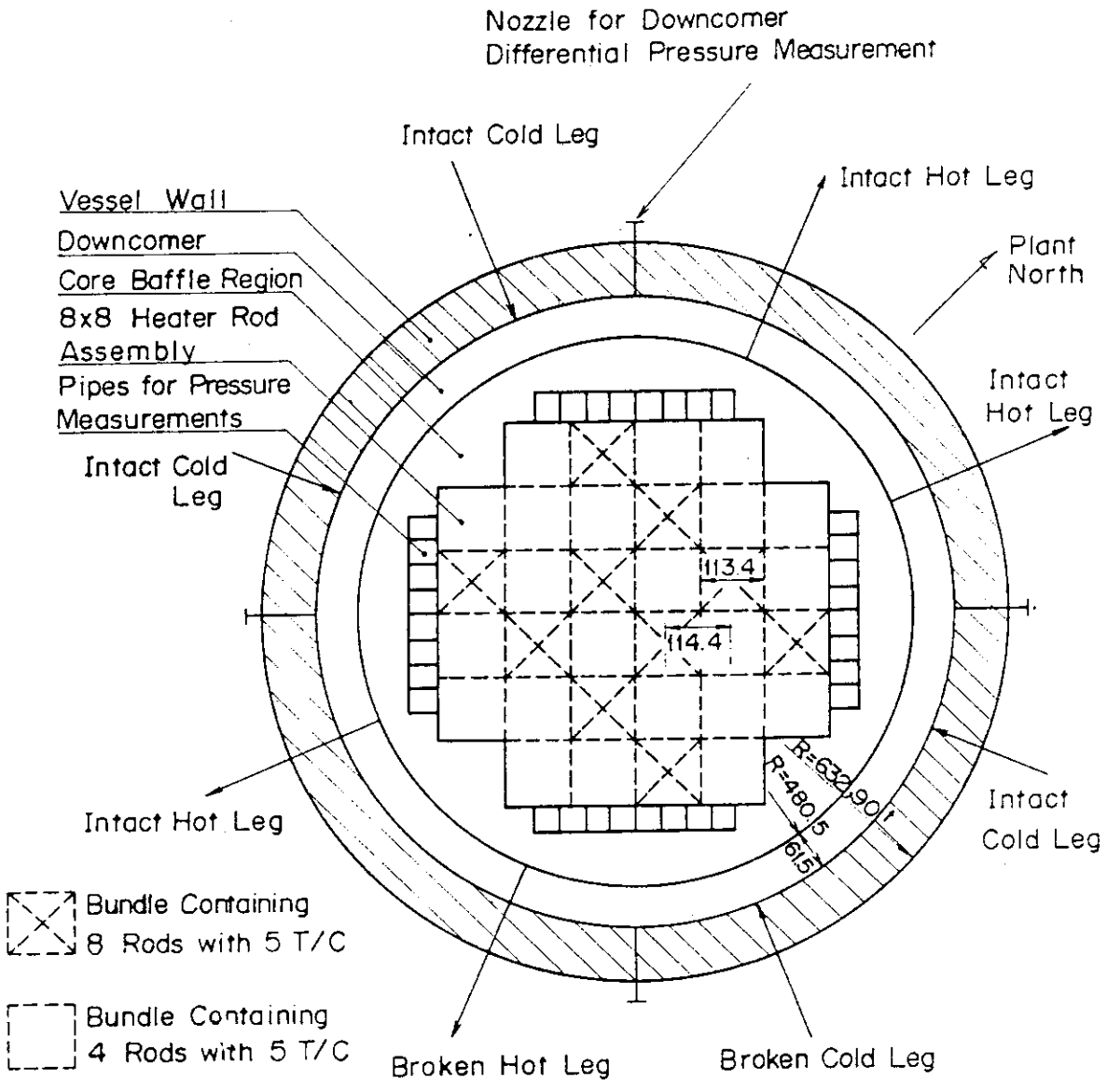

Fig.2.2 Cross section of pressure vessel

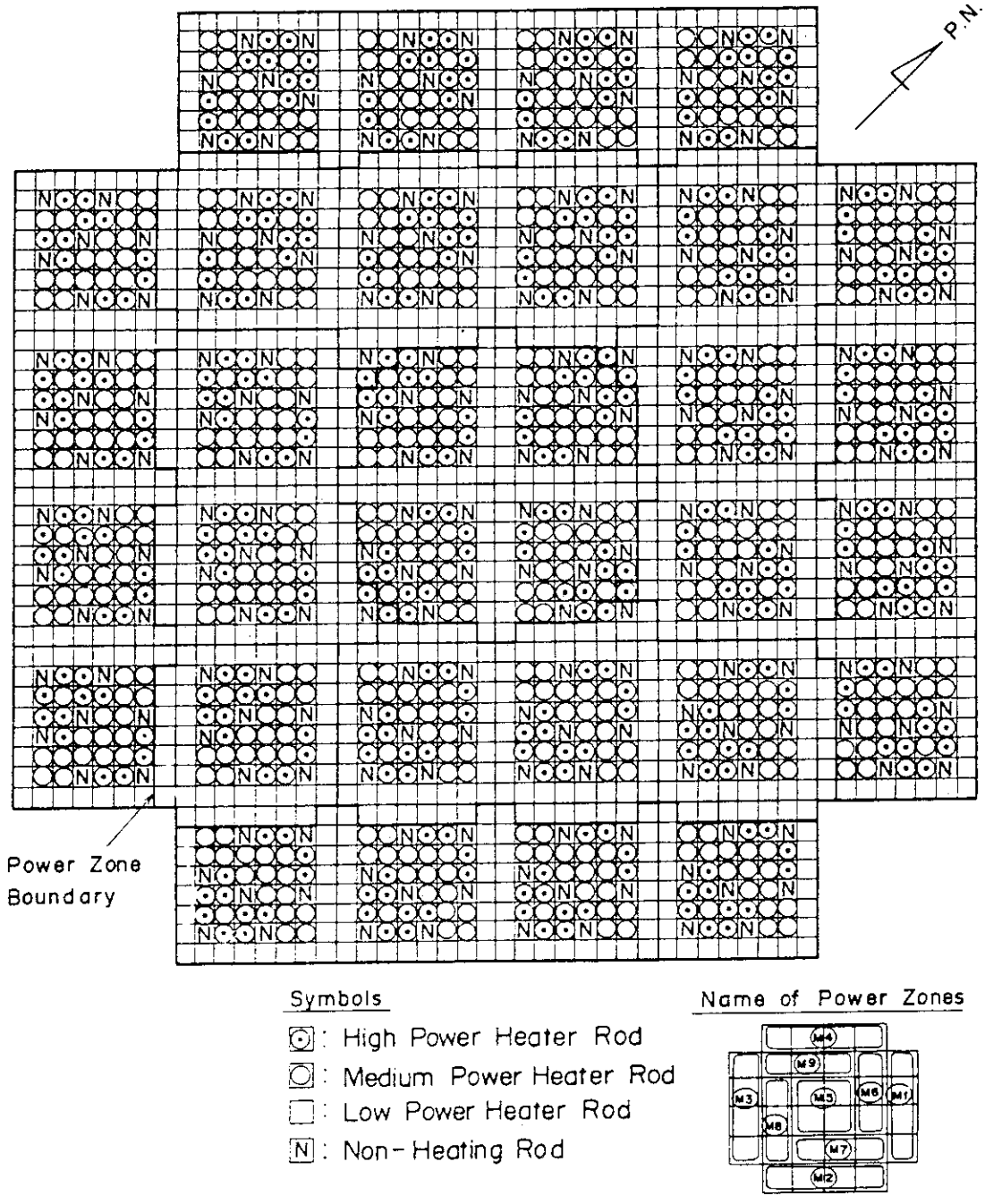

Fig.2.3 Configuration of rods in core

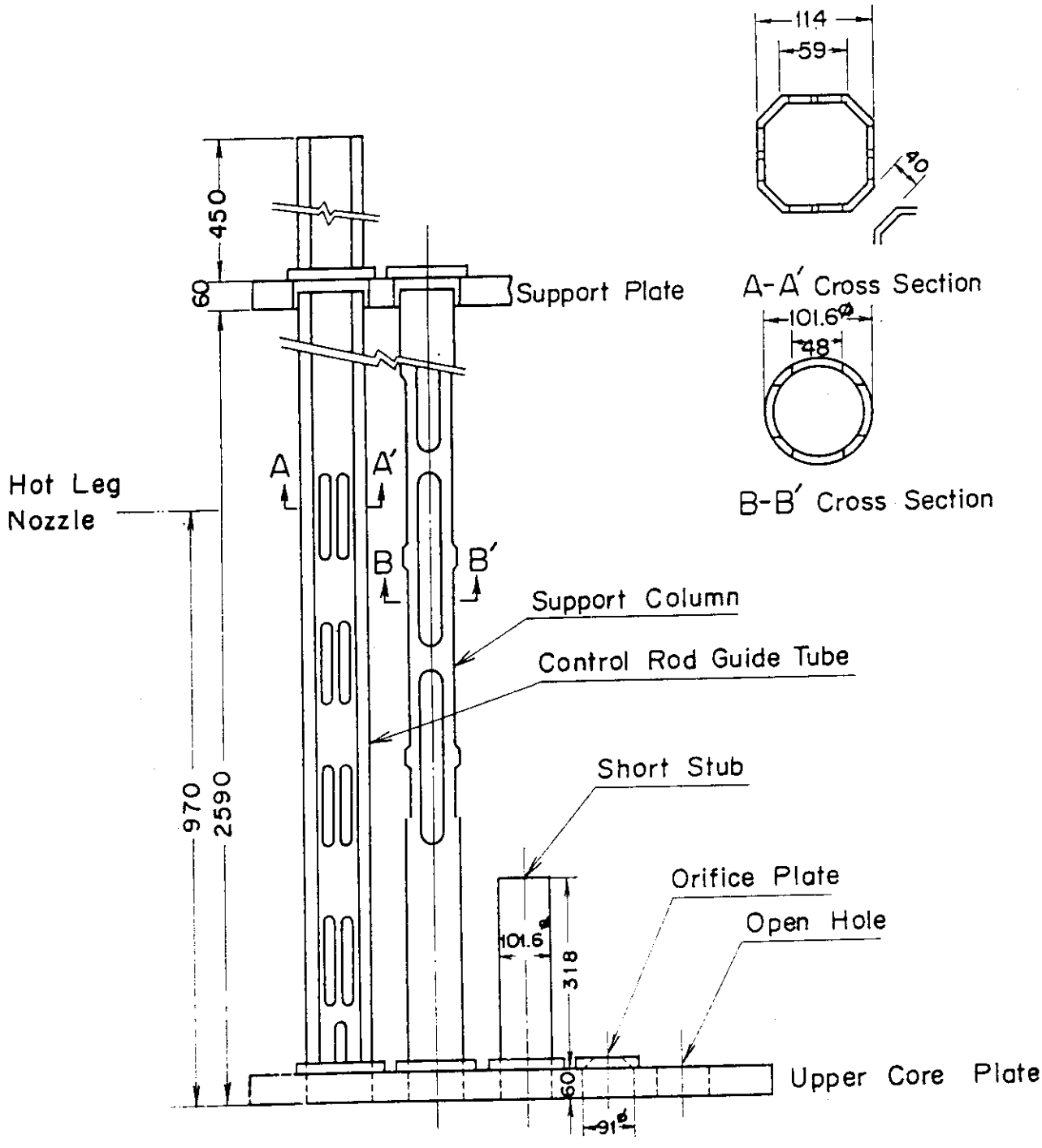

Fig.2.4 Conception of internals

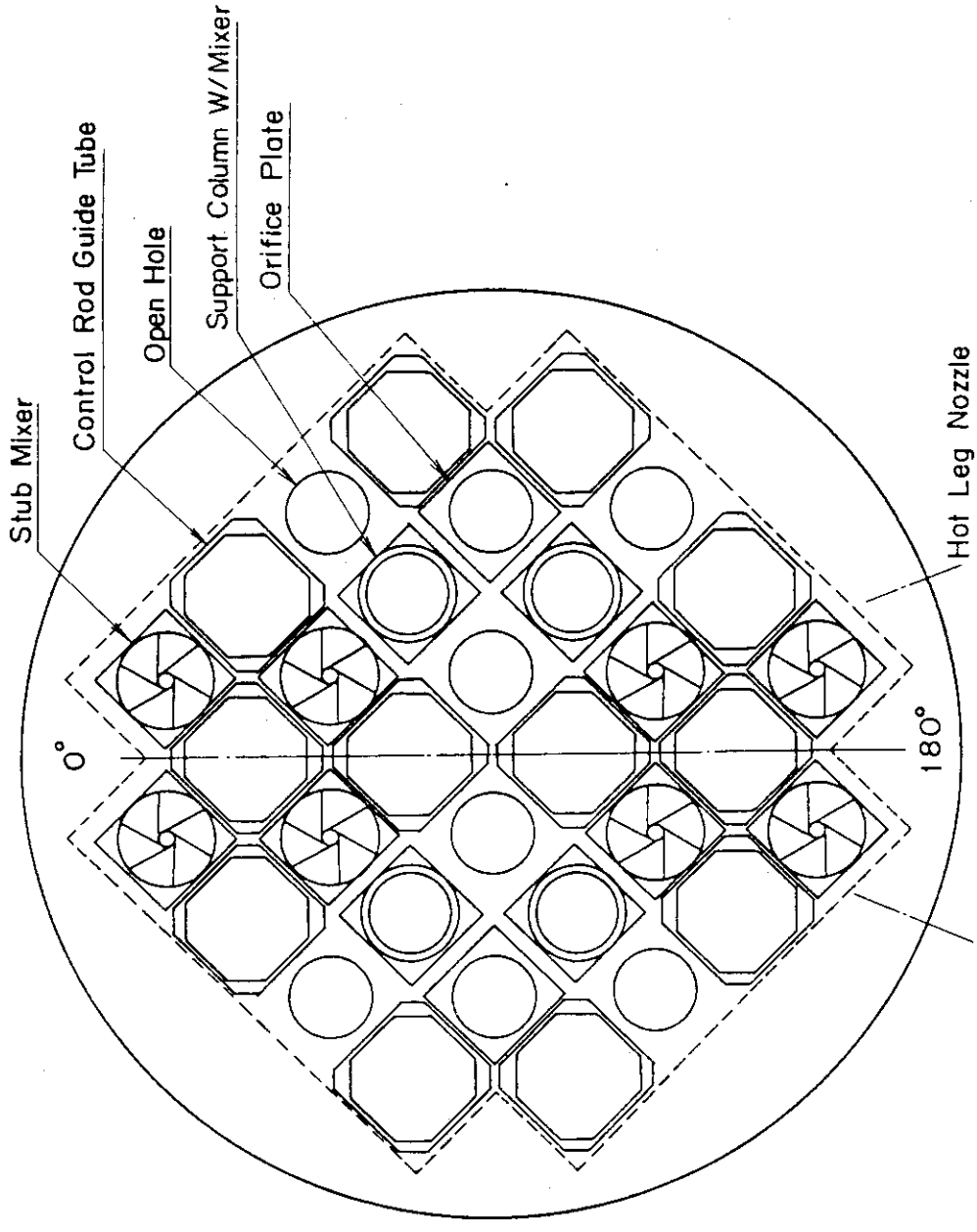

Fig.2.5 Arrangement of internals

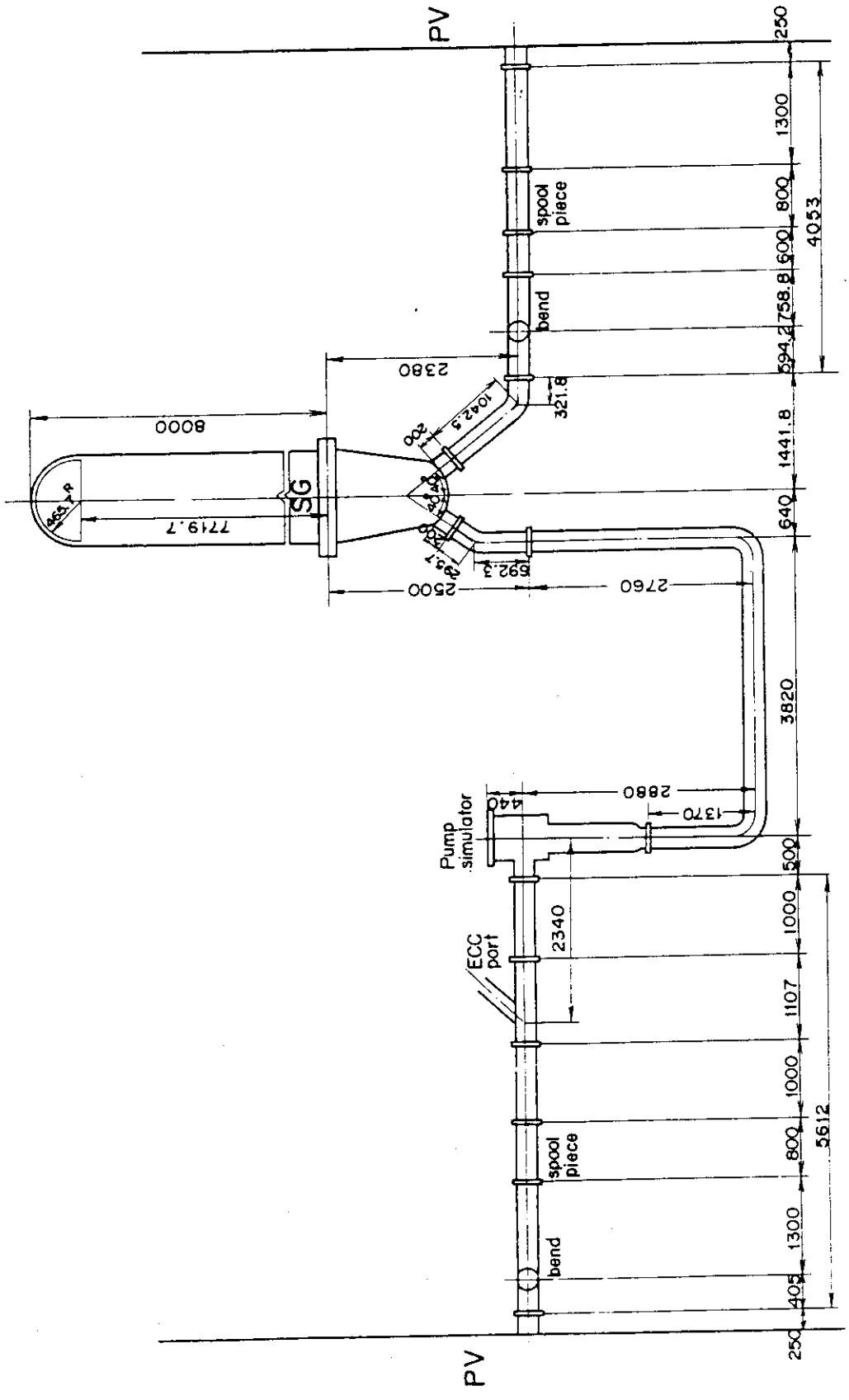

Fig.2.6 Primary loop

3. Results and Discussions

The system behavior during the experiment is discussed in this chapter. For C1-8, since the core power was prematurely interrupted during the experiment, the C1-18 results are mainly discussed.

The discussion of the C1-18 results is divided into three groups. The filled water behavior in the loop seal section is presented in Section 3.1. The discussion of the vessel differential pressure behavior is presented in Section 3.2, and the loop and the core behaviors are discussed in Section 3.3 and Section 3.4, respectively.

The C1-8 results are compared with the C1-18 results in Section 3.5.

3.1 Water behavior filled in loop seal section

Before the initiation of the experiment, saturated water was filled in each loop seal piping to 1.5 m level from the bottom of the piping.

Figure 3.1 shows the steam generator (SG) side and the pump-side differential pressures in the loop seal section. The pump-side differential pressure was measured between the bottom and the pump inlet which is 0.92 m elevation from the bottom. The positive values of them represent the higher pressure at the upstream.

The SG-side differential pressure significantly increases right after flood. This indicates that the filled water was pushed from the SG-side to the pump-side. That of the intact loop reaches about zero value at 10 seconds after flood. After 10 seconds, the SG-side differential pressure of the intact loop is decreased again. This means that some amount of the filled water returned from the pump side to the SG side.

The water which was filled in the intact loop seal section is pushed to the pump side again after 13 seconds because of the increase of the upper plenum pressure. The steam initiated to penetrate through the loop seal at 37 seconds after flood. The significant decrease of the pump-side differential pressure indicates that this steam penetration was remarkable after 55 seconds. The pump-side differential pressure is stable at about zero value after 65 seconds. Most of the filled water is considered to be blown away from the loop seal section to the cold leg at that time. This trend is also observed in the broken loop, however, the decrease of the SG-side differential pressure at 10 seconds

is not observed.

Figure 3.2 shows the SG-side differential pressure of the intact and the broken loop seal sections and the ECC injection rate into the intact cold leg. In the experiment, the ECC water was injected into the intact cold legs, but not into the broken cold leg. The differential pressures in both the intact and the broken loops rise immedeatly after the flood initiation. The steam was generated in the core after flooding, and the generated steam resulted in the increase of the upper plenum pressure, therefore, the filled water in the loop seal section was pushed from the SG-side to the pump-side. During the accumulator injection period at the cold leg, the SG-side differential pressure in the intact loop significantly increases and that is much greater than in the broken loop. It is considered that the steam condensation in the intact cold leg due to the subcooled water injection caused the pressure decrease in the intact cold leg, as a result, the filled water was pushed to the pump side. When the injection rate was reduced at 10 seconds, the steam condensation also diminished, and the filled water reentered into the SG-side of the loop seal section. After that, the filled water was pushed again to the pump side because of the increasing pressure in the upper plenum, then, the steam could penetrate through the filled water after about 50 seconds for the intact Loop-1.

Figure 3.3 shows the differential pressure between the bottom of the loop seal piping and the pump inlet in each loop. The decrease of them indicates the steam penetration through the loop seal section. The initiation of the differential pressure decrease in each loop occurs at the different timing between about 32 seconds and 50 seconds. The exact water level in the loop seal section prior to the experiment initiation and the reversed water mass during the accumulator injection period are considered to affect the timing of the initiation of the steam penetration. The differential pressures stay at nearly constant value after the sudden decrease. Most of the water in the loop seal section was blown away.

These behaviors of the filled water were also confirmed by the flow observation at the locations in Loop-1 shown in Fig.3.1. The steam bubble passed through the horizontal bottom piping of the intact loop seal section around 10 seconds, and the steam and water mixture flow was observed at the pump inlet during the period from 50 seconds through 70 seconds. The separate flow was observed at the bottom piping

of the loop seal during 50 to 60 seconds. After that, water was not observed there. Much water was observed at the pump outlet through 70 seconds. After 70 seconds, the water intermittently passed through the pump outlet piping. These flow observations indicated that the first steam penetration occurred at 10seconds and the significant penetration initiated at 50 seconds, then, most of the filled water was blown away at about 70 seconds.

3.2 Vessel differential pressure behavior

Figure 3.4 compares the differential pressure in the downcomer, the lower plenum and the core. During the accumulator injection period, the downcomer differential pressure steeply increases. When the ECC injection rate was reduced, the increasing rate of the downcomer differential pressure lowers. At that time, the accumulated water mass in the downcomer is less for C1-18 than for C1-5. It is considered that some amount of the injected water flowed into the loop seal section for C1-18, as described in the former section, caused the less water mass supplied into the downcomer, and the less accumulated mass in the downcomer.

The difference between the differential pressures in the downcomer and the core is the driving force for the steam penetration through the blocked loop seal section. This difference increased the upper plenum pressure which pushed the filled water in the SG-side loop seal section to the pump side. When the water level in the SG-side loop seal section reached the top of the bottom piping of the loop seal section, the steam penetration initiated. Since the flow area of the pump was about twice of that of the loop seal piping, the calculated water level in the pump-side loop seal section was about 2.05 m at that time. For C1-18, when the significant steam penetration occured in the broken loop at 32 seconds, the difference of the differential pressures in the downcomer and the core reaches 20 kPa that is equivalent to the saturated water head of 2.06 m. This value is nearly the same as the calculated water level in the pump-side loop seal section.

As described above, the steam penetration initiated when the difference of the differential pressures in the downcomer and the core exceeds the effective water head at the top of the bottom piping of the loop seal section when all of the filled water was assumed to be accumulated only in the pump-side and the bottom pipings of the loop seal

section, not in the SG-side.

For C1-18, the initiation of the significant steam penetration is later in Loop-1 and Loop-3 than in the broken loop (Loop-4). Because ECC water was not injected into the broken cold leg, the potential cause of this delay was the reversed water mass.

When the significant steam penetration initiated, the filled water in the intact loop seal sections and the accumulated water in the intact c-ld legs were forced to flow into the downcomer, consequently, the accumulated water mass in the downcomer increases consequently at around 50 seconds. The downcomer differential pressure continues to increase through the time when the filled water was almost discharged from the loop seal section at 65 seconds. Since the peak value of the differential pressure is greater than the saturated value of that which is close to the downcomer overflow level, some of the accumulated water could overflow into the containment. The downcomer differential pressure for C1-18 is almost the same as that for C1-5 after 200 seconds.

The core differential pressure for C1-18 is suppressed before the significant steam penetration through the loop seal section at 50 seconds. That recovers at 65 seconds when the filled water in the loop seal section was blown away. And that value is identical to the C1-5 result after about 80 seconds, though the downcomer differential pressure was still higher for C1-18 than for C1-5. The core differential pressure is nearly steady after that time.

The differential pressure between the top of the core and the top of the vessel is compared between C1-18 and C1-5 in Fig.3.5. Water does not accumulate above the core for C1-18 before 50 seconds due to no significant steam flow in the core caused by the filled water in the loop seal section, while the water accumulation for C1-15 initiates immediately after the flood initiation. The accumulated water mass above the core is slightly less for C1-18 than for C1-5 after that.

3.3 Loop behavior

The differential pressure in the broken cold leg nozzle is compared in Fig.3.6. For C1-18, the steam generated in the core penetrated through the filled water in the loop seal section at 37 seconds and flows into the containment via the broken cold leg nozzle.

This steam flow slightly increased the differential pressure in the broken cold leg nozzle. The steam penetration accompanied with the water discharge increased the accumulated water mass in the downcomer, and the downcomer overflow initiated. Since the steam flow increased in the intact loops due to the cleared intact loop seal sections and the downcomer water overflow, the differential pressure in the broken cold leg nozzle significantly increases after 65 seconds. The differential pressure gradually decreases after that reaches the peak value at 130 seconds. The value and the trend of the differential pressure for C1-18 are nearly the same as those for C1-5 after about 200 seconds.

Figure 3.7 compares the differential pressure in the intact and the broken loops. For C1-18, the differential pressures in both loops before the significant steam penetration represent the difference of the filled water heads between the pump-side and the SG-side of the loop seal section due to no significant steam flow in the loops. And after 65 seconds, those represent the pressure drop caused by the flow resistance in the loop. For the broken loop, that reaches 19.5 kPa when the significant steam penetration initiates at 32 seconds. This value is almost the same as the difference of the differential pressure of the downcomer and the core at that time, as mentioned in the former section. For the intact loop (Loop-1), the steam penetration delays about 20 seconds and the differential pressure reaches 24 kPa. This behavior shows that the filled water mass in the loop seal section of Loop-1 was increased by the reversed water. The sudden increase of the accumulated core water mass caused the increased steam generation rate in the core, and the higher downcomer differential pressure allowed the higher pressure drop in the loop for C1-18 than for C1-5 after 65 seconds. The higher differential pressure in the broken cold leg nozzle for C1-18 promoted this behavior for the broken loop. After 200 seconds, the differential pressures in both loops for C1-18 are nearly the same as those for C1-5.

Figure 3.8 shows the comparison of the fluid temperatures in the inlet and the outlet plenum of the steam generator. The inlet temperatures of both experiments are nearly identical to the saturation temperatures. The outlet temperature for C1-18 increases at 50 seconds. This confirmes that the steam flow in this loop initiated at this time. The value of the outlet temperature for C1-18 is identical to that for

C1-5 after 100 seconds.

3.4 Core behavior

Figure 3.9 compares the core flooding rate between C1-18 and C1-5. For C1-5, the flooding rate is very high at the initiation of the transient due to the steep increase of the downcomer differential pressure which is the driving force of the core flooding. For C1-18, the steep increase of the downcomer differential pressure was also observed, as shown in Fig.3.1, however, since the filled water head in the loop seal section deducted the driving force, the flooding rate is significantly lower in an early transient than that for C1-5. The deduction of the driving force was taken out when the steam penetrated through the loop seal section at about 32 seconds, then the flooding rate increases. After the steam penetrated all of four loop seal section, the flooding rate significantly increases until 60 seconds. The flooding rate reduces again after 60 seconds. The value of the flooding rate for C1-18 is very similar to that for C1-5 after about 80 seconds.

The fluid temperature at the core inlet and the core saturation temperature are compared in Fig.3.10. The fluid temperatures of both experiments at the core inlet show the significant subcooling. The direct injection of the subcool ECC water into the lower plenum affected this fluid subcooling.

Figure 3.11 compares the clad surface temperatures of the average-powered rod (TE18Y rod). For C1-5, the increasing rate of the surface temperature reduces immediately after the flood initiation due to the steam flow in the core caused by the steam generation in the lower part of the core. On the contrary, for C1-18, the increasing rate does not reduce because of no significant steam flow caused by the blockage of the loop seal section. As a result, the surface temperatures are significantly higher, the turnaround time is longer, especially on 1.015 m elevation, and the quench time is also longer for C1-18 than for C1-5.

The calculated heat transfer coefficients of the maximum-powered rod (TE32X13) midplane are compared in Fig.3.12. The lower water accumulation in the core and the lower flooding rate in an early transient resulted in the lower heat transfer coefficient for C1-18 than

for C1-5. That for C1-18 increases around about 65 seconds, however, the value is still lower for C1-18 than that for C1-5. The void fraction near the core midplane are compared in the Fig.3.13. The void fractions for C1-18 decrease after about 50 seconds, while those for C1-5 decrease immediately after the flood initiation. Though the saturated value of each elevation for C1-18 is similar to that for C1-5, the void fraction between 1.83 m and 2.44 m for C1-18 is higher through 240 seconds than that for C1-5. This higher void fraction seems to cause the lower heat transfer coefficient.

Figure 3.14 presents the comparison of the turnaround times in the core medium-powered region (B region). As expected from the rod surface temperature responses, the turnaround time at the elevation of 1.05 m is significantly longer for C1-18 than for C1-5 due to less water accumulation in the core. Since the core water accumulation was steeply increasing during the period from 50 seconds to 60 seconds, as shown in Fig.3.4, the steam generation rate must be significantly increased. The increased steam flow promoted the heat transfer, as shown in Fig.3.12, and resulted in the relatively earlier turnaround time at 1.83 m elevation for C1-18. Figure 3.15 compares the turnaround temperatures in the core medium-powered region (B region). The turnaround temperature at each elevation is quite higher for C1-18. This tendency is significant for the elevation of 1.05 m. The maximum turnaround temperature in the core is 1134 K for C1-18 and 1039 K for C1-5. The lower heat transfer coefficient in an early transient which was caused by the loop seal section blockage resulted in the higher turnaround temperature. Figure 3.16 shows the comparison of the quench times in the core medium-powered region (B region). The quench times are also longer for C1-18, however, the difference is not so significant. The early recovery of the core water mass contributed to reduce the effect of the blocked loop seal section on the core quench behavior.

3.5 Comparison of C1-8 with C1-18

The C1-8 experiment was conducted under nominally the same conditions as those for C1-18. In the test, since the rod surface temperature exceeded the designed allowable temperature, the power supply to the core was prematurely interrupted at that time.

The differential pressure in the SG-side loop seal section is compared between C1-8 and C1-18 in Fig.3.17. They are identical to each other through about 30 seconds. The effects of the steam condensation and the reversed water, as decribed in Section 3.1, are also observed in C1-8 result. After 30 seconds, the differential pressure for C1-8 is slightly lower than that for C1-18. Figure 3.18 compares the differential pressure between the bottom of the loop seal section and the pump inlet. Though the tendency of them is very similar to each other, the timing of the initiation of the steam penetration through the loop seal section delays for C1-8. For the broken loop (Loop-4), the delay is not so significant, but for the intact loop (Loop-1), the steam penetration is more than 20 seconds later, and it occurs after turning off the core power supply.

Figure 3.19 shows the comparison of the differential pressure in the downcomer, the lower plenum and the core. The tendency is quite similar to each other. However, the downcomer differential pressure is slightly lower for C1-8 than for C1-18 before the initiation of the significant steam penetration. The downcomer differential pressure is very important for these experiments, because that is the driving force of the steam penetration through the loop seal section. The slightly lower downcomer differential pressure for C1-8 reduces the differential pressure between the hot leg and the cold leg and results the delayed steam penetration into the loop seal section, as shown in Fig.3.18. The steep increase of the core accumulated water mass due to the steam penetration is also delayed and occurs after interrupting the core power supply.

The accumulator injection rate, as shown in Fig.3.20, is about 1.39×10^{-3} m^3/s lower on the average for C1-8 than for C1-18. The difference of the injected water mass between C1-8 and the C1-18 is equivalent to about 0.15 m difference of the collapsed water level in the downcomer. It is considered that the less injected water mass caused the lower downcomer differential pressure, consequently, the delayed steam penetration through the loop seal section.

Figure 3.21 compares the surface temperatures of the maximum powered rod (TE32X). For C1-18, the temperature rise reduces at about the same time as the initiation of the steam penetration. Since the steam penetration is delayed for C1-8, the temperature continue to

increase before that and reaches 1163 K, then the power to the core central region was reduced by 20%. At last, the temperature reaches 1173 K which is the maximum allowable temperature, and the core power was turned off.

The little lower accumulator injection rate for C1-8 caused the delayed steam penetration through the loop seal section and resulted in the higher rod temperature.

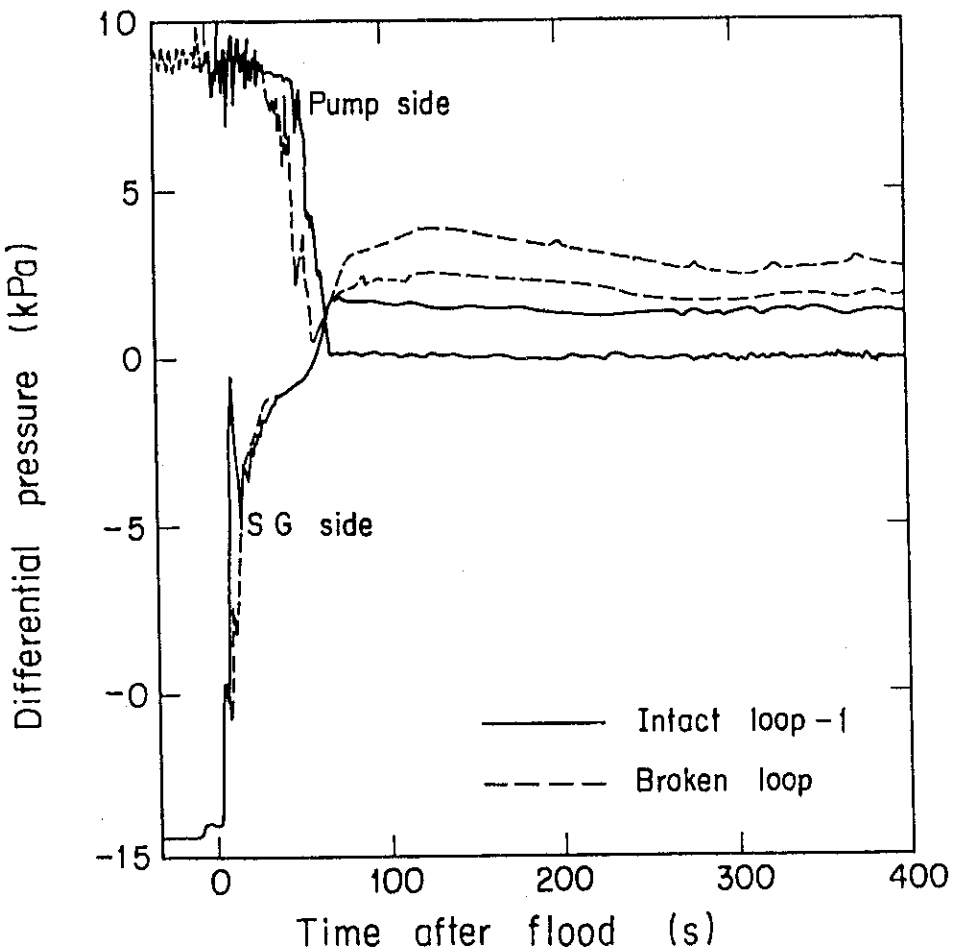

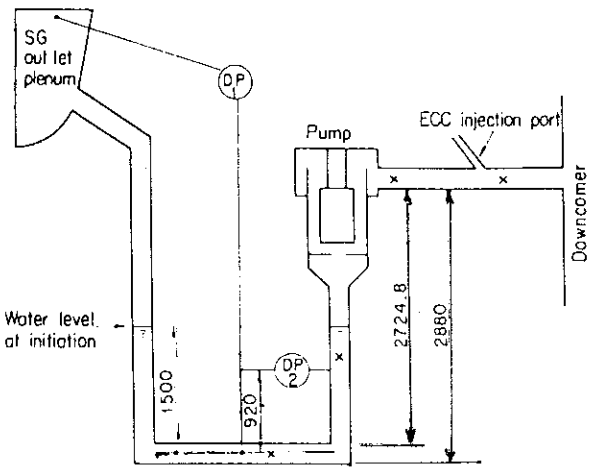

Note DP1: Differential pressure in SG side of loop seal section

DP2: Differential pressure between bottom of loop seal section and pump inlet (pump side)

x: flow observation window

Fig.3.1 Differential pressures in SG-side and pump-side loop seal section

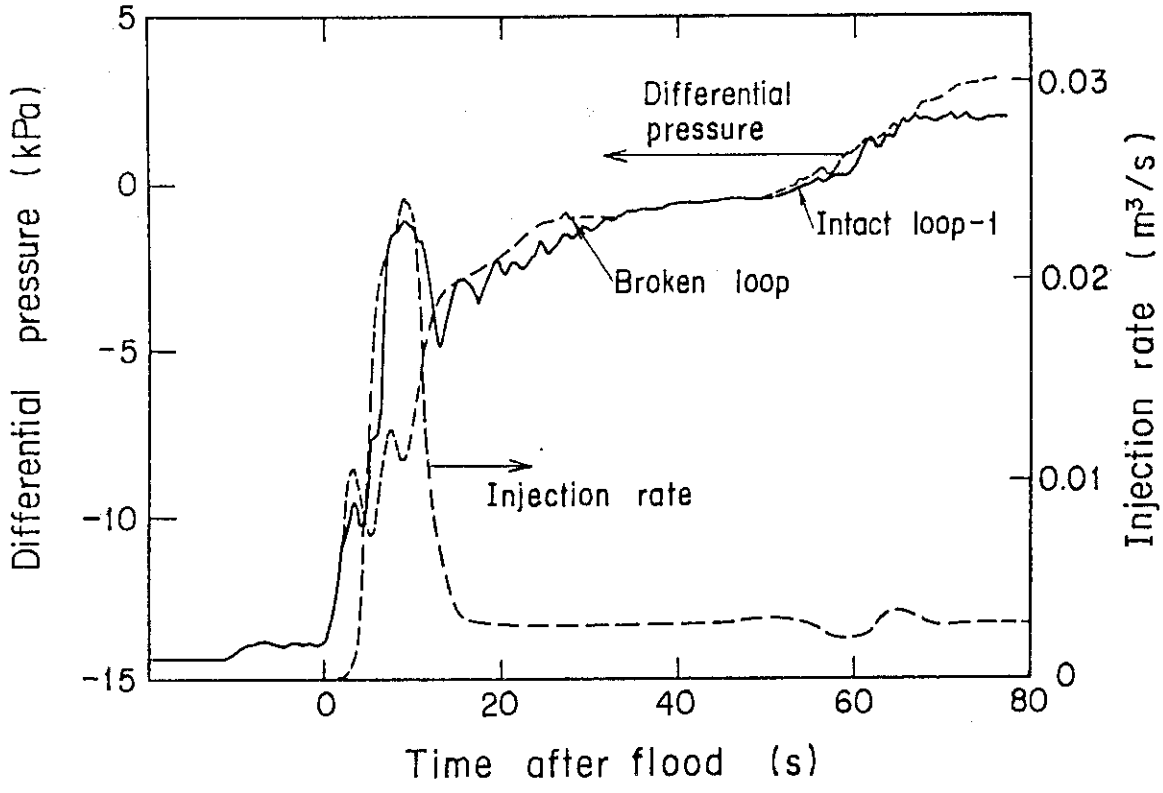

Fig.3.2 SG-side differential pressure and ECC injection rate into cold leg

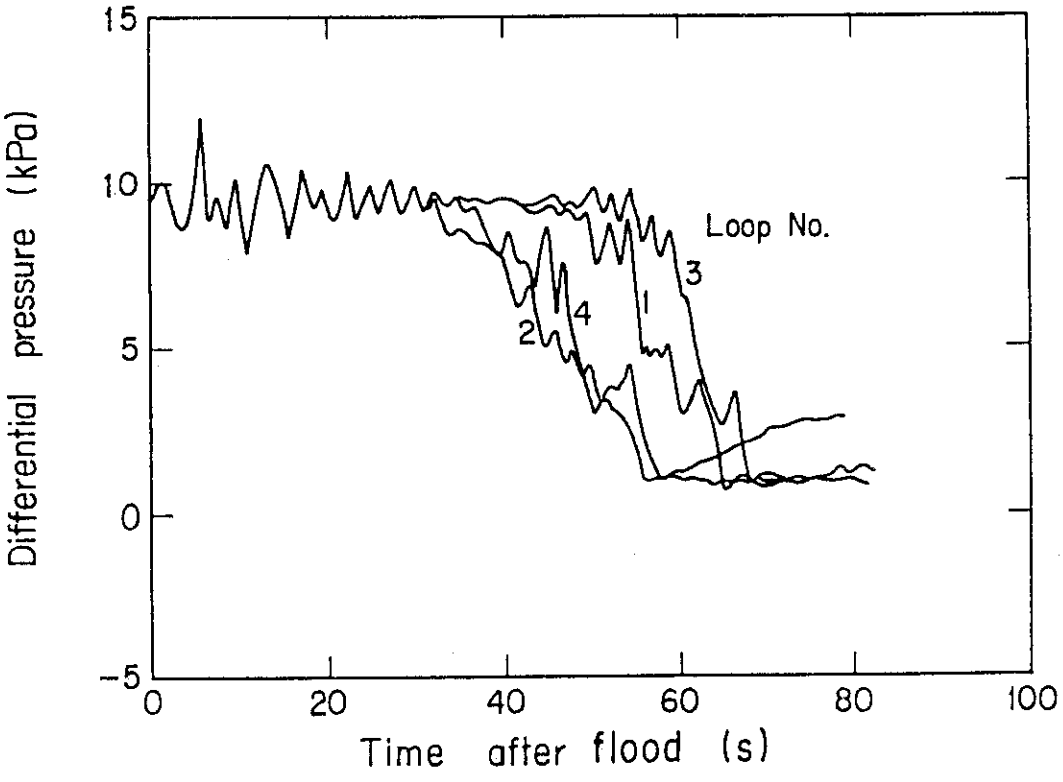

Fig.3.3 Differential pressure between bottom of loop seal section and pump inlet

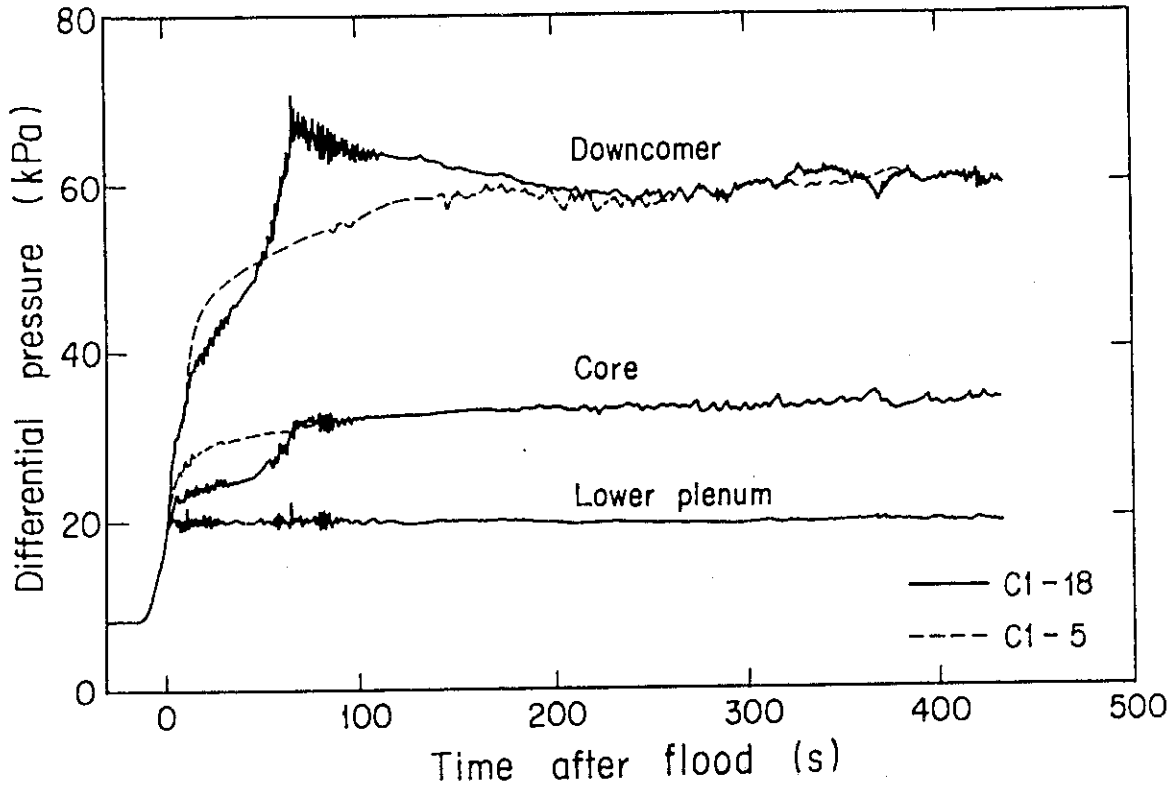

Fig.3.4 Differential pressures in downcomer, core and lower plenum

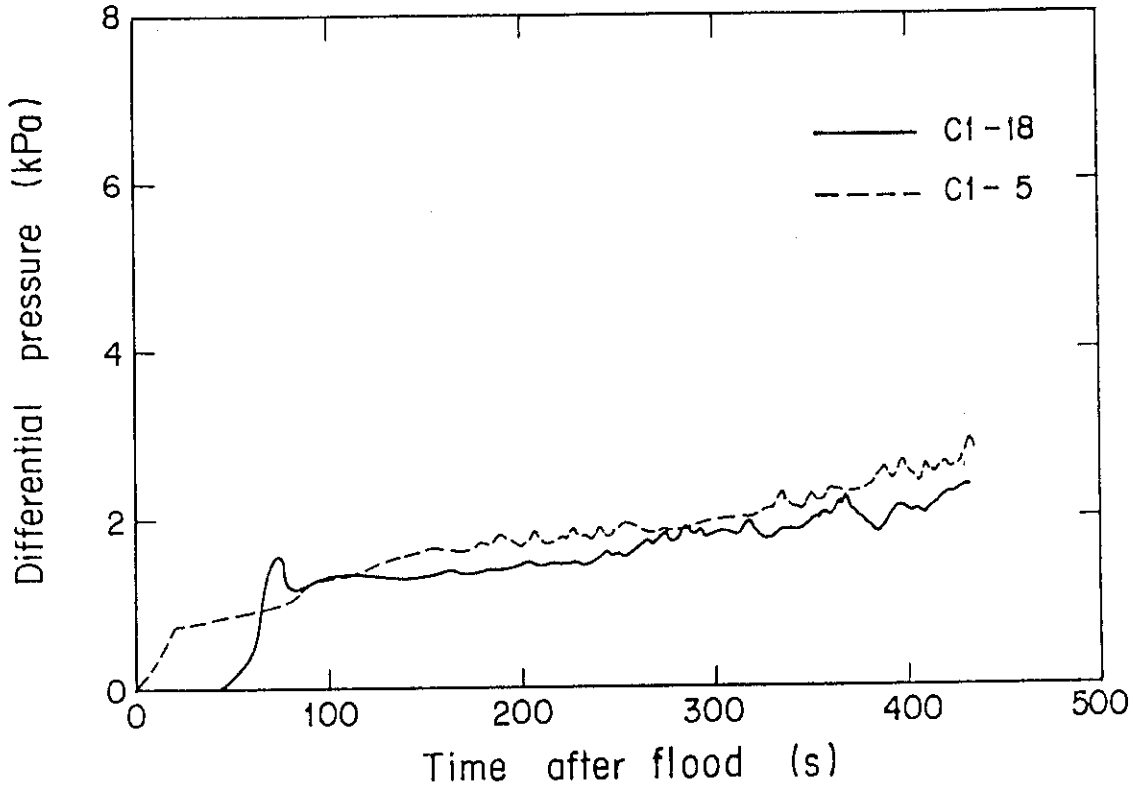

Fig.3.5 Differential pressure above core

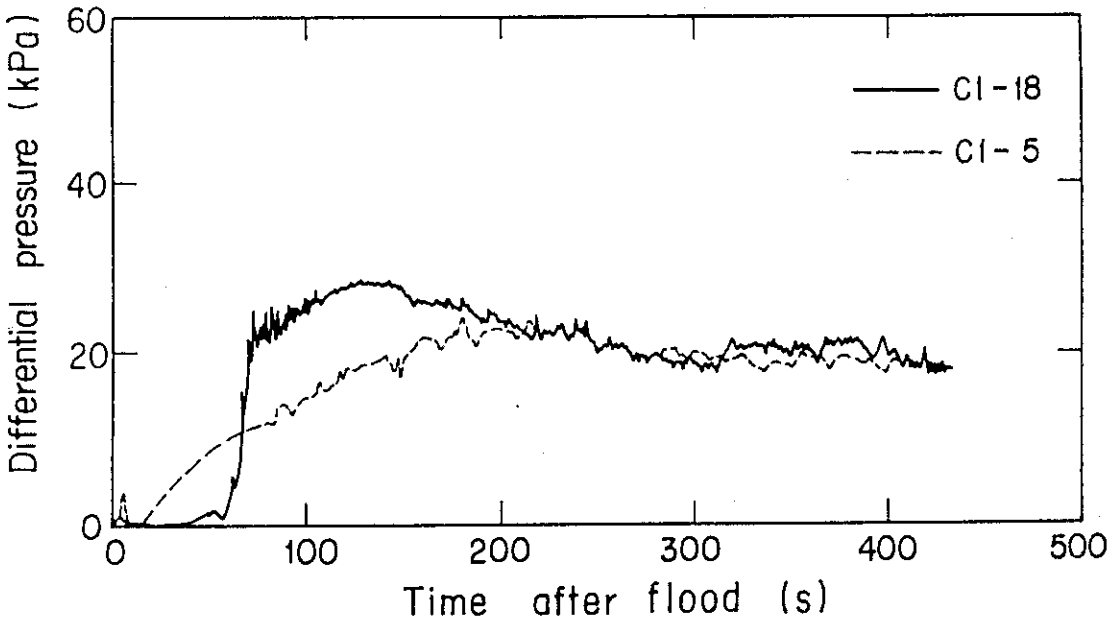

Fig.3.6 Differential pressure in broken cold leg nozzle

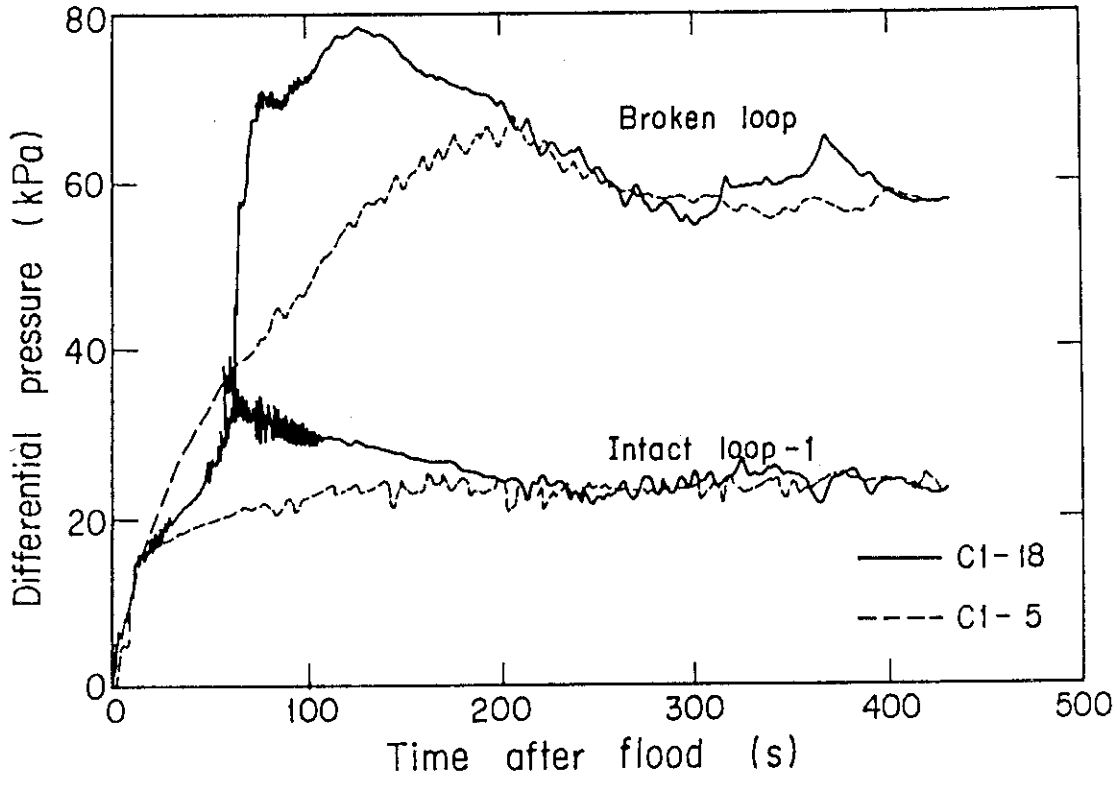

Fig.3.7 Differential pressures in intact and broken loops

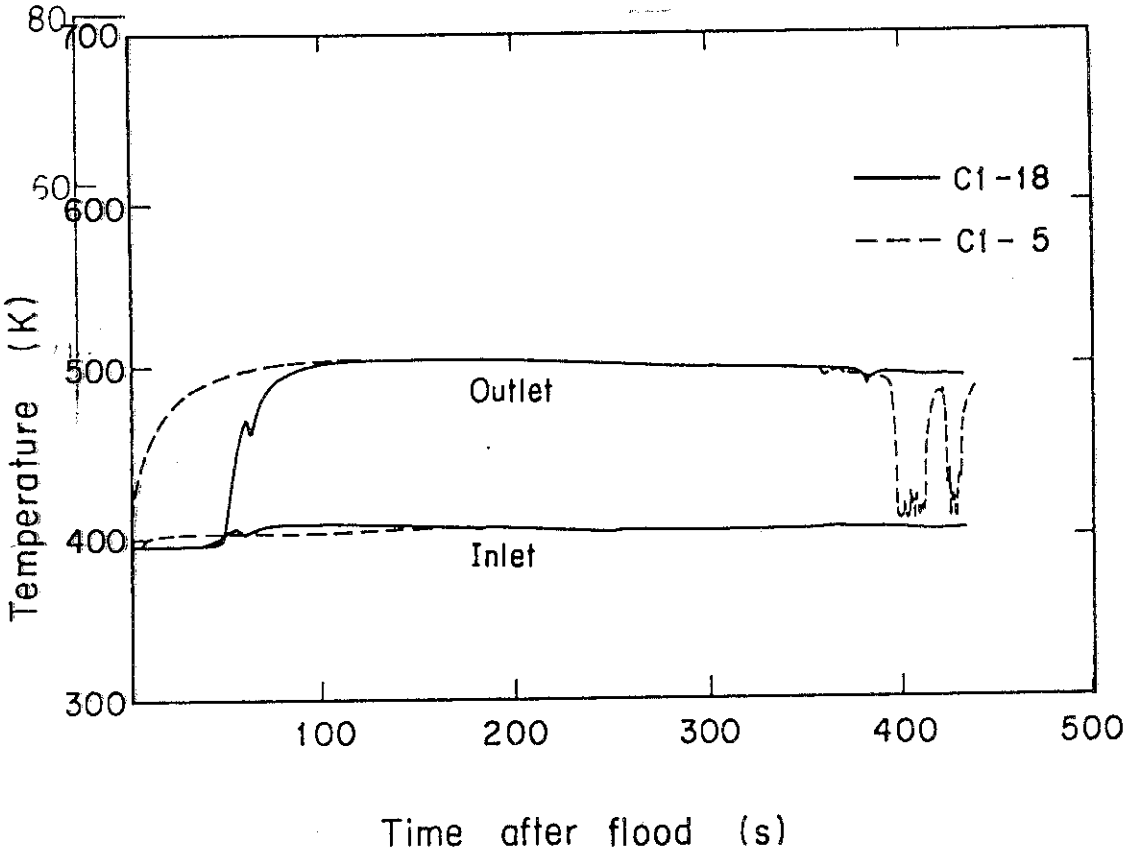

Fig.3.8 Fluid temperatures in inlet and outlet plenum of steam generator

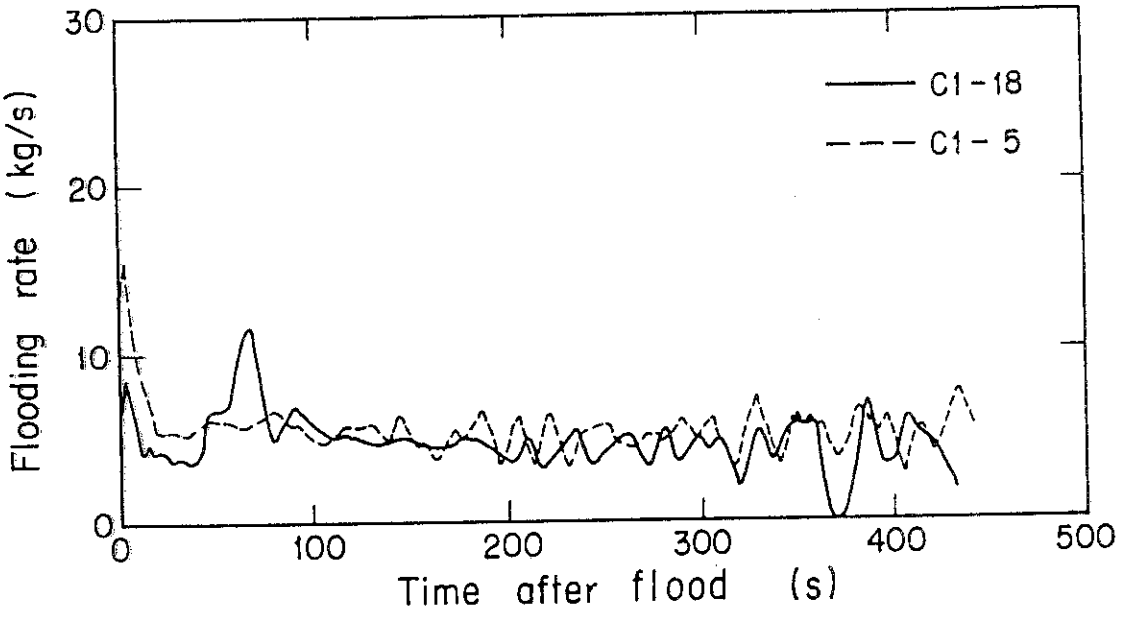

Fig.3.9 Core flooding rate

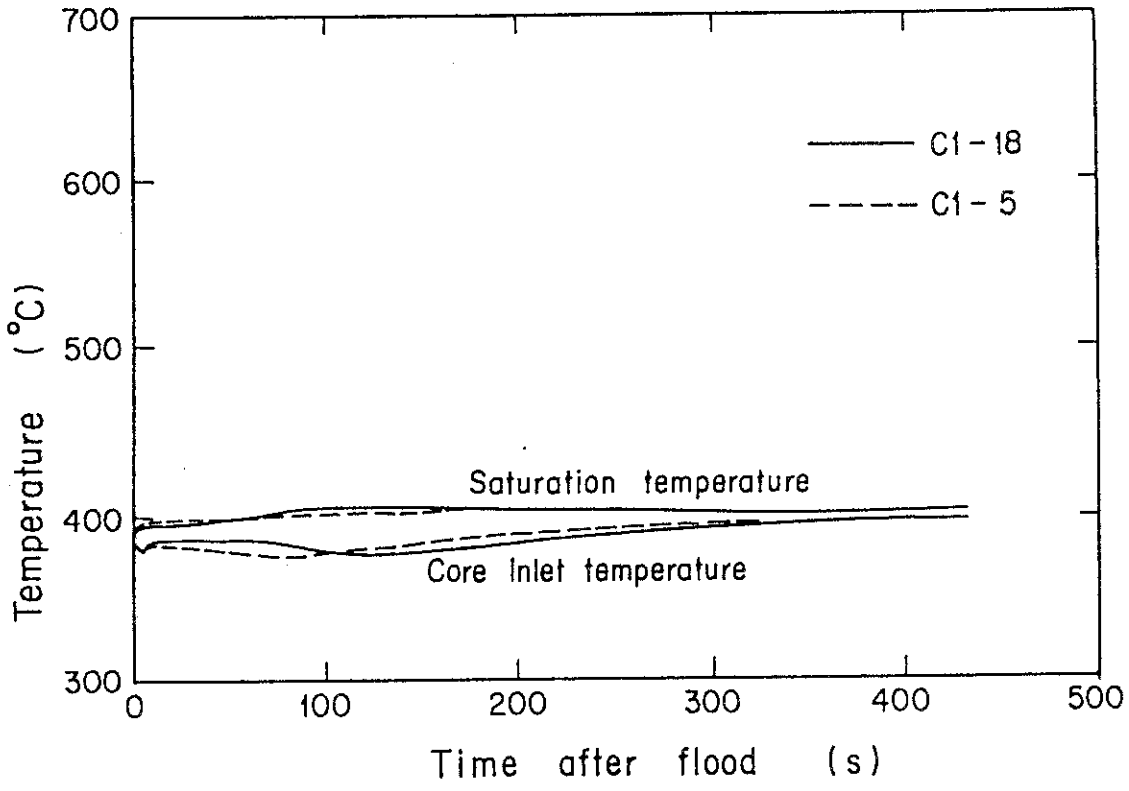

Fig.3.10 Core inlet fluid temperature and saturation temperature

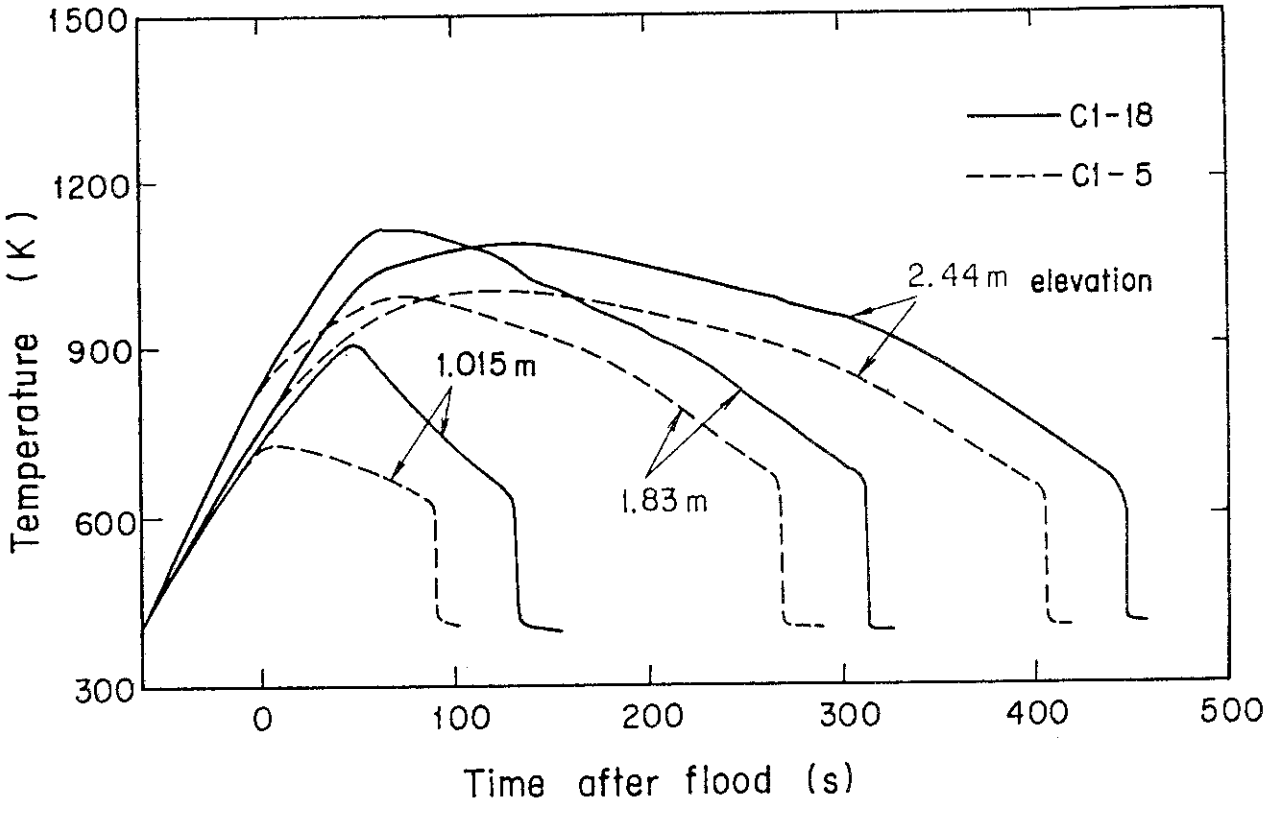

Fig.3.11 Clad surface temperatures of average-powered rod (TE18Y rod)

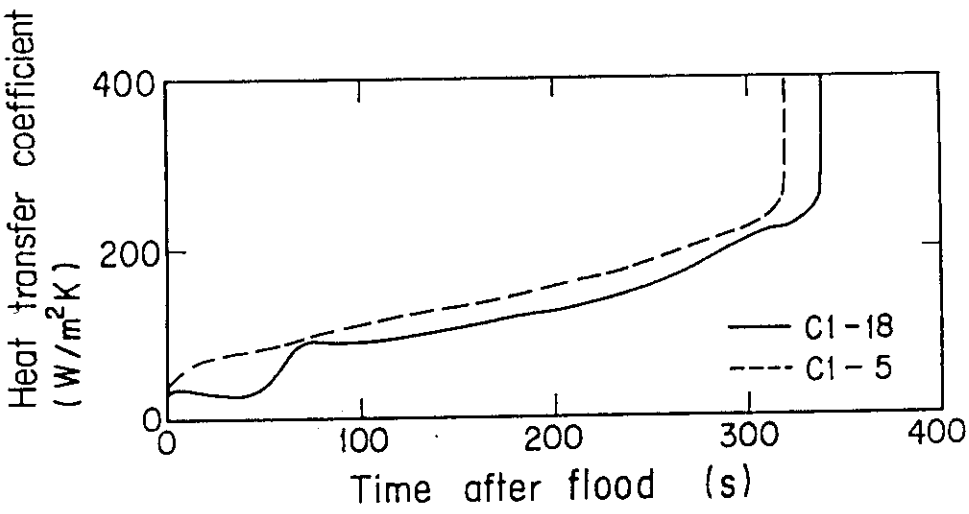

Fig.3.12 Heat transfer coefficient on maximum-powered rod midplane

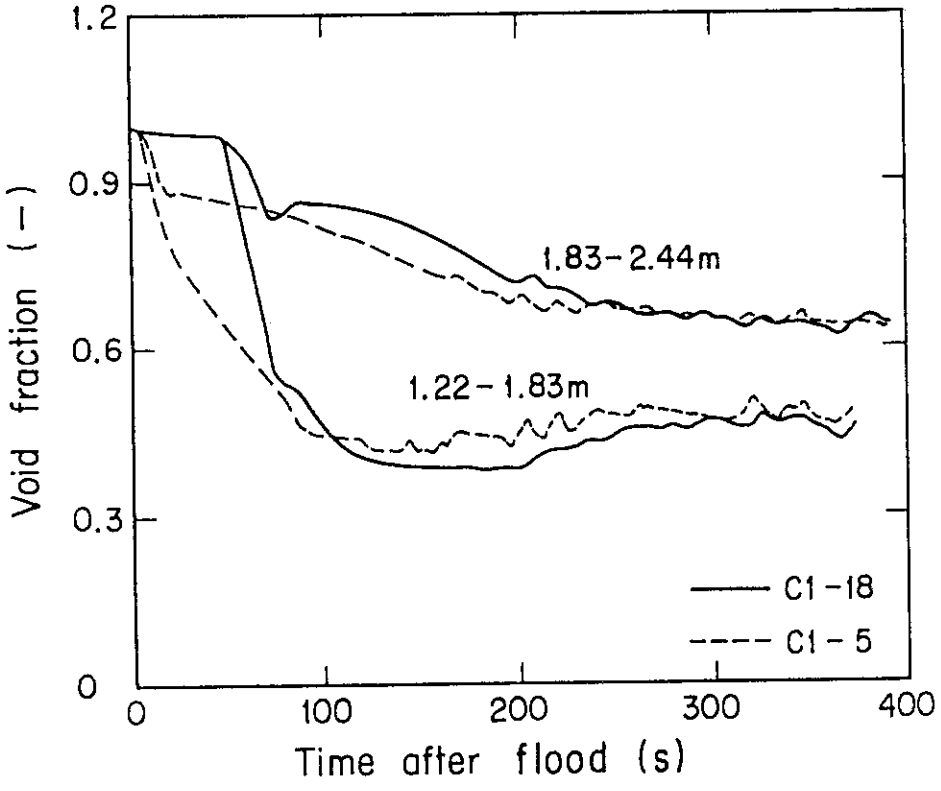

Fig.3.13 Core void fraction

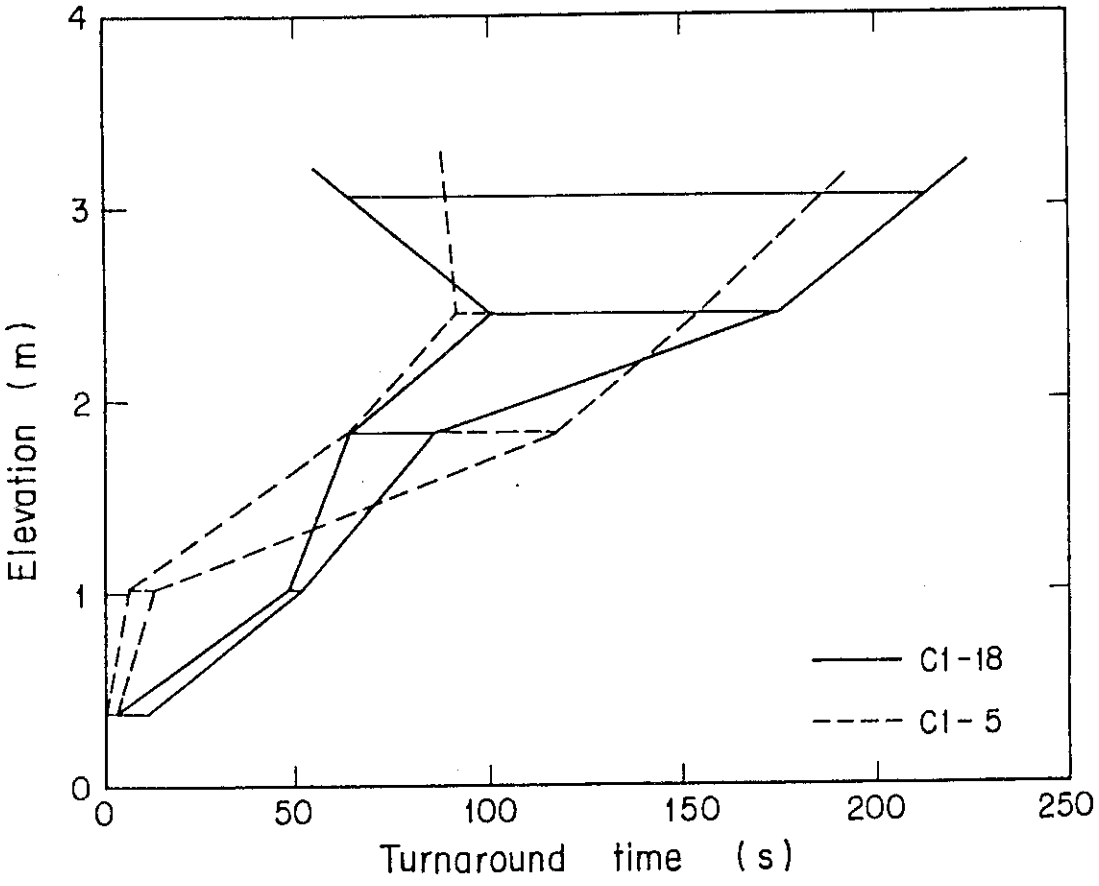

Fig.3.14 Turnaround times in core medium-powered region (B region)

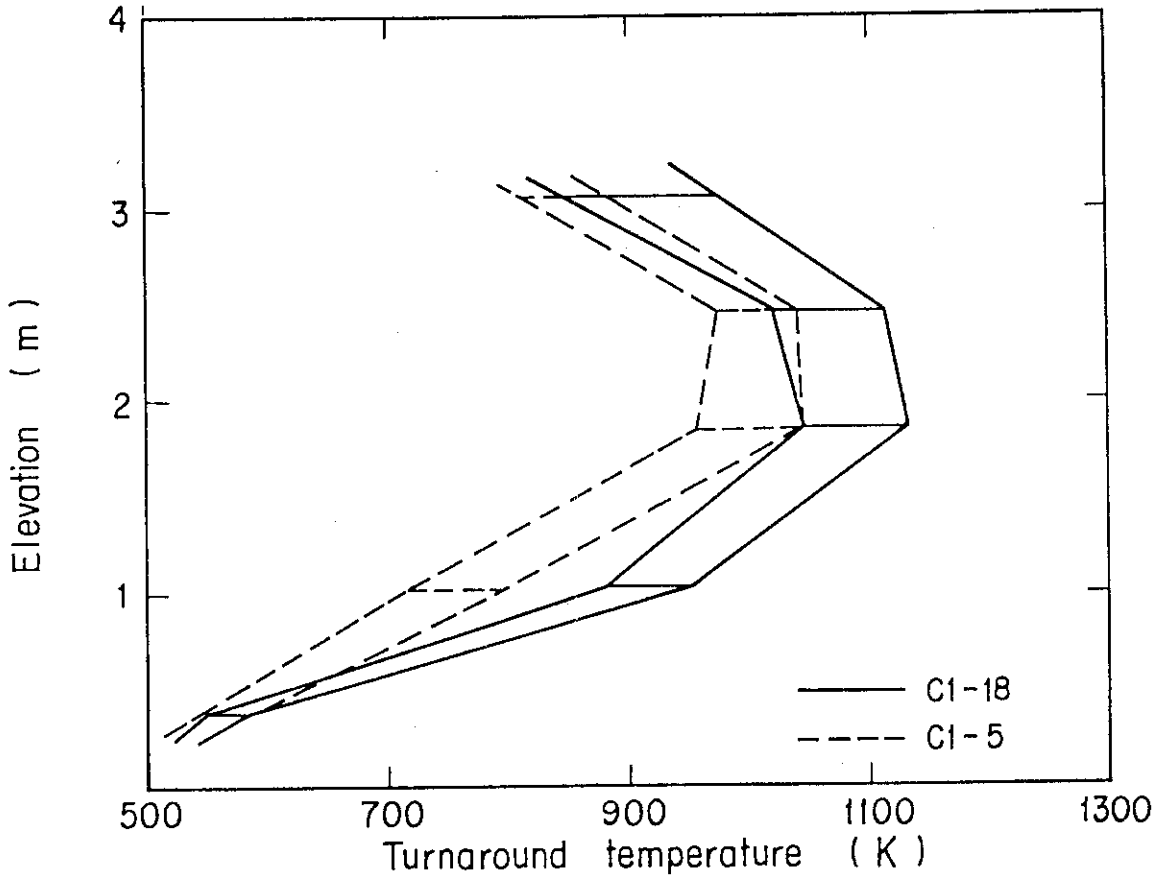

Fig.3.15 Turnaround temperatures in core medium-powered region (B region)

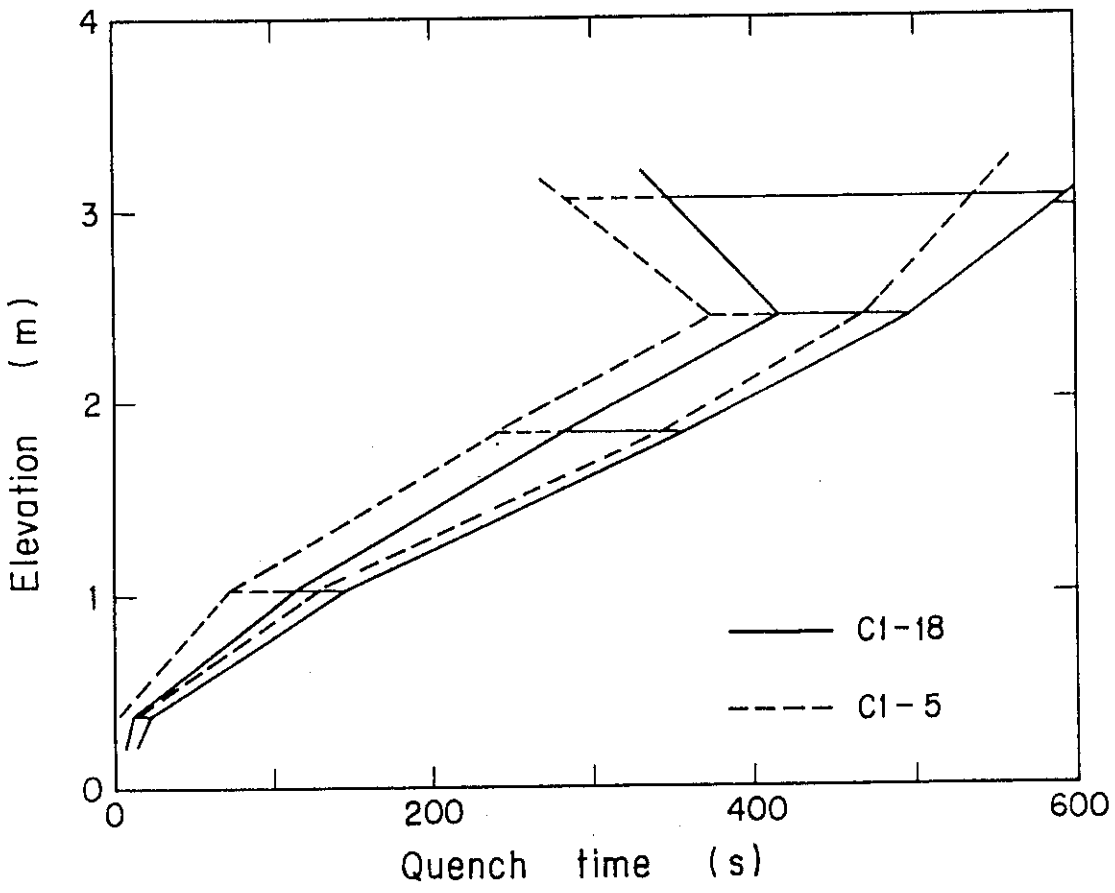

Fig.3.16 Quench times in core medium-powered region (B region)

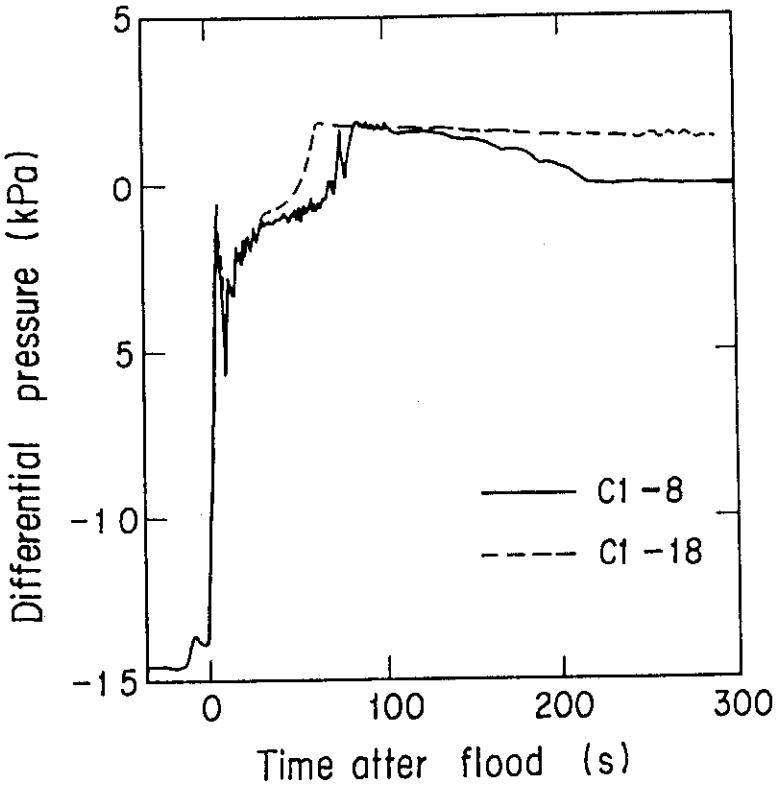

Fig.3.17 Comparison of differential pressure in SG-side loop seal section

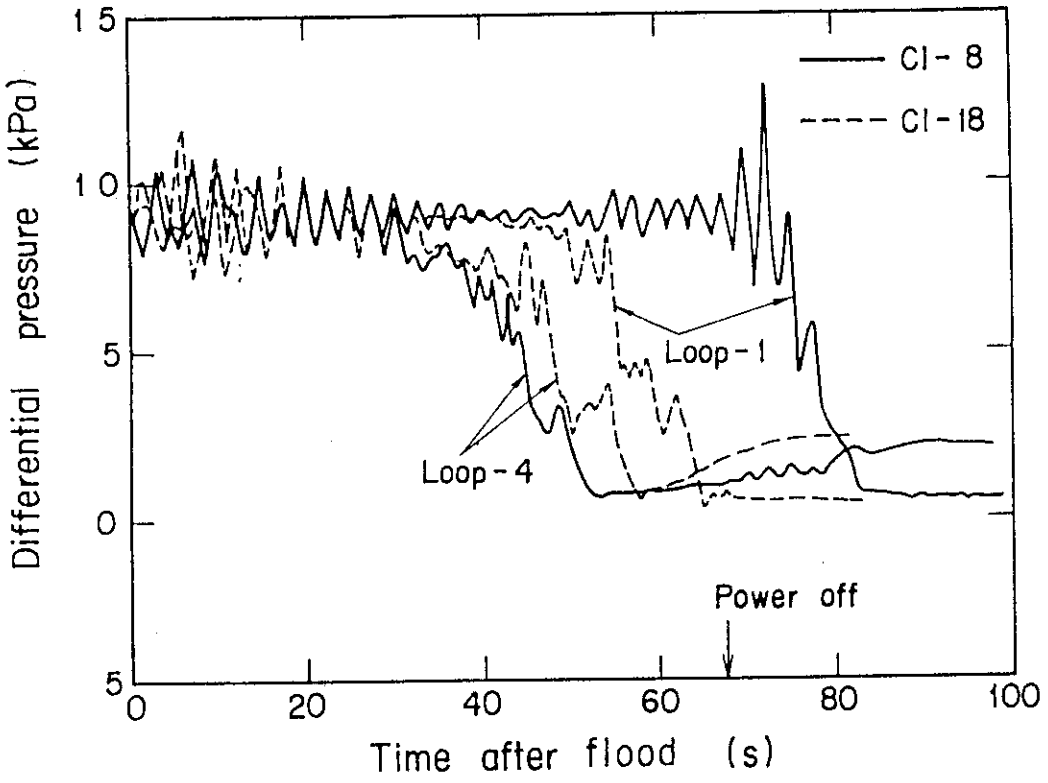

Fig.3.18 Comparison of differential pressure between bottom of loop seal section and pump inlet

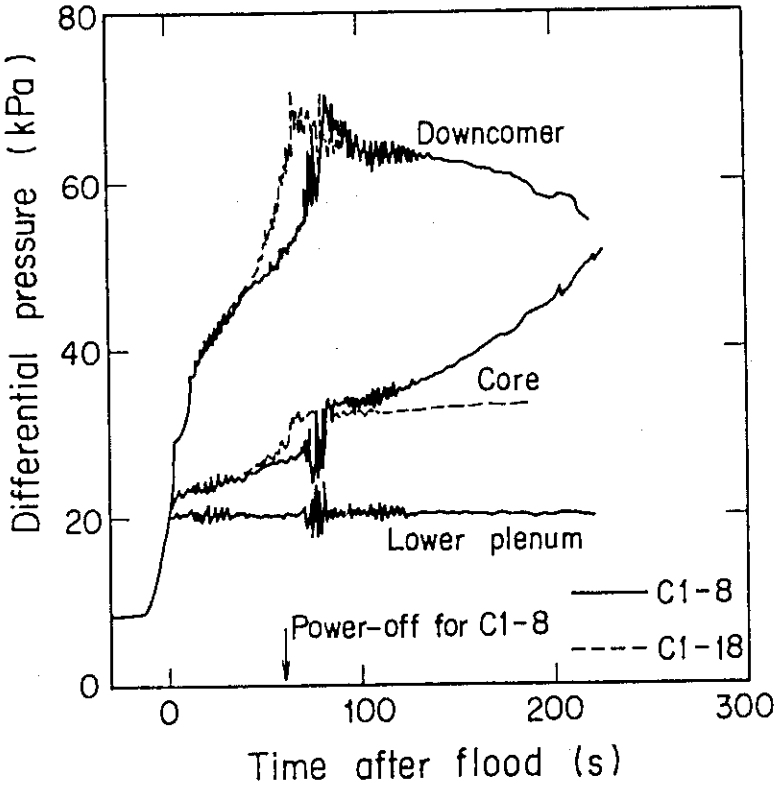

Fig.3.19 Comparison of differential pressures in downcomer, lower plenum and core

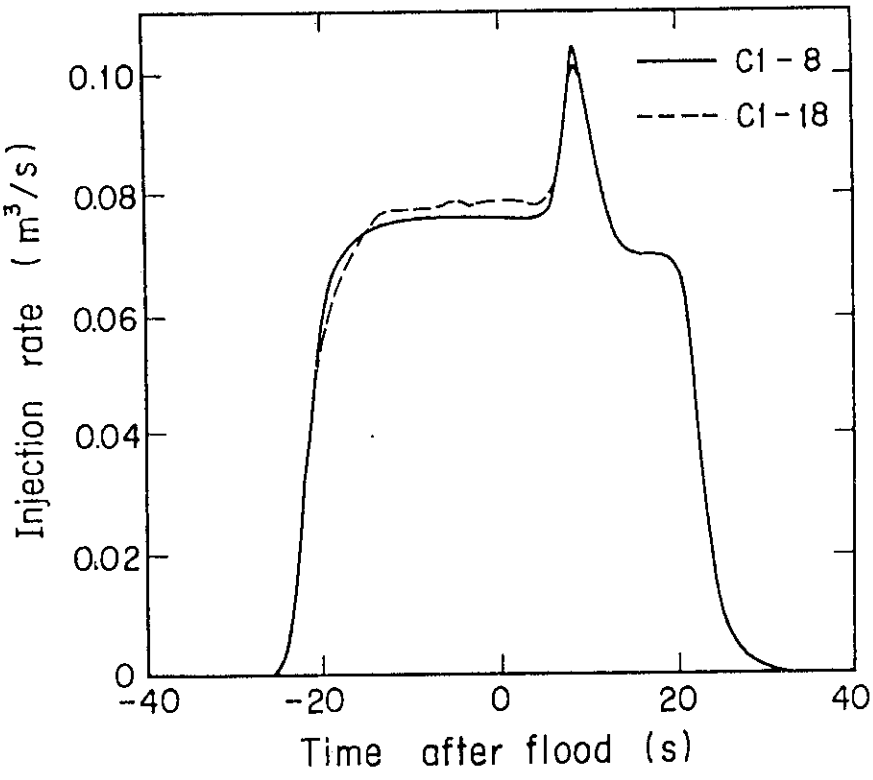

Fig.3.20 Comparison of accumulator injection rate

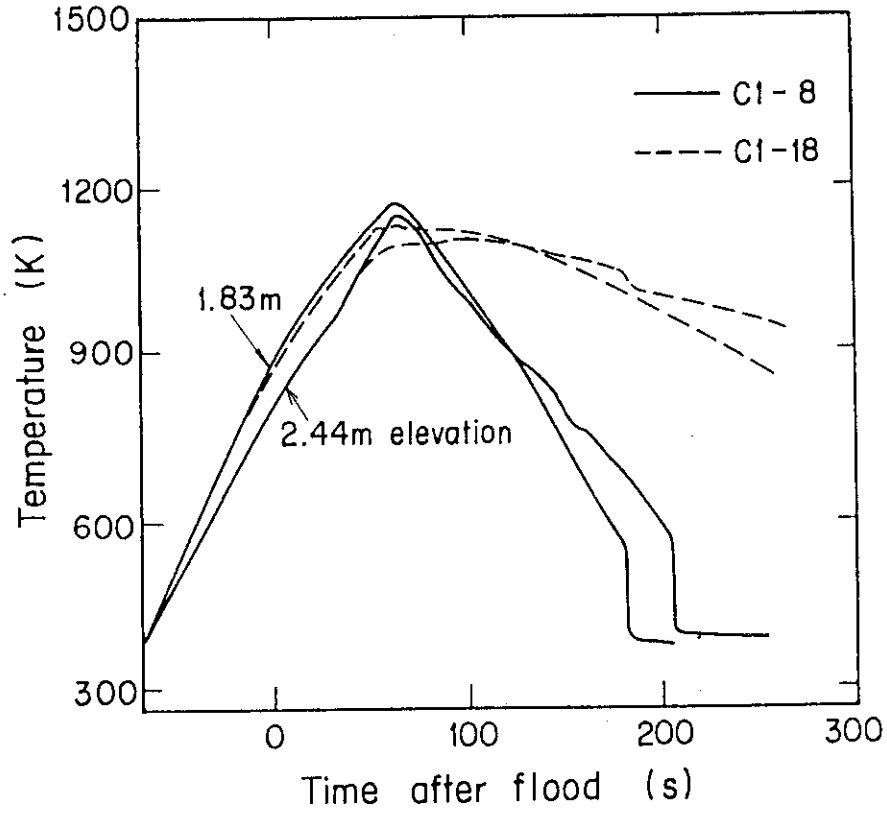

Fig.3.21 Comparison of surface temperatures of maximum-powered rod (TE32X rod)

4. Conclusions

In order to study the effect of the water seal in the loop seal section on the reflood phenomena, C1-18 and C1-8 were conducted. In these experiments, the loop seal section was filled with the saturated water by the elevation of 1.5 m. The results of C1-18 were compared with those of C1-5 which was performed without the water seal in the loop seal section. The C1-8 results were also compared with the C1-18 results.

For C1-18

- Filled water behavior in the loop seal section
  1) The filled water was pushed from the SG side to the pump side of the loop seal section immediately after the flood initiation due to the pressure increase in the upper plenum.
  2) This movement was accelerated by the steam condensation in the intact cold leg and/or in the upper part of the downcomer during the period that the subcooled accumulator water was injected into the intact cold leg. A small amount of the steam penetrated through the loop seal section in this period.
  3) During this period, the reverse water flow was observed at the outlet of the pump. The water mass in the loop seal section seemed to increase.
  4) The significant steam penetration through the broken loop seal section occurred at 32 seconds after BOCREC and most of the filled water was blown away until 65 seconds.
  5) The initiation of the steam penetration in the intact loop was about 18 seconds later than that in the broken loop. The increased water mass due to the reversed water caused this delay.

- System behavior
  1) The core water accumulation was suppressed before the significant steam penetration through the loop seal section. Therefore, the differential pressure in the downcomer was much higher than that in the core.
  2) The difference between the differential pressures in the downcomer and the core is the driving force of the steam penetration through the loop seal section. The steam penetration initiates

when the water level in the SG-side loop seal section reaches just below the top of the bottom piping. For C1-18, the significant steam penetration through the broken loop seal section initiated at 32 seconds after BOCREC and at this time, the driving force was equal to the water head in the pump-side loop seal section.

3) Simultaneously with the significant steam penetration, the core water mass increased and reached the identical value to that for C1-5.
4) Since the discharged water from the loop seal section increased the accumulated water mass in the downcomer, the initiation of the downcomer overflow was earlier for C1-18 than for C1-5. The mixture of the steam and the overflowed water caused the significant pressure drop in the broken cold leg nozzle.
5) The differential pressure of the each system component was similar to that for C1-5 after about 200 seconds. The effect of the filled water in the loop seal section was considered to disappear at that time.

o Core behavior

1) No steam flow in the core before the significant steam penetration resulted the low heat transfer coefficient in the core and the low flooding rate.
2) After the significant steam penetration, the high flooding rate was observed in a short period. The accumulated water mass in the core also increased at that time. Thus, the core heat transfer coefficients increased.
3) Because of the low heat transfer coefficient in an early transient for C1-18, the turnaround temperatures were high. The maximum turnaround temperature was 1.34 K which was about 100 K higher than that for C1-5.
4) The quench times in the core were not so different with those for C1-5. The early recovery of the core water mass reduced the effect of the loop seal section blockage on the quench behavior.

Comparison of C1-18 with C1-8

1) In C1-8, the initiation of the significant steam penetration was later and the temperature rise of the core was higher than those for C1-18.
2) The accumulator injection rate for C1-8 was slightly lower and caused the slightly lower differential pressure in the downcomer, accordingly the lower driving force of the steam penetration.
3) Therefore, it took more time for the steam to penetrate through the loop seal section and that allowed the higher temperature rise of the core. The maximum temperature in the core exceeded the designed allowable temperature, then the supplied power was prematurely turned off.
4) As described above, the ECC injection rate affected the initiation of the steam penetration through the loop seal section.

Acknowledgements

The authors are very grateful to Dr. M. Nozawa, Deputy Director General of Tokai Research Establishment, JAERI, Dr. S. Katsuragi, Director of Nuclear Safety Research Center, and Dr. K. Hirano, Deputy Head of Department of Nuclear Safety Research for their hearty suggestion and encouragement.

They are deeply indebted to Mr. T. Iguchi, Mr. J. Sugimoto, Dr. H. Akimoto, and Mr. T. Okubo for their analytical support. They would like to express their appreciation to Mr. H. Adachi, Dr. Y. Sudo, Mr. M. Sobajima, Mr. T. Iwamura, Mr. M. Osakabe, and Mr. A. Ohnuki for their useful discussions, Messrs. K. Sekiguchi, Y. Fukaya, N. Suzuki, T. Oyama, T. Wakabayashi, Y. Niitsuma, J. Matsumoto, T. Nishikizawa, and H. Sonobe for their contribution to the facility operation, to Messrs. R.K. Fujita and D.H. Miyasaki, resident engineers from USNRC, and to Dr. P.J. Schally, resident engineer from BMFT, for their devoted help.

References

1) Murao, Y., et al., "Evaluation Report on CCTF Core-I Reflood Test C1-5 (Run 14)", JAERI-M 83-027, (Jan. 1983)

2) Murao, Y., et al., "CCTF Core-I Test Result", JAERI-M 82-073 (Jul. 1982).

Acknowledgements

The authors are very grateful to Dr. M. Nozawa, Deputy Director General of Tokai Research Establishment, JAERI, Dr. S. Katsuragi, Director of Nuclear Safety Research Center, and Dr. K. Hirano, Deputy Head of Department of Nuclear Safety Research for their hearty suggestion and encouragement.

They are deeply indebted to Mr. T. Iguchi, Mr. J. Sugimoto, Dr. H. Akimoto, and Mr. T. Okubo for their analytical support. They would like to express their appreciation to Mr. H. Adachi, Dr. Y. Sudo, Mr. M. Sobajima, Mr. T. Iwamura, Mr. M. Osakabe, and Mr. A. Ohnuki for their useful discussions, Messrs. K. Sekiguchi, Y. Fukaya, N. Suzuki, T. Oyama, T. Wakabayashi, Y. Niitsuma, J. Matsumoto, T. Nishikizawa, and H. Sonobe for their contribution to the facility operation, to Messrs. R.K. Fujita and D.H. Miyasaki, resident engineers from USNRC, and to Dr. P.J. Schally, resident engineer from BMFT, for their devoted help.

References

1) Murao, Y., et al., "Evaluation Report on CCTF Core-I Reflood Test C1-5 (Run 14)", JAERI-M 83-027, (Jan. 1983)
2) Murao, Y., et al., "CCTF Core-I Test Result", JAERI-M 82-073 (Jul. 1982).

Appendix A

Definition of Tag. IDs in Appendix B through Appendix D

Figure list

1. Definition of Tag.ID for clad surface temperatures

Notation : TENNWAM

NN : Bundle number

WA : Power zone

WA = X1, X2 : High power (Local power factor 1.1)

WA = Y1, Y2 : Medium power (Local power factor 1.0)

WA = Z1, Z2 : Low power (Local power factor 0.95)

M : Elevation

	Elevation (m)	Axial power factor
1	0.38	0.568
2	1.015	1.176
3	1.83	1.492
4	2.44	1.312
5	3.05	0.815

2. Definition of power zone and bundle number

See Fig. A-1

3. Definition of Tag.ID for void fraction

See Fig. A-2

4. Definition of Tag.ID for average linear power of heater rod in each power unit zone

See Fig. A-3

5. Definition of carry-over rate fraction (C.R.F)

$$CRF = \frac{\dot{m}_{UP} + \dot{m}_{L}}{\dot{m}_{CR} + \dot{m}_{UP} + \dot{m}_{L}}$$

The calculated data within ±25 s are averaged:

$$(CRF)_i = \frac{1}{101} \sum_{k=i-50}^{i+50} (CRF)_k$$

where

ΔP_{UP} : Average of measured data at four orientations

ΔP_{CR} : Same as above

$$\dot{m}_{UP} = A_{up} \frac{d}{dt} (\Delta P_{UP})$$

$$\dot{m}_{CR} = A_{CR} \frac{d}{dt} (\Delta P_{CR})$$

$$\dot{m}_L = \sum_{k=1}^{4} \dot{m}_{pk}$$

$\dot{m}$: mass flow rate or mass accumulation rate

ΔP: differential pressure

suffix

UP: upper plenum

CR: core

L : loop

p : primary pump

6. Definition of Tag.ID for differential pressure through downcomer, upper plenum, core and lower plenum

See Fig. A-4

7. Definition of Tag.ID for differential pressure through intact and broken loop and broken cold leg nozzle

See Fig. A-5

8. Definition of Tag.ID for fluid temperature in inlet and outlet plenum and secondary of steam generator

See Fig. A-6

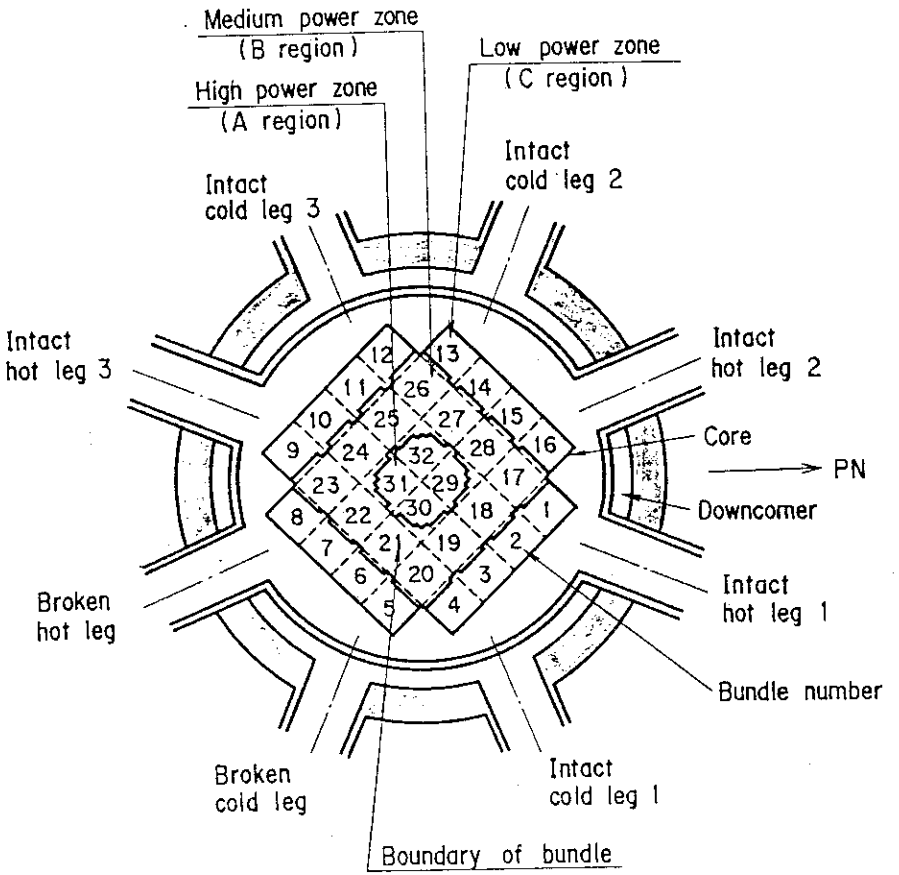

Fig. A-1 Definition of power zones and bundle numbers

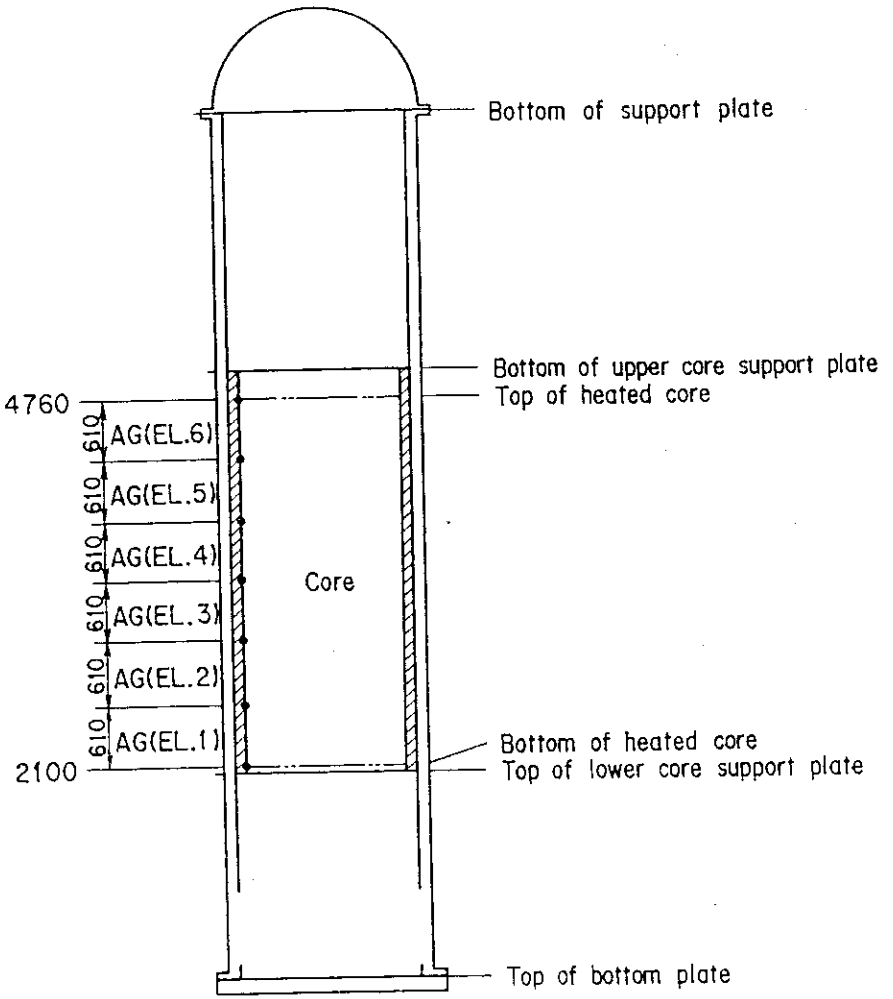

Fig. A-2 Definition of Tag.ID for void fraction (AG(EL.1) ~ AG(EL.6))

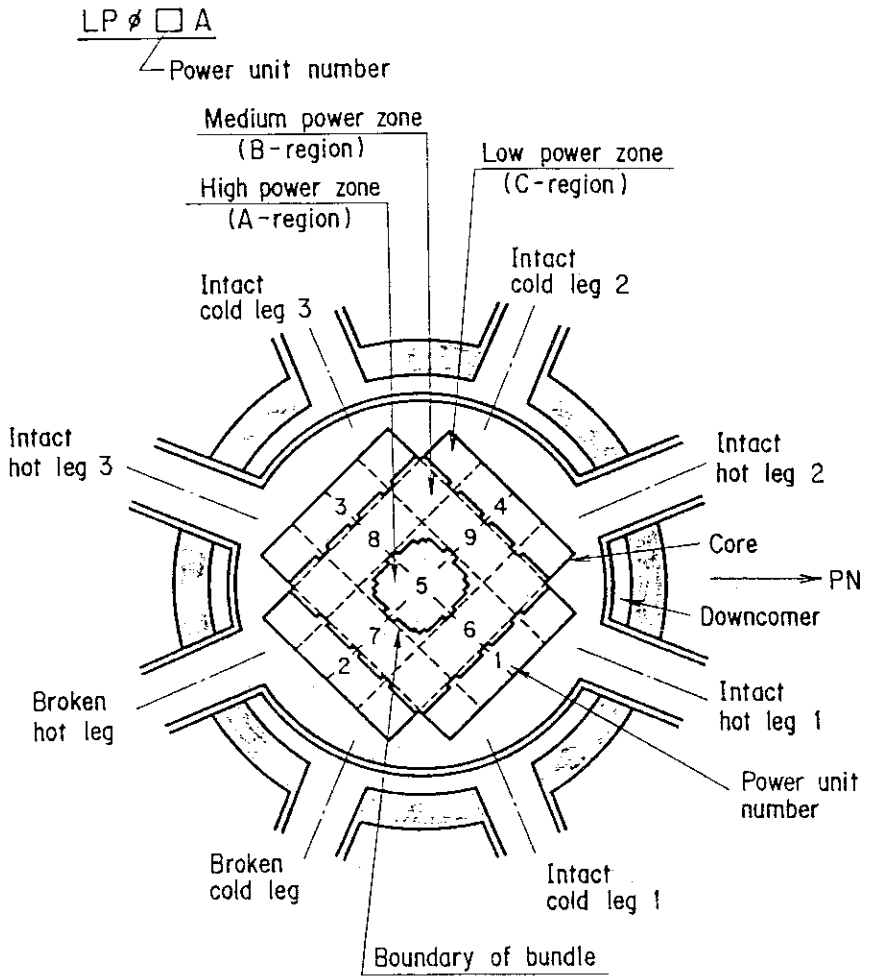

Fig. A-3 Definition of Tag.ID for average linear power of heater rod in each power unit zone (LP01A ~ LP09A)

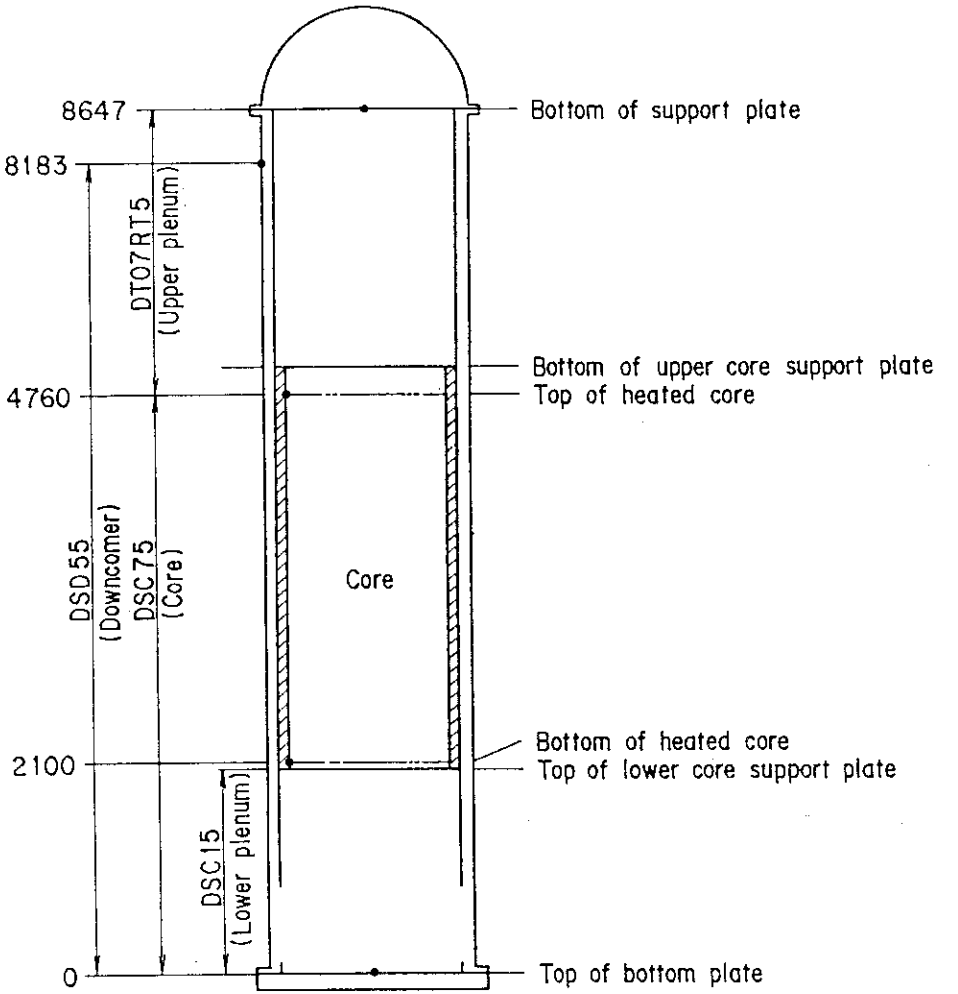

Fig. A-4 Definition of Tag.ID for differential pressure through downcomer, upper plenum, core, and lower plenum (DSD55, DT07TR5, DSC75, DSC15)

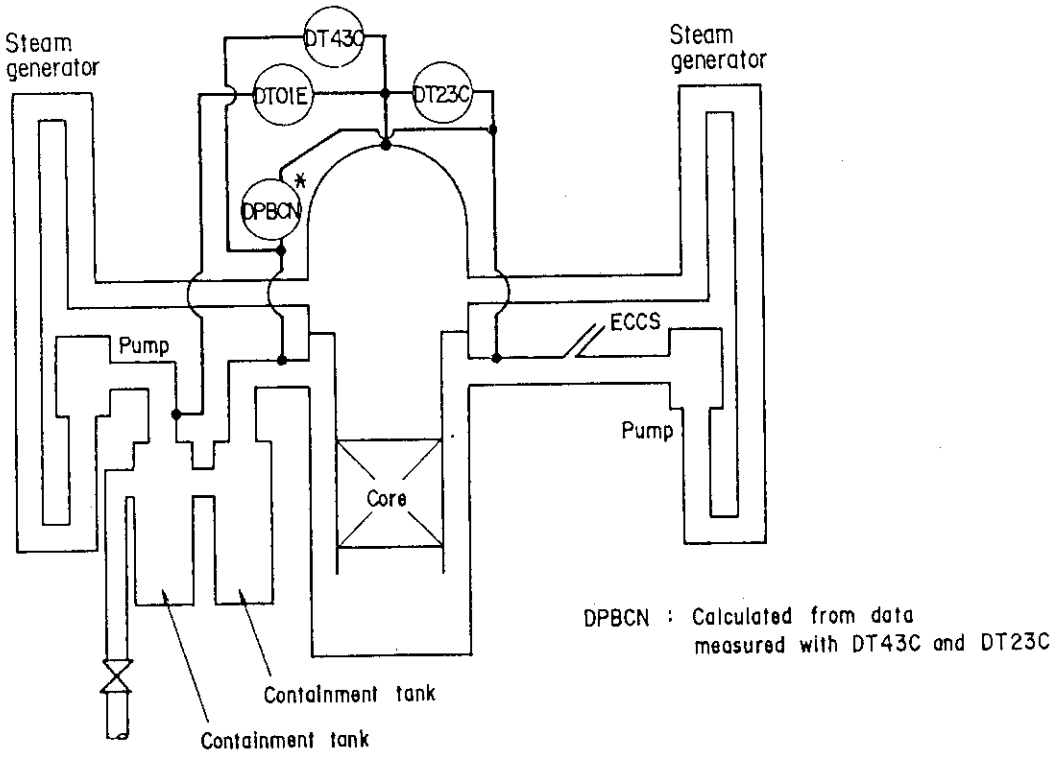

Fig. A-5 Definition of Tag.ID for differential pressure through intact and broken loop and broken cold leg nozzle (DT23C, DT01B, DPBCN)

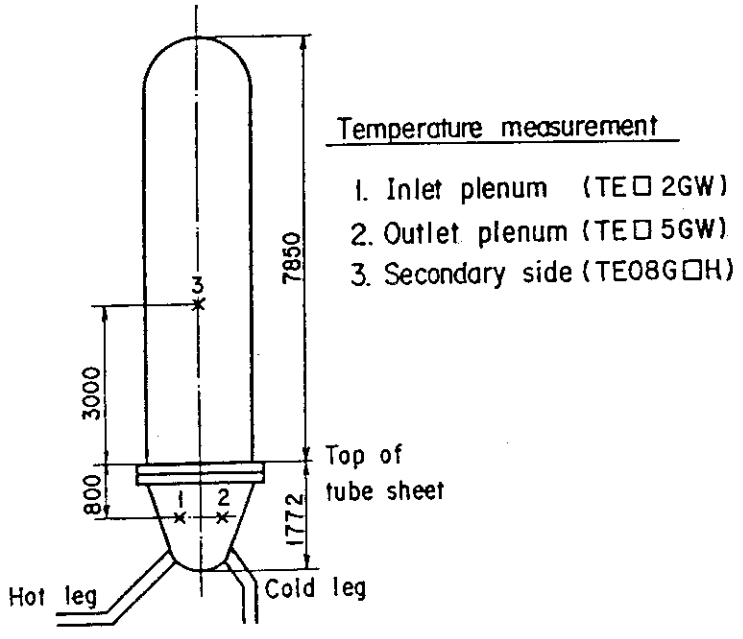

Fig. A-6 Definition of Tag.ID for fluid temperature in inlet and outlet plenum and secondary of steam generator (TE□2GW, TE□5GW, TE08G□H)

Appendix B

Main results for Test C1-18 (Run 37)

Table and Figure List

Table B-1 Summary of test conditions

1. TEST TYPE : LOOP SEAL WATER FILLING TEST
2. TEST NUMBER : RUN 037 3. DATE : March 10, 1981
4. POWER : A: TOTAL: 9.40 MW; B:LINEAR: 1.41 KW/M
5. RELATIVE RADIAL POWER SHAPE :

   A: ZONE: A B C

   B: RATIO: 1.153 : 1.079 : 0.885
6. AXIAL POWER SHAPE : CHOPPED COSINE
7. PRESSURE (KG/CM^2A) :

   A: SYSTEM: 1.96, B: CONTAINMENT 1.95,

   C: STEAM GENERATOR SECONDARY: 53.6
8. TEMPERATURE (DEG.C) :

   A: DOWNCOMER WALL 166, B: VESSEL INTERNALS 108,

   C: PRIMARY PIPING WALL 120, D: LOWER PELNUM LIQUID 114,

   E: ECC LIQUID 38.8, F: STEAM GENERATOR SECONDARY 263,

   G: CORE TEMPERATURE AT ECC INITIATION 597
9. ECC INJECTION TYPE: C

   A: COLD LEG, B: LOWER PLENUM, C: LOWER PLENUM + COLD LEG
10. PUMP K-FACTOR : $\sim$ 15
11. ECC FLOW RATES AND DURATION :

    A: ACCUMULATOR 285 M^3/HR FROM 0 TO 24 SECONDS

    B: LPCI 30.2 M^3/HR FROM 24 TO 805 SECONDS

    C: ECC INJECTION TO LOWER PLENUM : FROM 0 TO 17.5 SECONDS

    (VALVE OPENING AND CLOSING TIMES ARE INCLUDED IN THE INJECTION DURATION)
12. INITIAL WATER LEVEL IN LOWER PLENUM : 0.88 M.
13. POWER CONTROL : ANS x 1.2 + ACTINIDE (30 SEC AFTER SCRAM)
14. EXPECTED BOCREC TIME FROM ECC INITIATION 12 SEC
15. EXPECTED PEAK TEMPERATURE AT BOCREC 600 C

Table B-2 Chronology of events

EVENT	TIME (sec)
Test Initiated (Heater Rods Power on) (Data Recording Initiated)	0
Accumulator Injection Initiated	55
Power Decay Initiated (Bottom of Core Recovery)	67.5 (67.5)
Accumulator Injection Switched from Lower Plenum to Cold Leg	72.5
Accumulator Injection Ended and LPCI Injection Initiated	79.0
All Heater Rods Quenched	626
Power Off	680
LPCI Injection Ended	860
Test Ended (Data Recording Ended)	1009

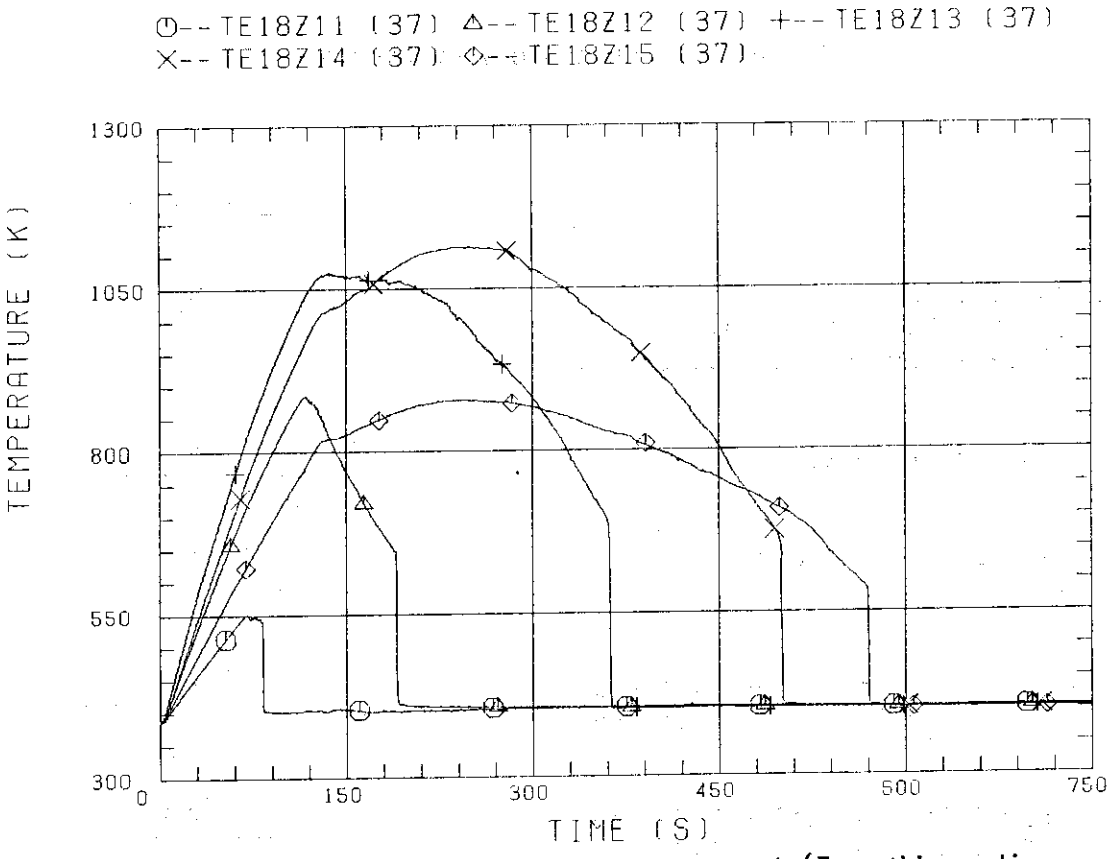

Fig. B-1 Surface temperature on low power rod (Z-rod)in medium power region (B region) (average power rod)

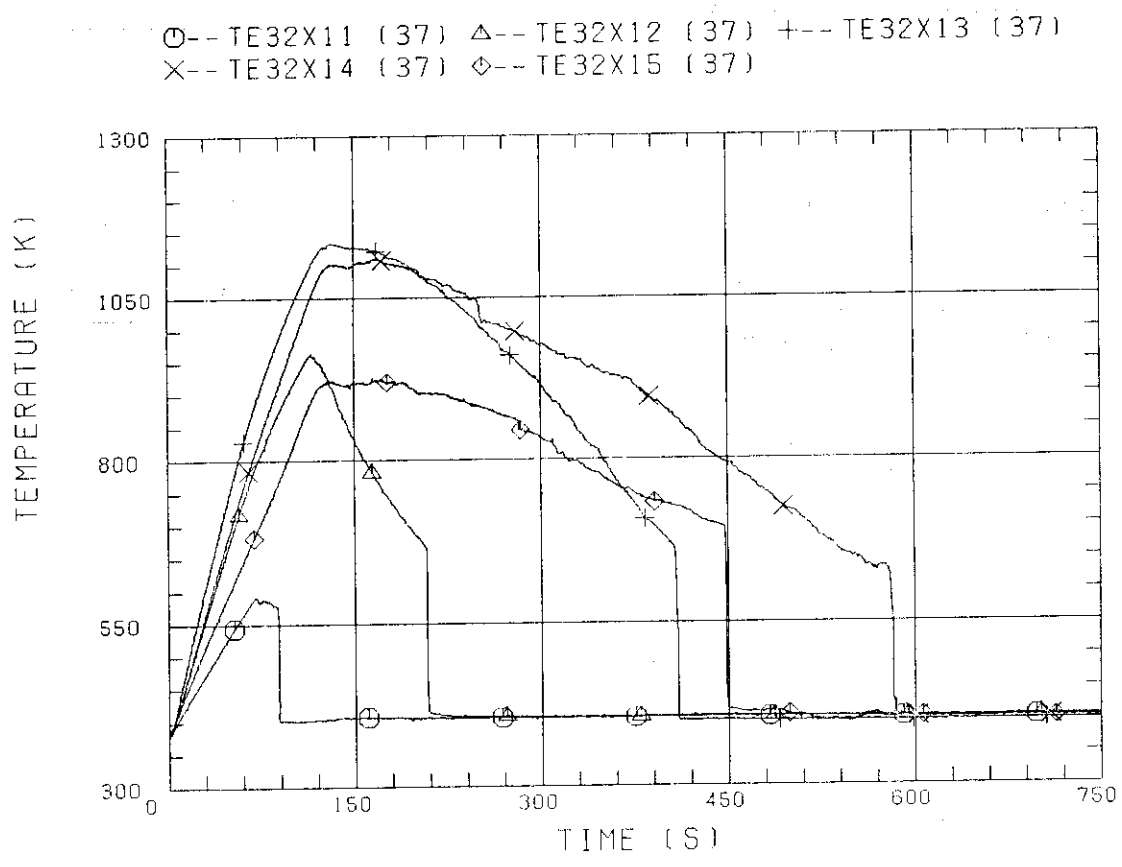

Fig. B-2 Surface temperature on high power rod (X-rod)in high power region (A region) (peak power rod)

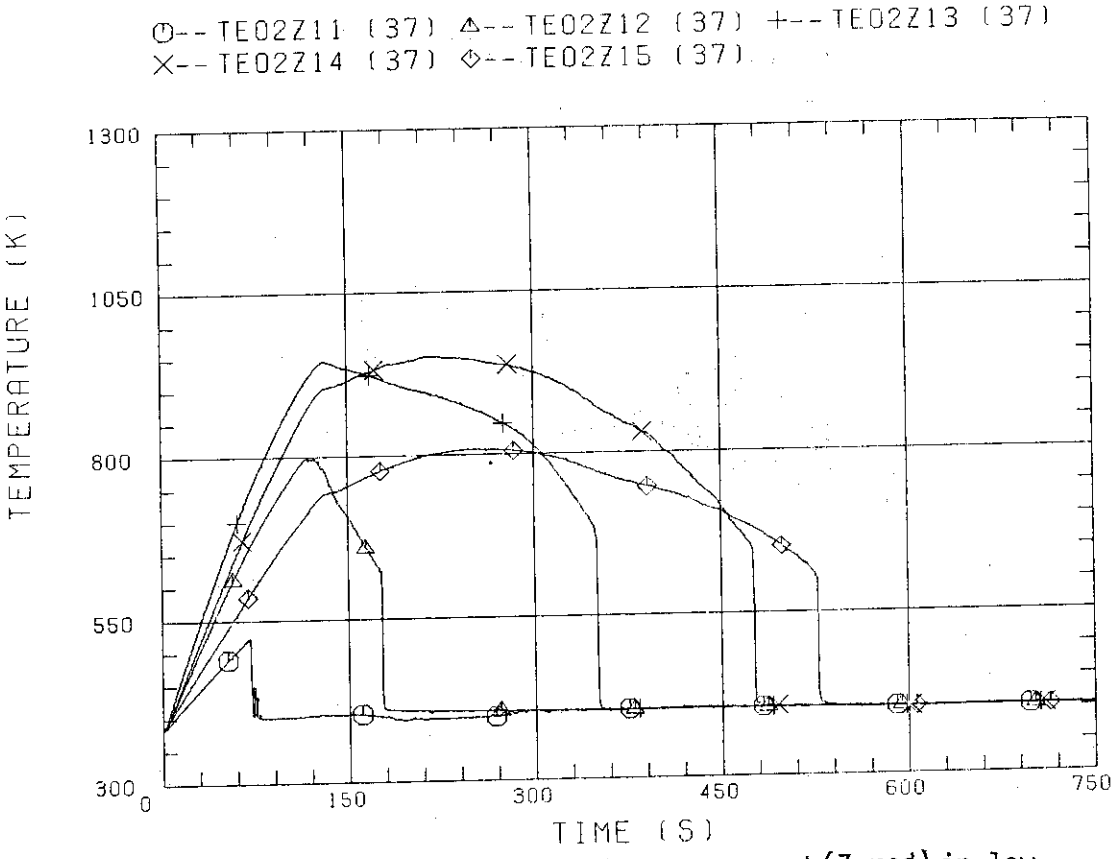

Fig. B-3 Surface temperature on low power rod (Z-rod) in low power region (C region) (lowest power rod)

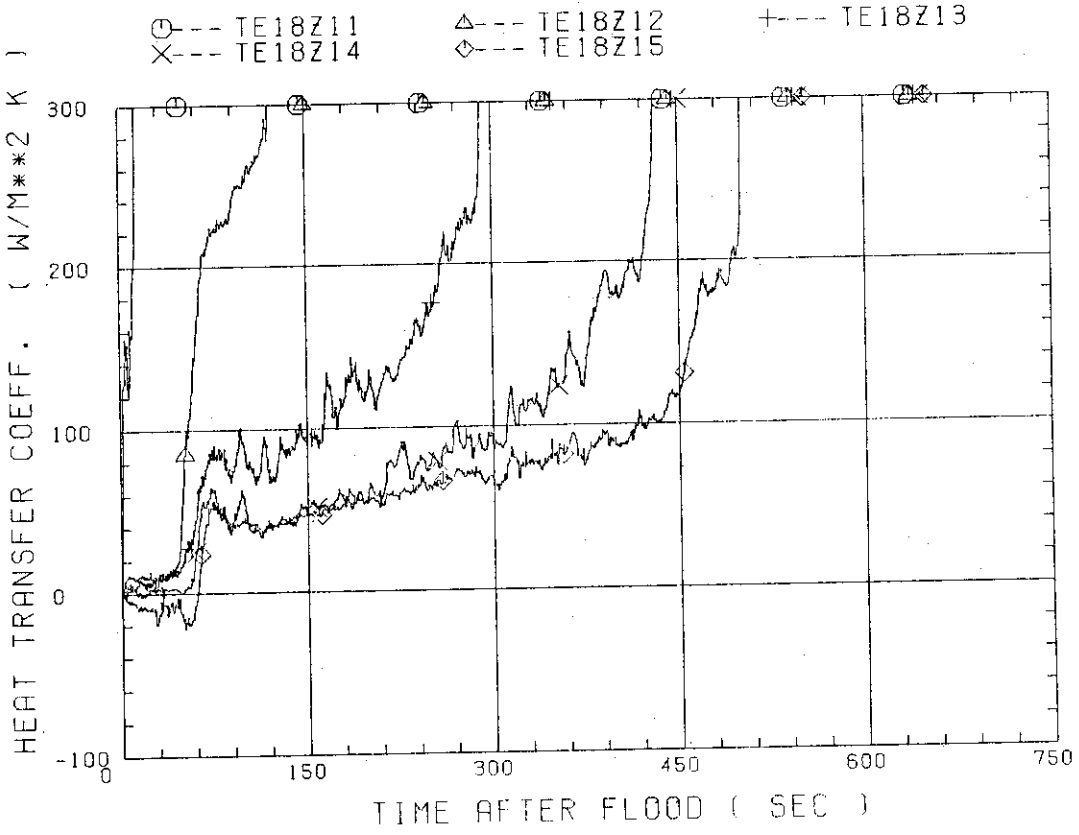

Fig. B-4 Heat transfer coefficient at midplane of low power rod (Z-rod) in medium power region (B region) (average power rod)

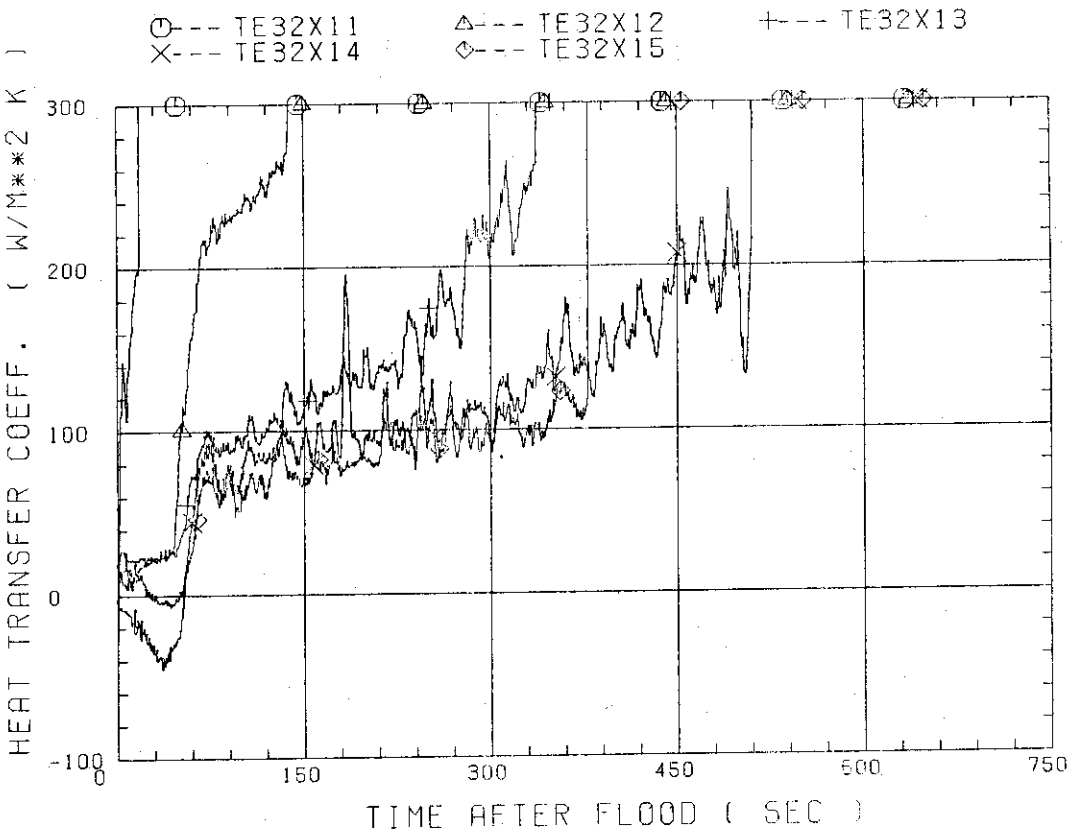

Fig. B-5 Heat transfer coefficient at midplane of high power rod (X-rod) in high power region (A region) (peak power rod)

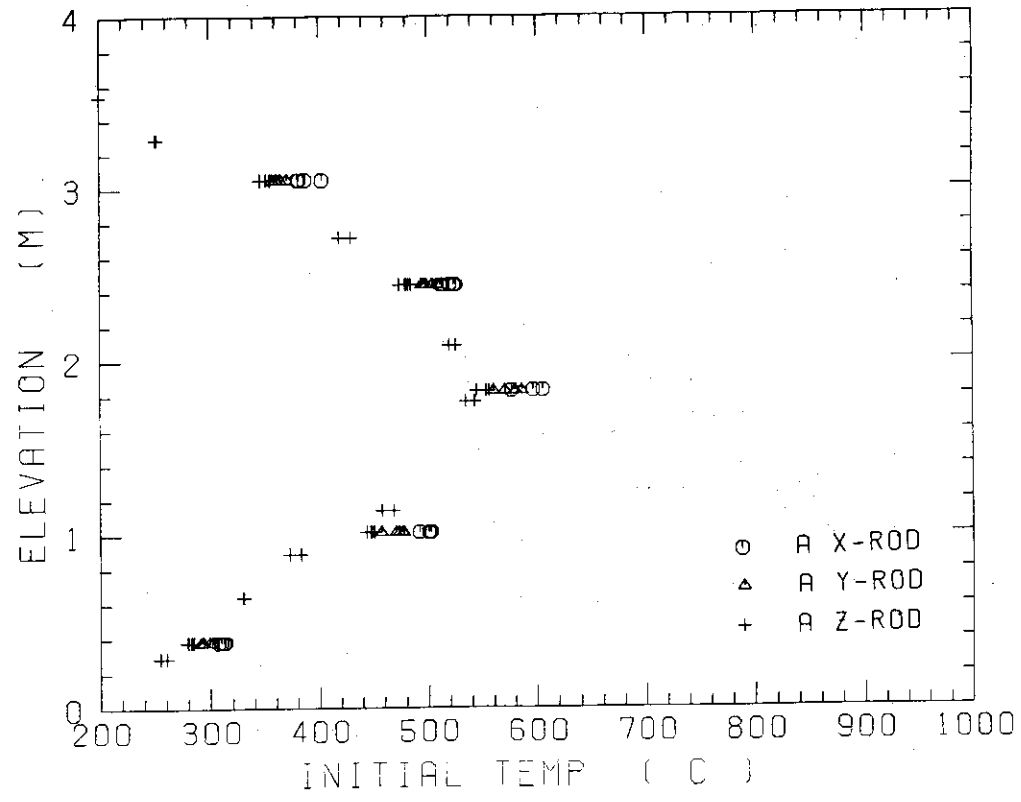

Fig. B-6 Initial rod surface temperature in high power region (A region)

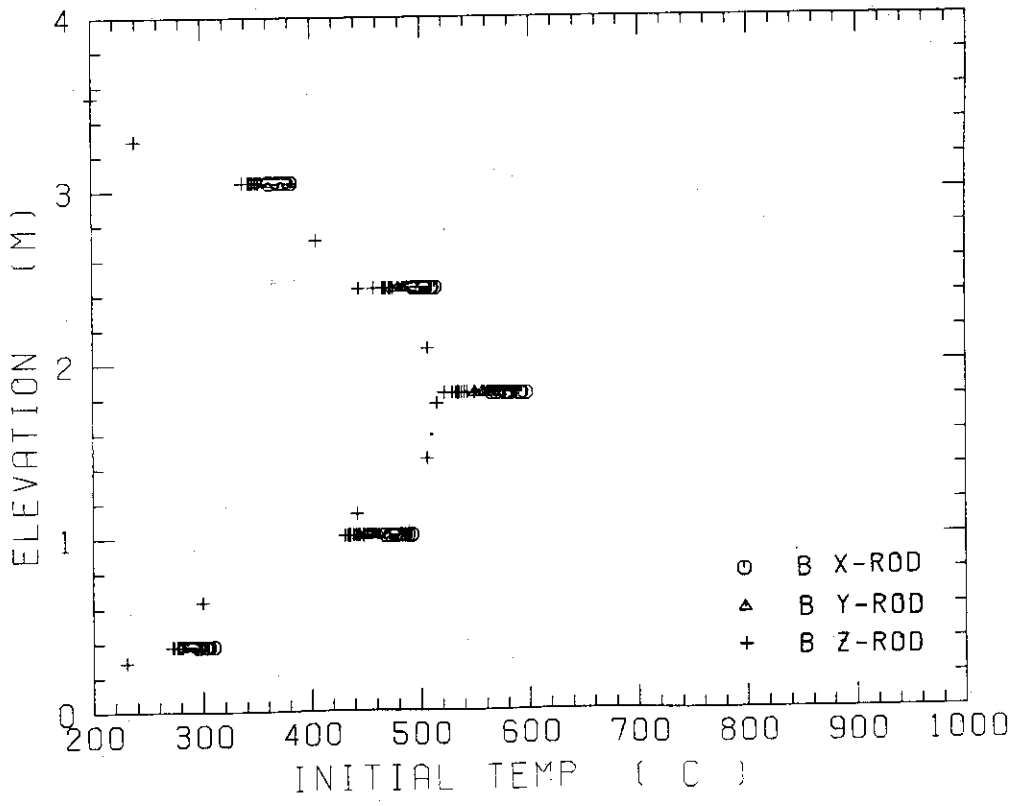

Fig. B-7 Initial rod surface temperature in medium power region (B region)

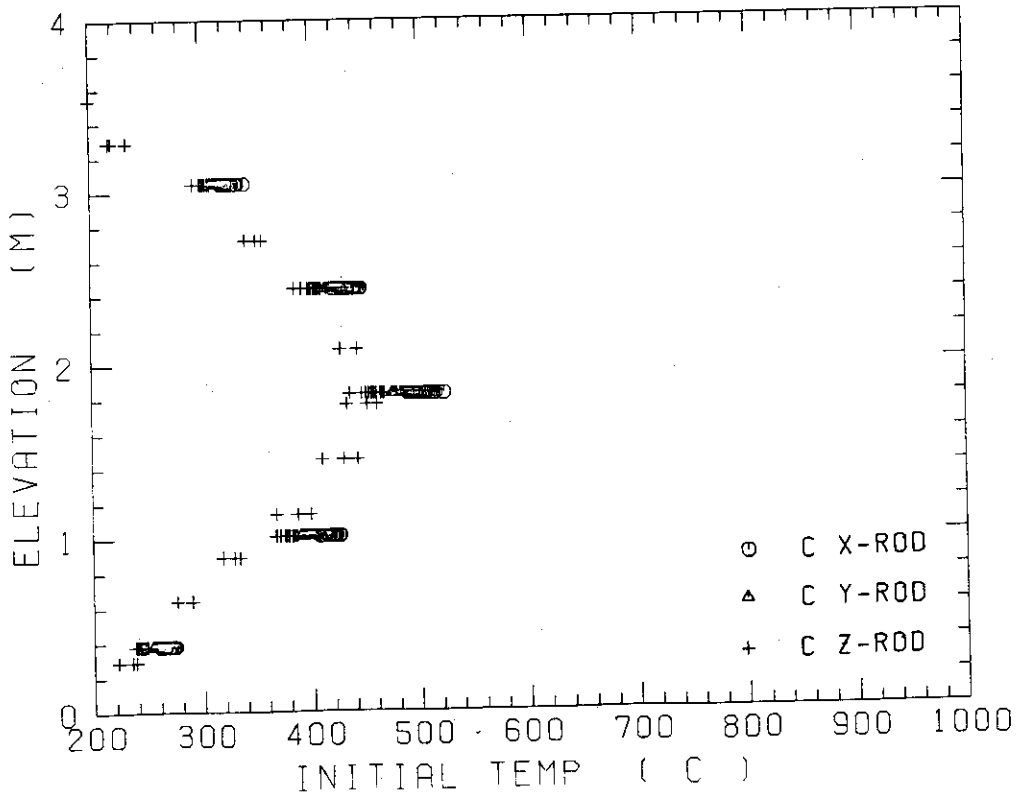

Fig. B-8 Initial rod surface temperature in low power region (C region)

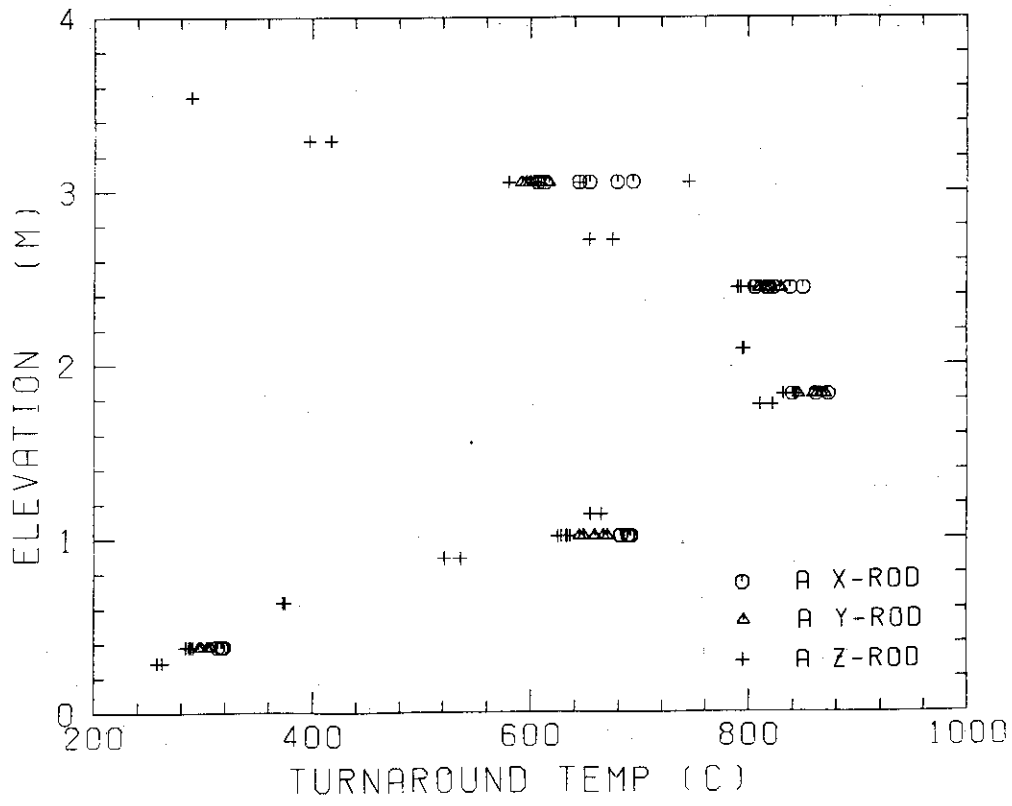

Fig. B-9 Turnaround temperature in high power region (A region)

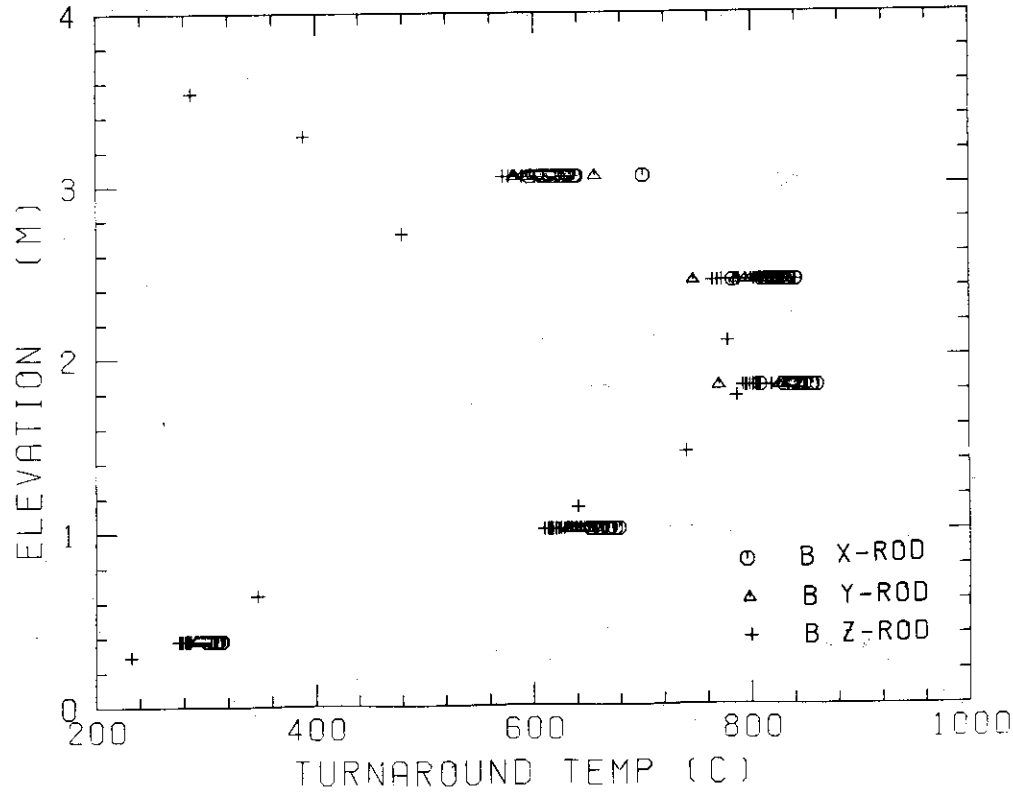

Fig. B-10 Turnaround temperature in medium power region (B region)

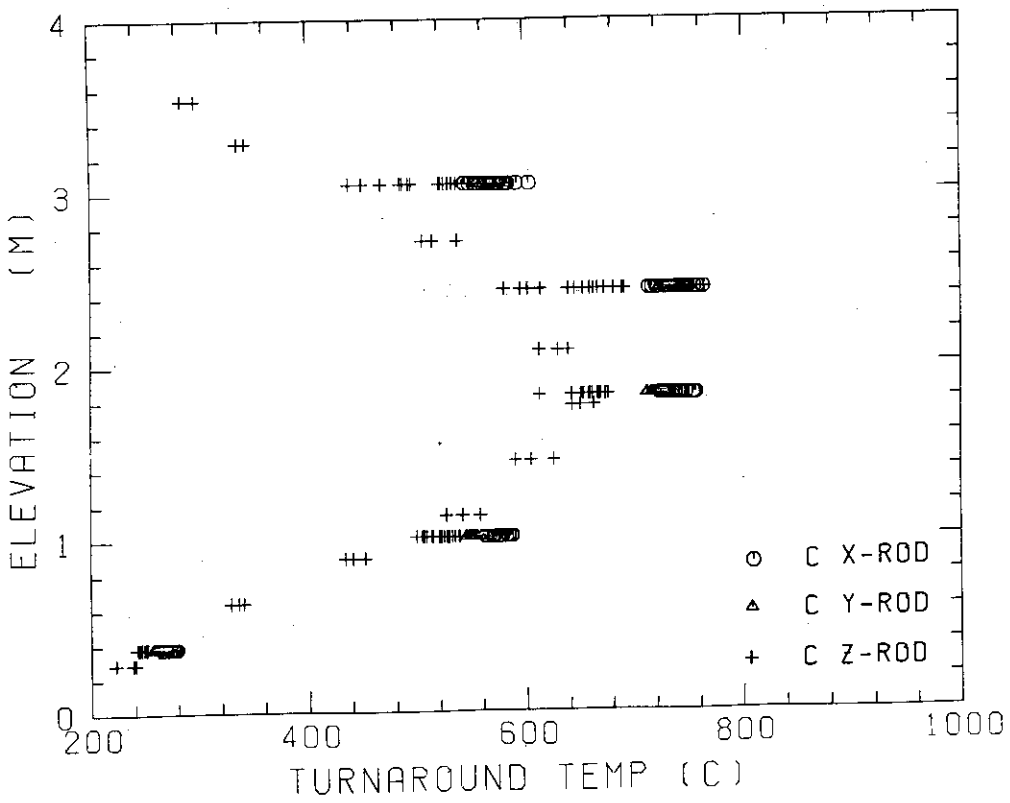

Fig. B-11 Turnaround temperature in low power region (C region)

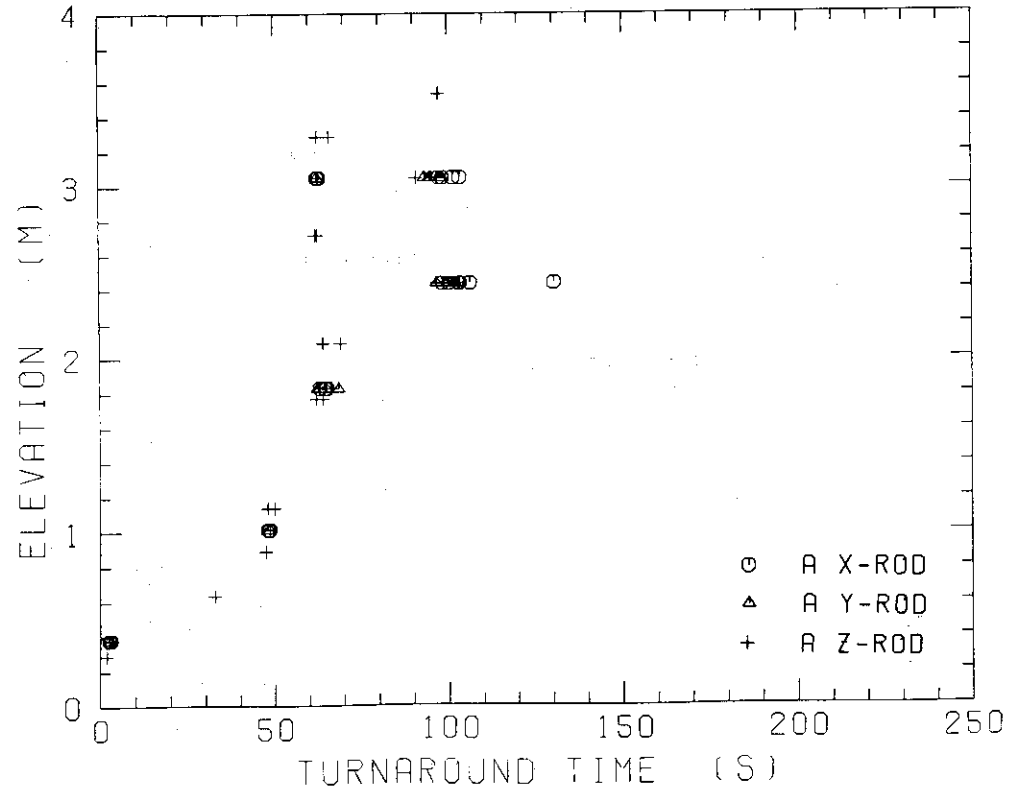

Fig. B-12 Turnaround time in high power region (A region)

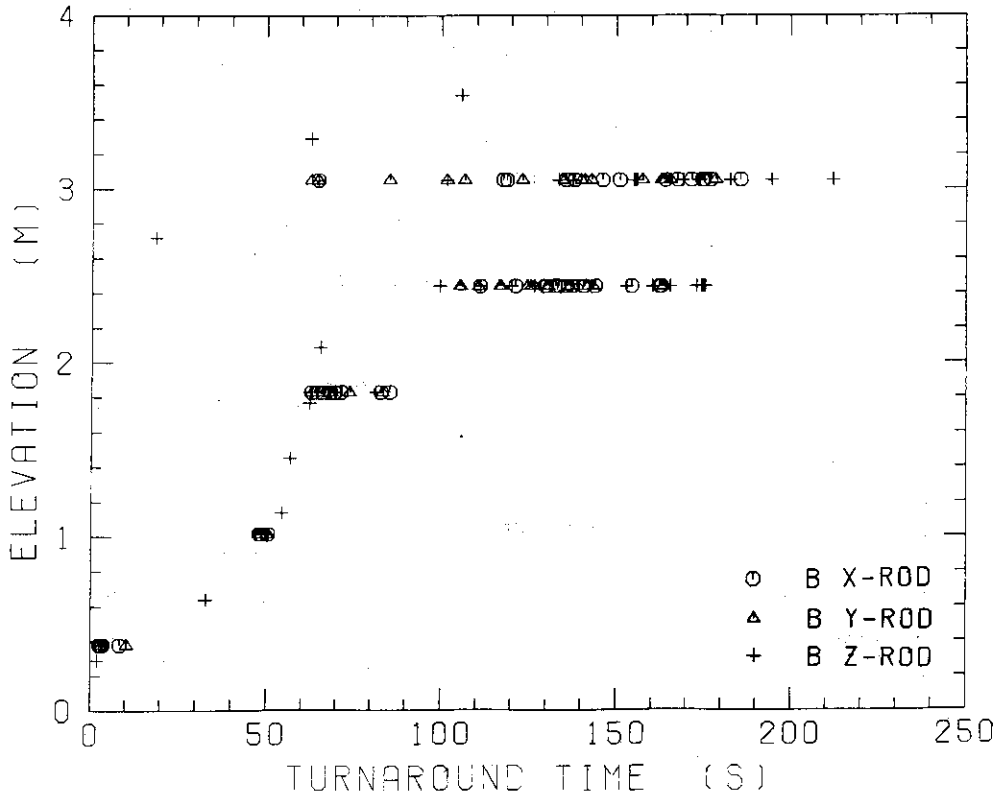

Fig. B-13 Turnaround time in medium power region (B region)

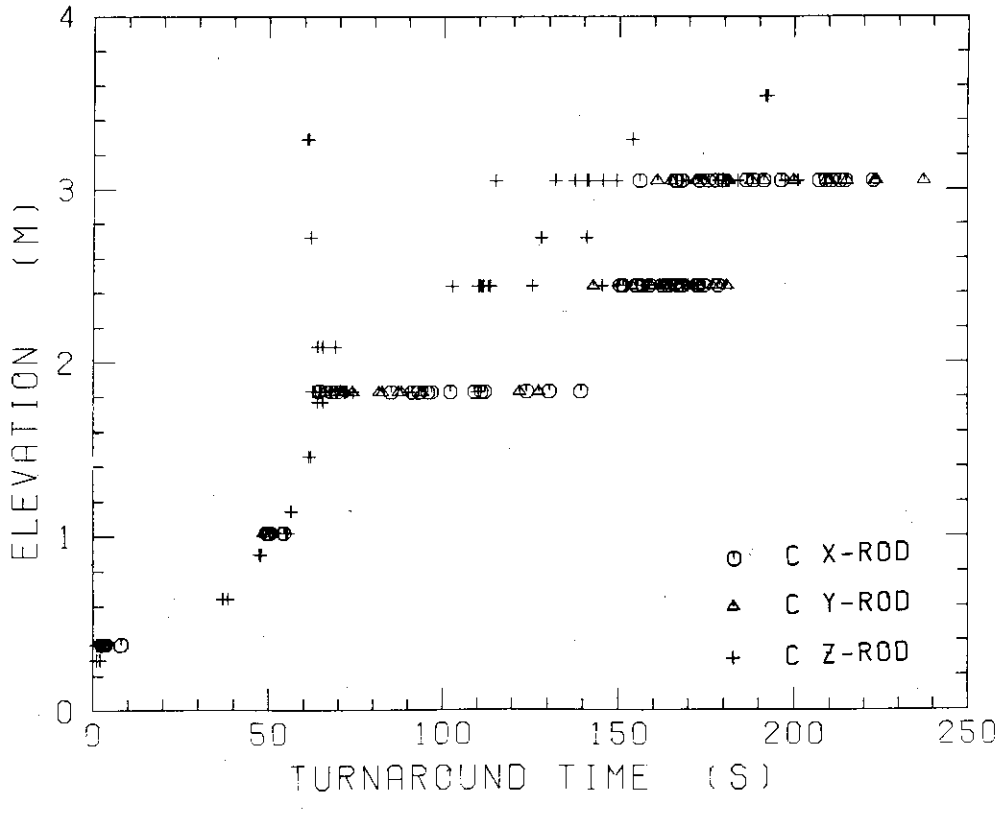

Fig. B-14 Turnaround time in low power region (C region)

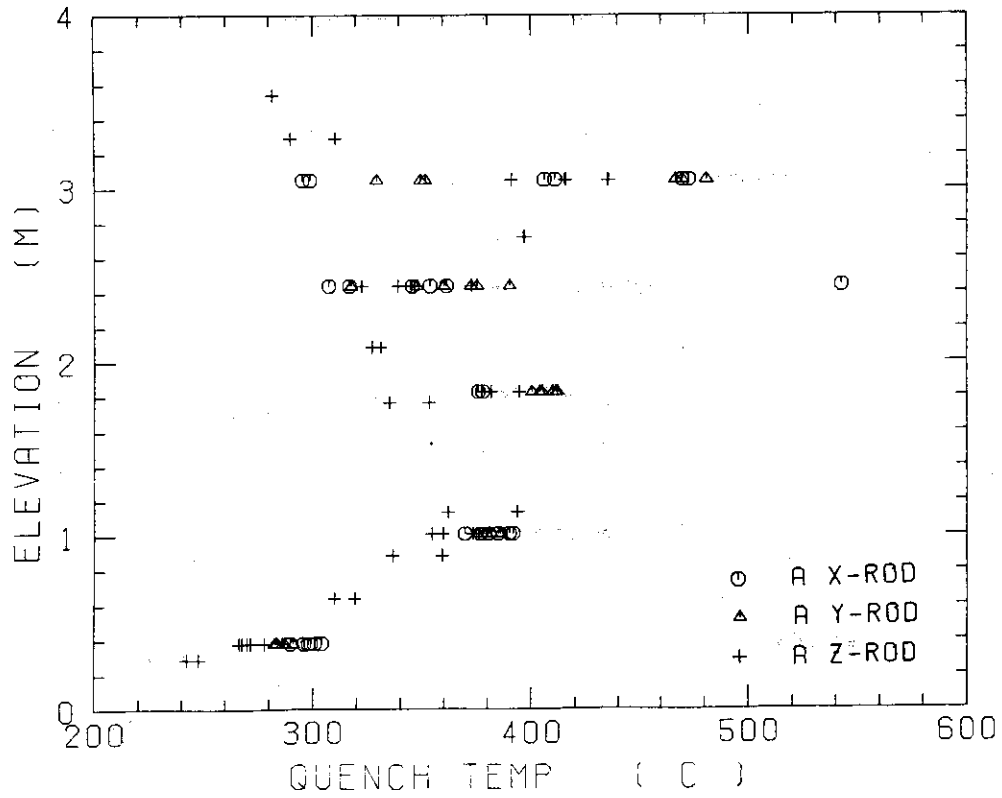

Fig. B-15 Quench temperature in high power region (A region)

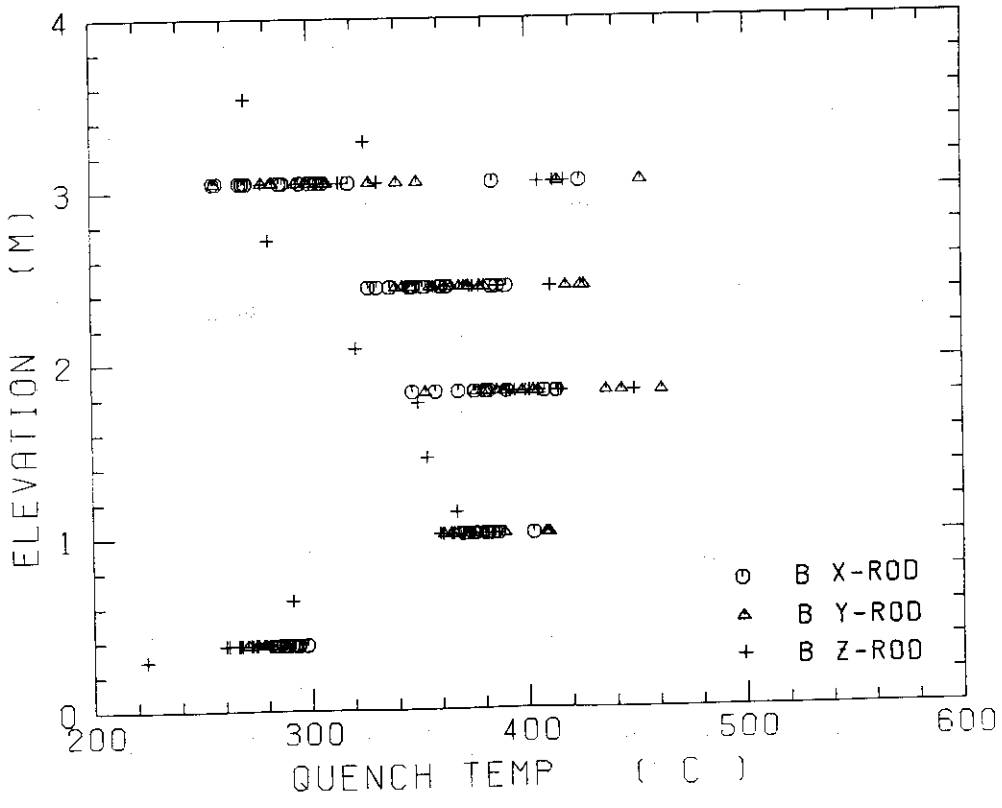

Fig. B-16 Quench temperature in medium power region (B region)

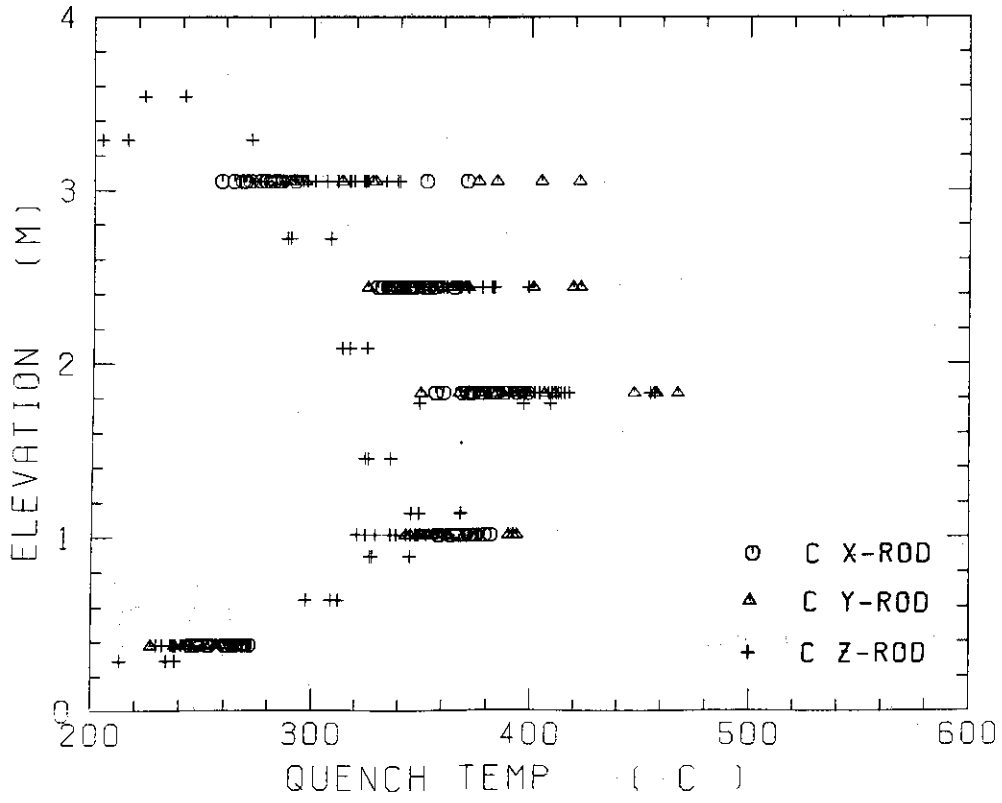

Fig. B-17 Quench temperature in low power region (C region)

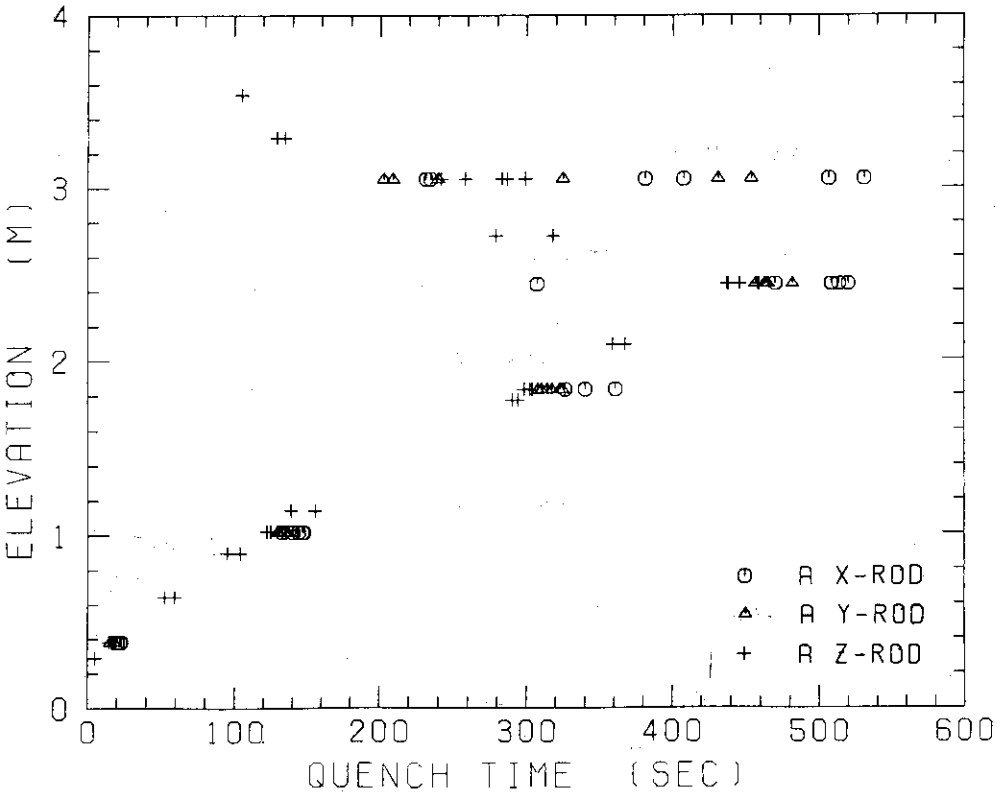

Fig. B-18 Quench time in high power region (A region)

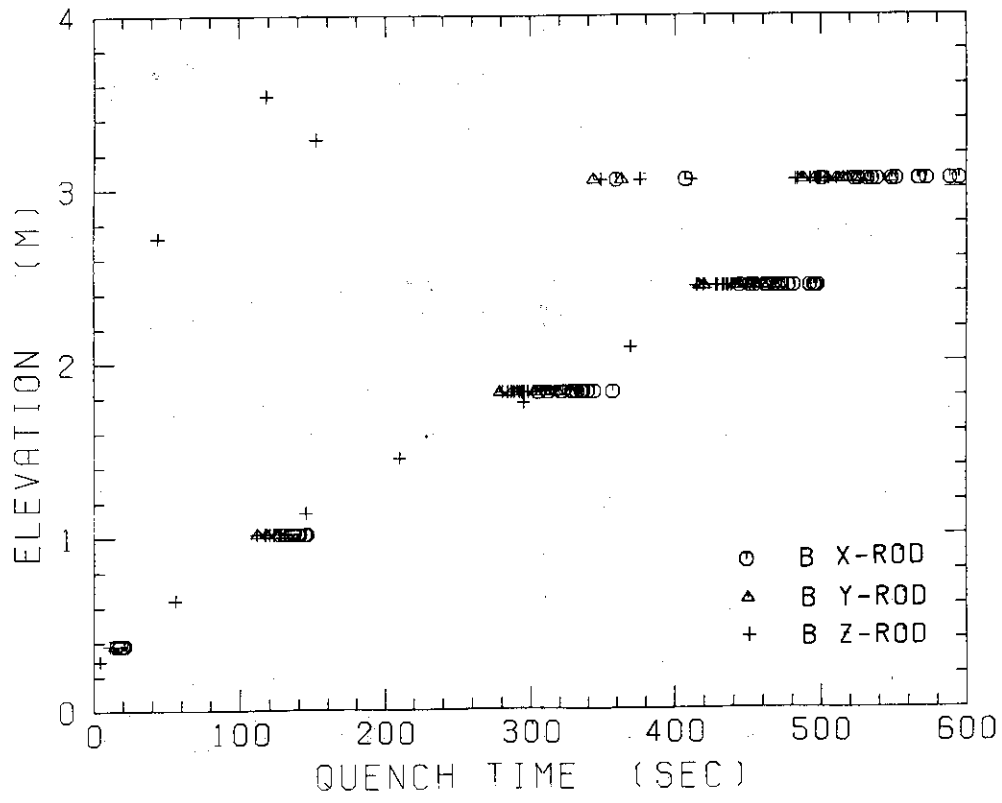

Fig. B-19 Quench time in medium power region (B region)

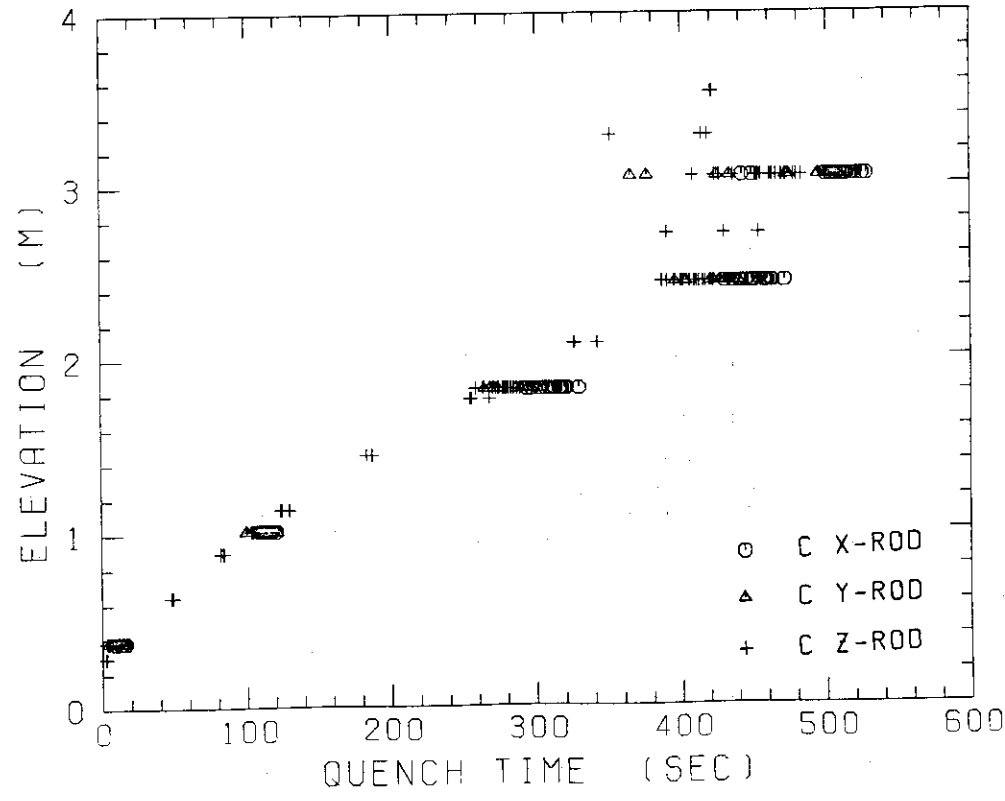

Fig. B-20 Quench time in low power region (C region)

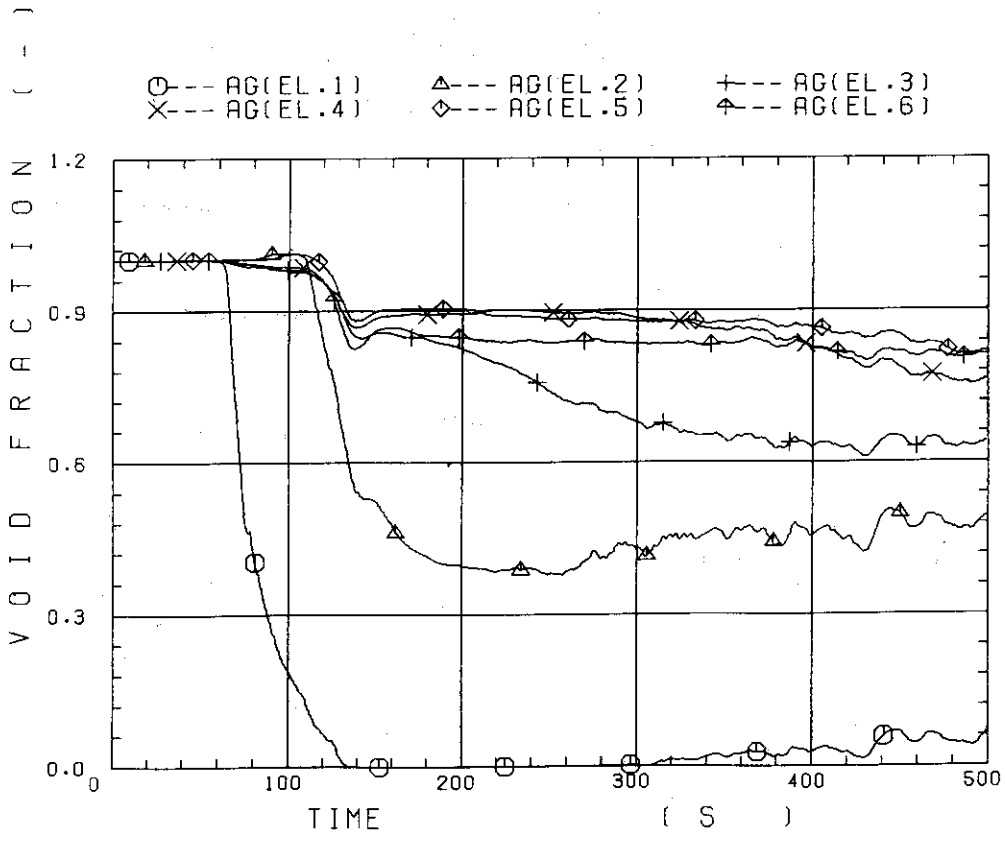

Fig. B-21 Void fraction in core

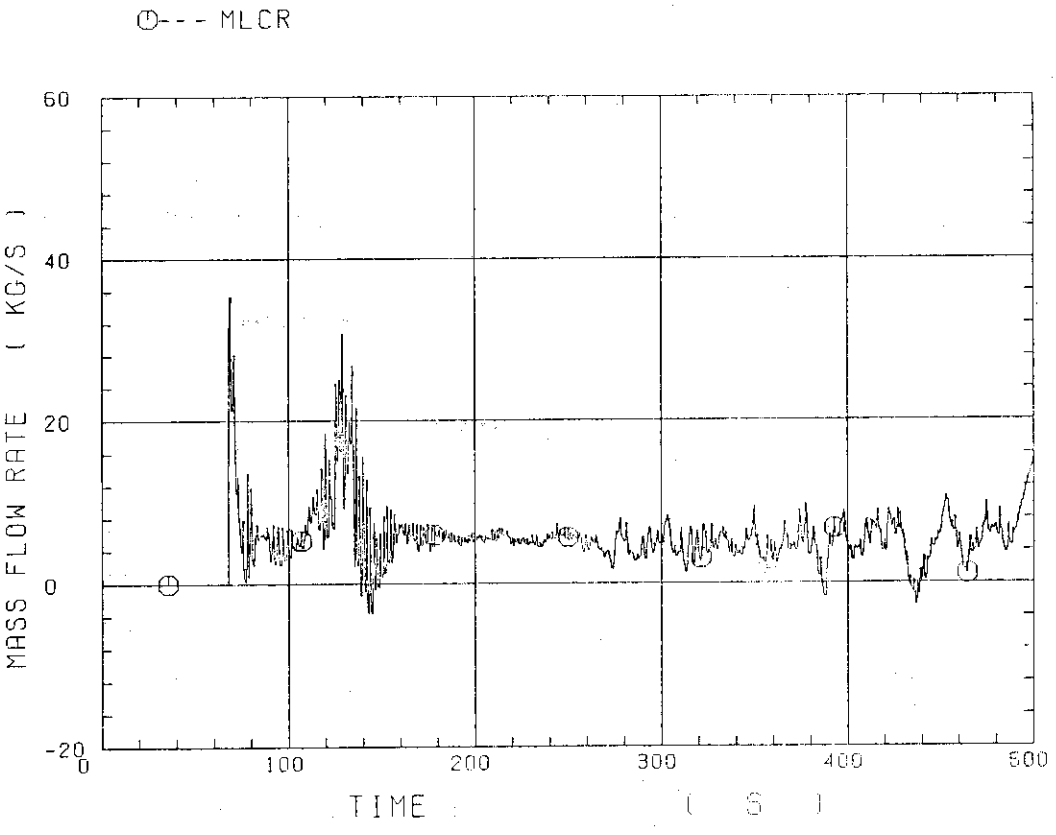

Fig. B-22 Evaluated core inlet mass flow rate

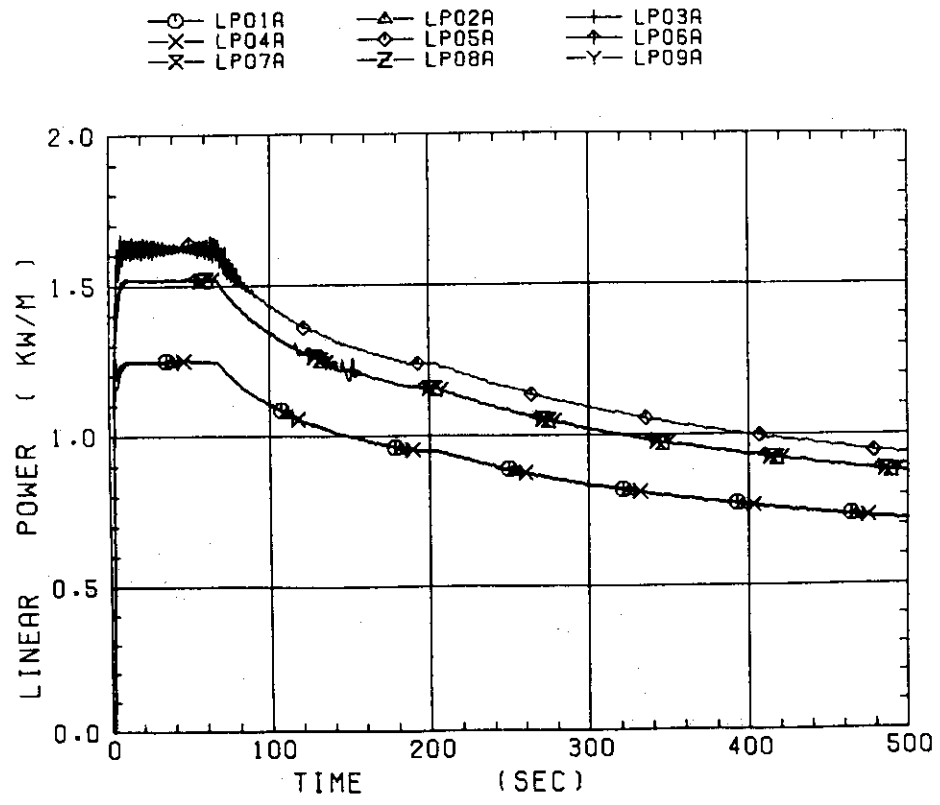

Fig. B-23 Average linear power of heater rod in each power unit zone

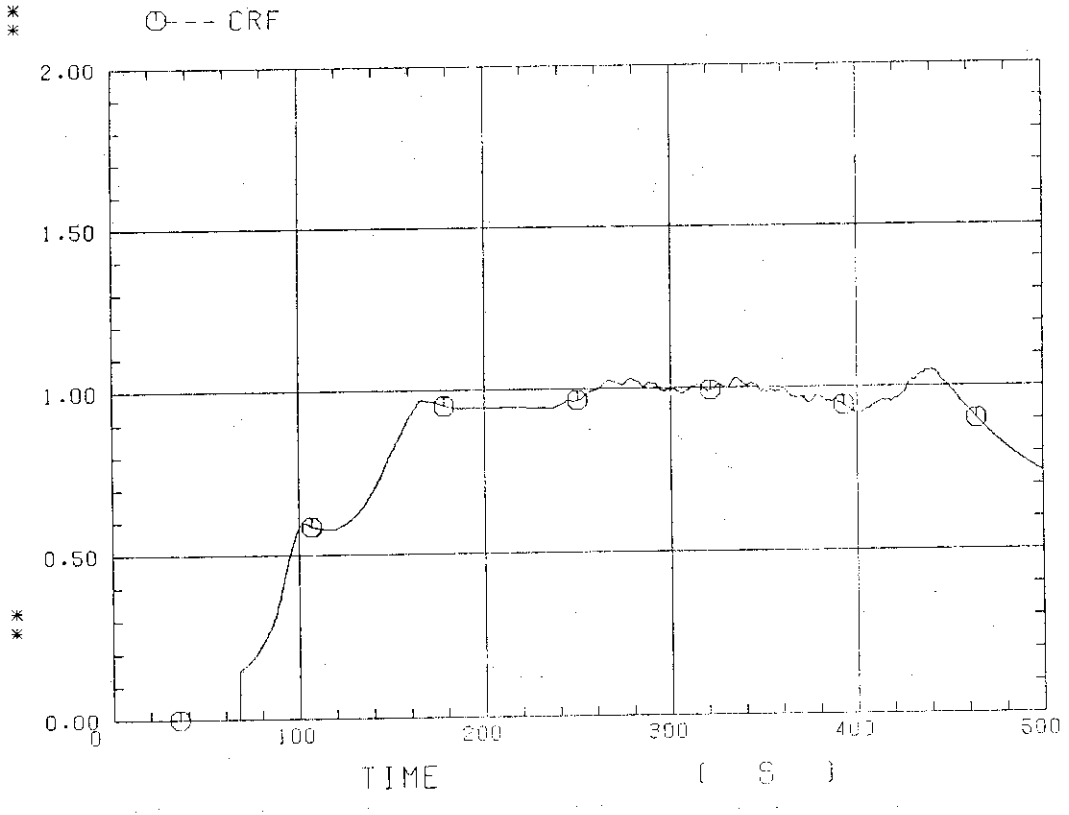

Fig. B-24 Carry-over rate fraction

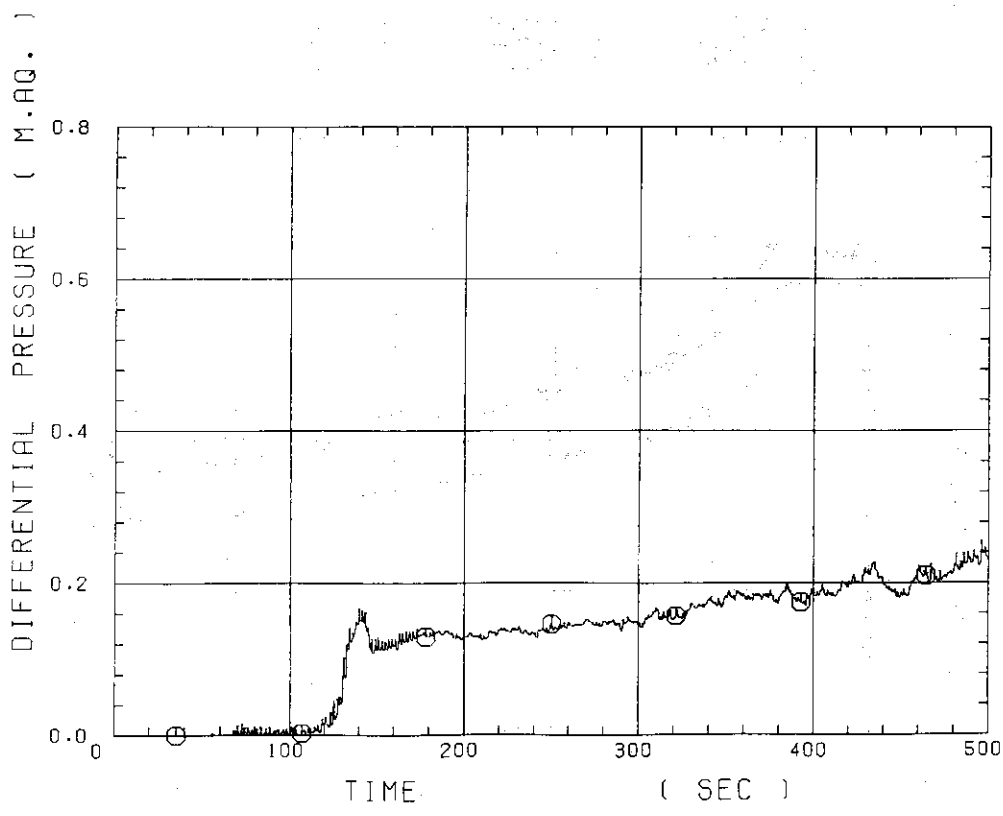

Fig. B-25 Differential pressure through upper plenum

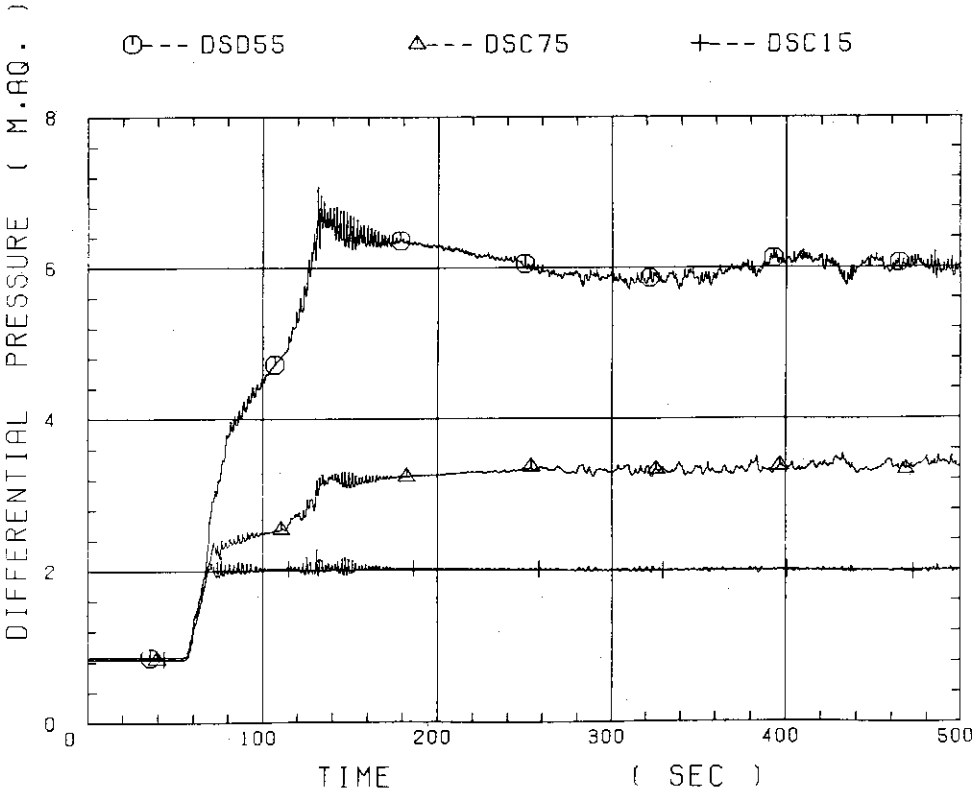

Fig. B-26 Differential pressure through downcomer, core, and lower plenum

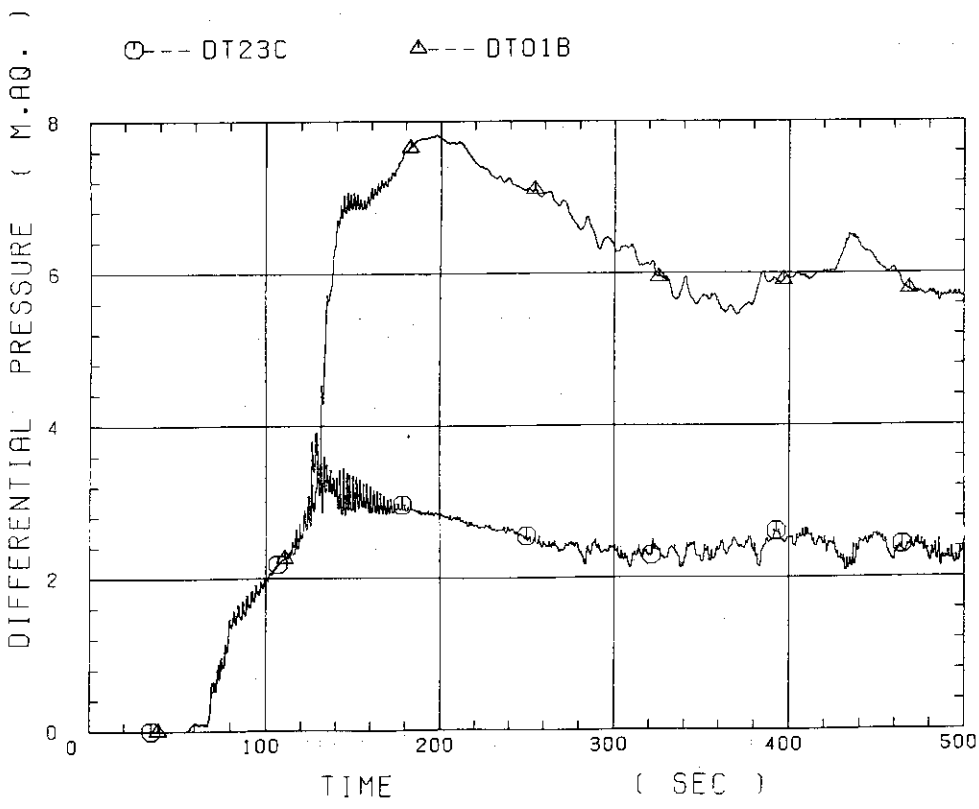

Fig. B-27 Differential pressure through intact and broken loops

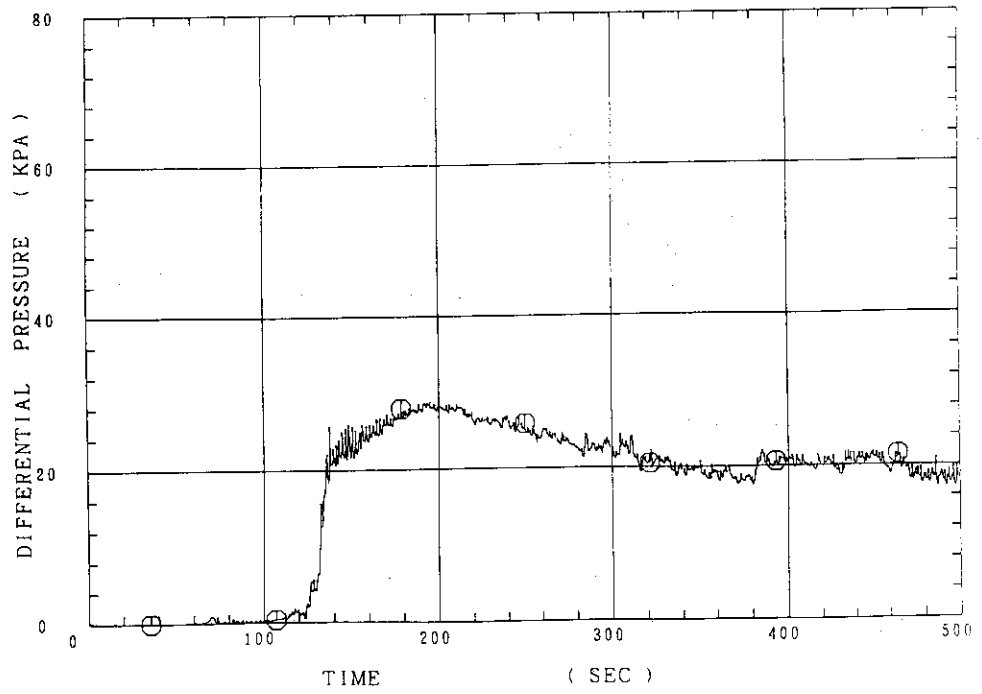

Fig. B-28 Differential pressure through broken cold leg nozzle

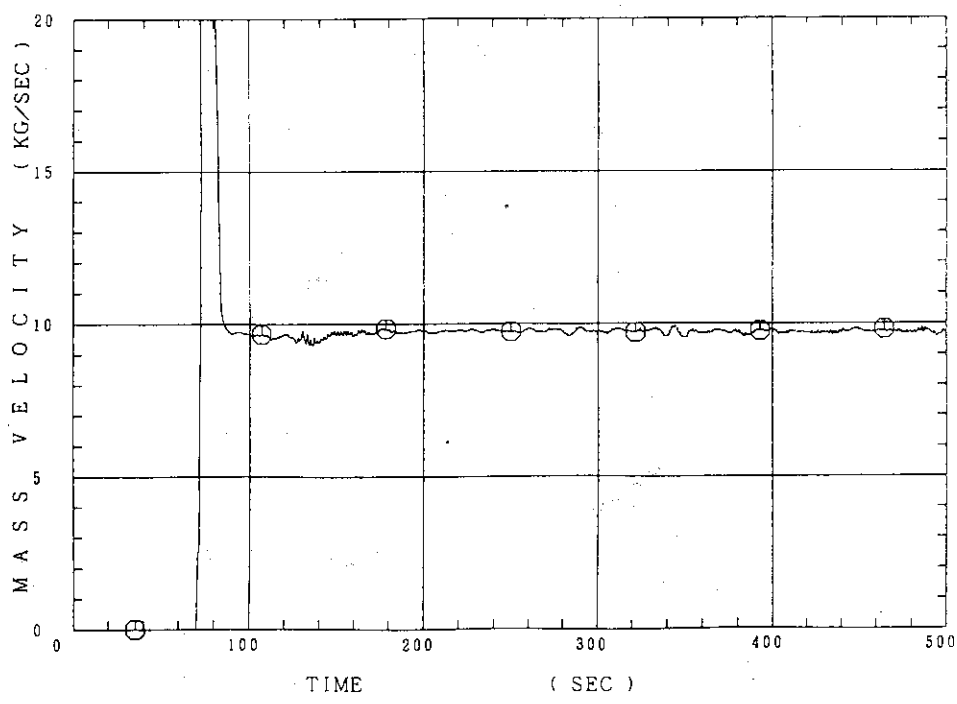

Fig. B-29 Total water mass flow rate from intact loops to downcomer

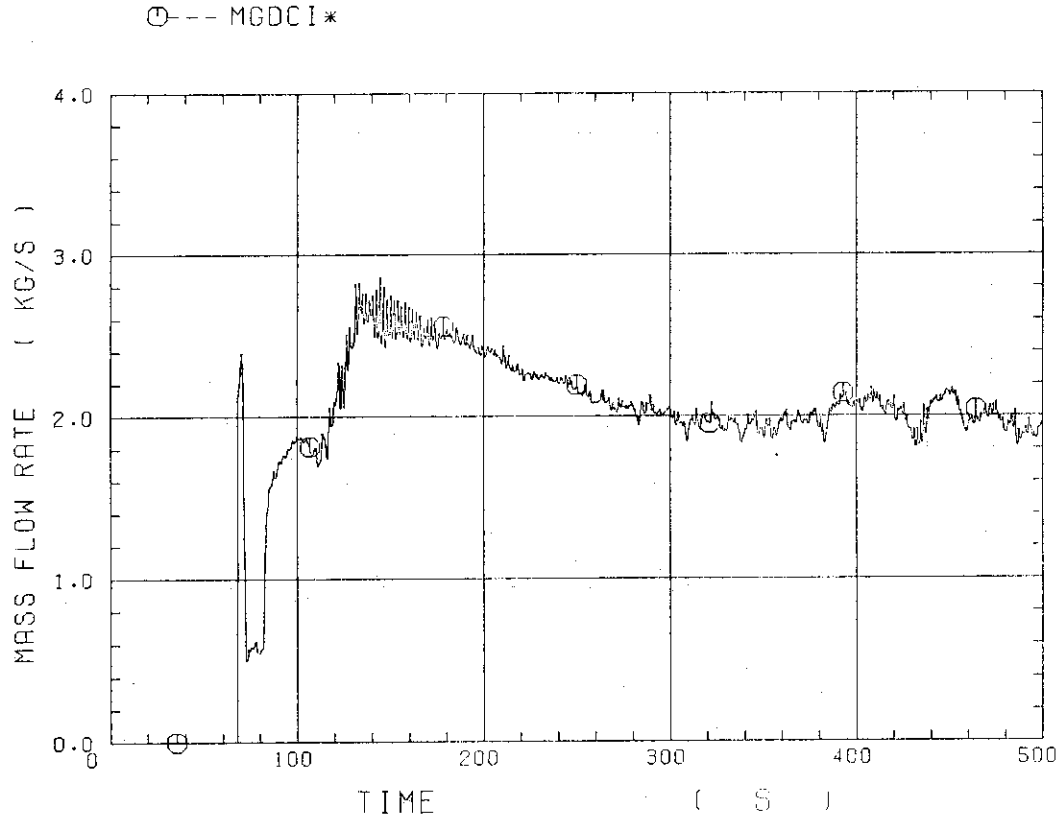

Fig. B-30 Total steam mass flow rate from intact loops to downcomer

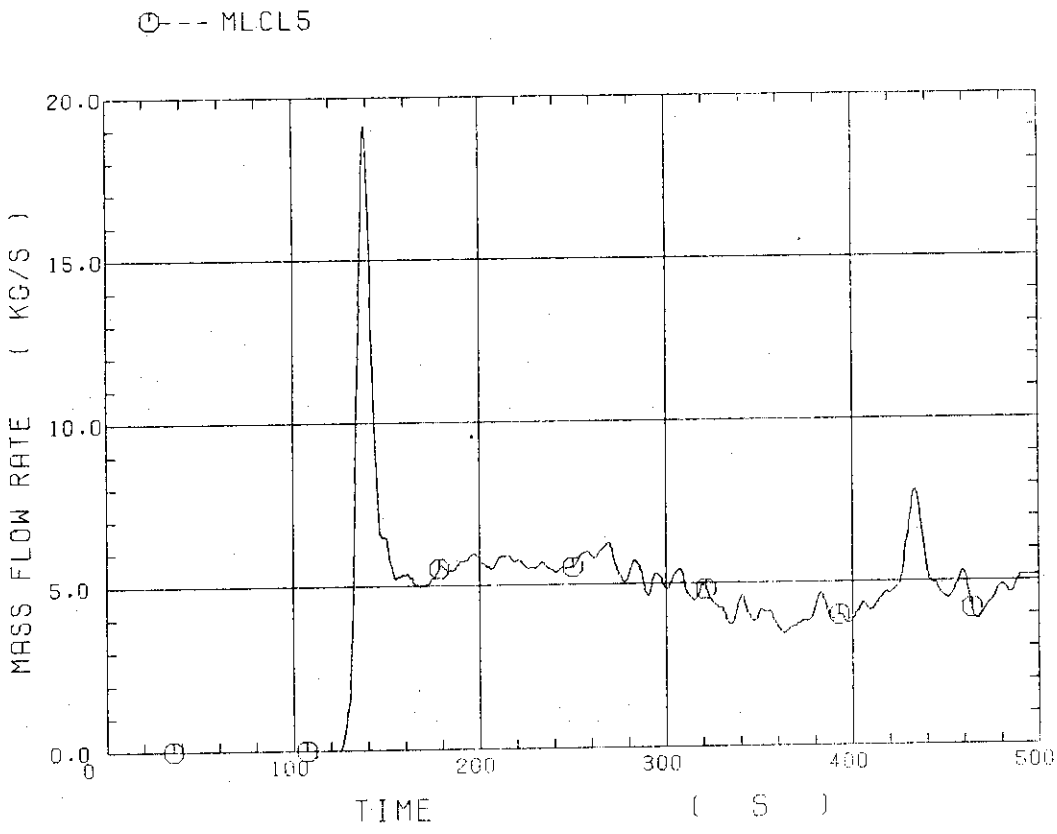

Fig. B-31 Water mass flow rate through broken cold leg nozzle

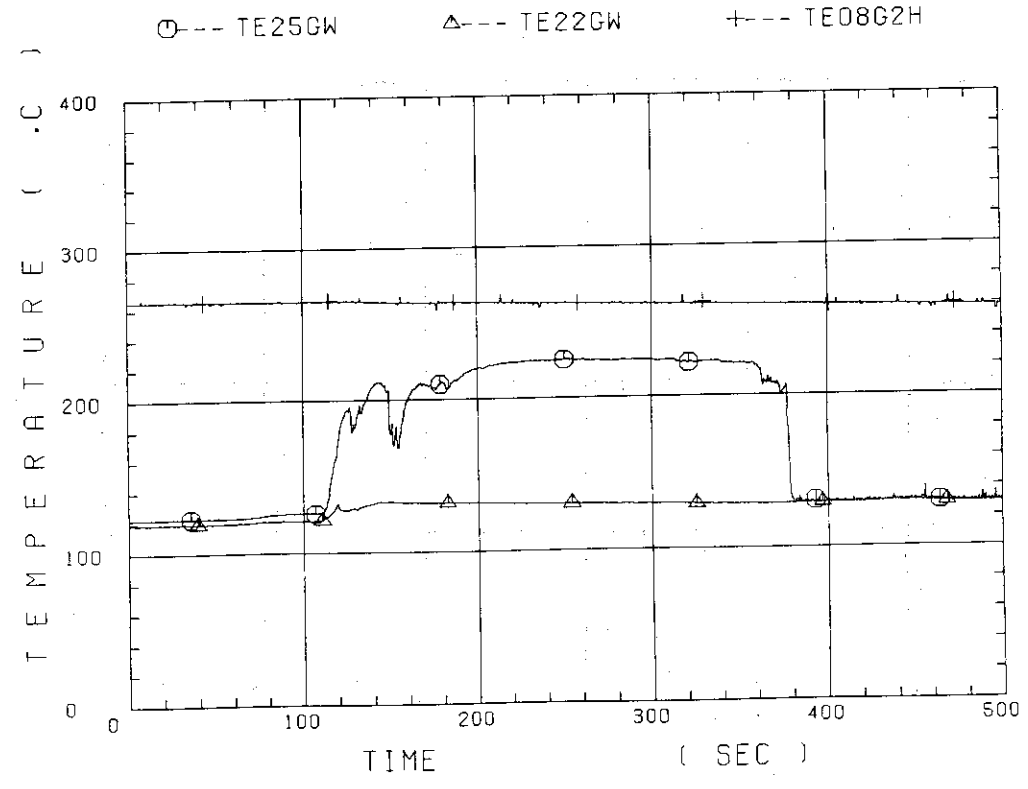

Fig. B-32 Fluid temperature in inlet plenum, outlet plenum, and secondary of steam generator 1

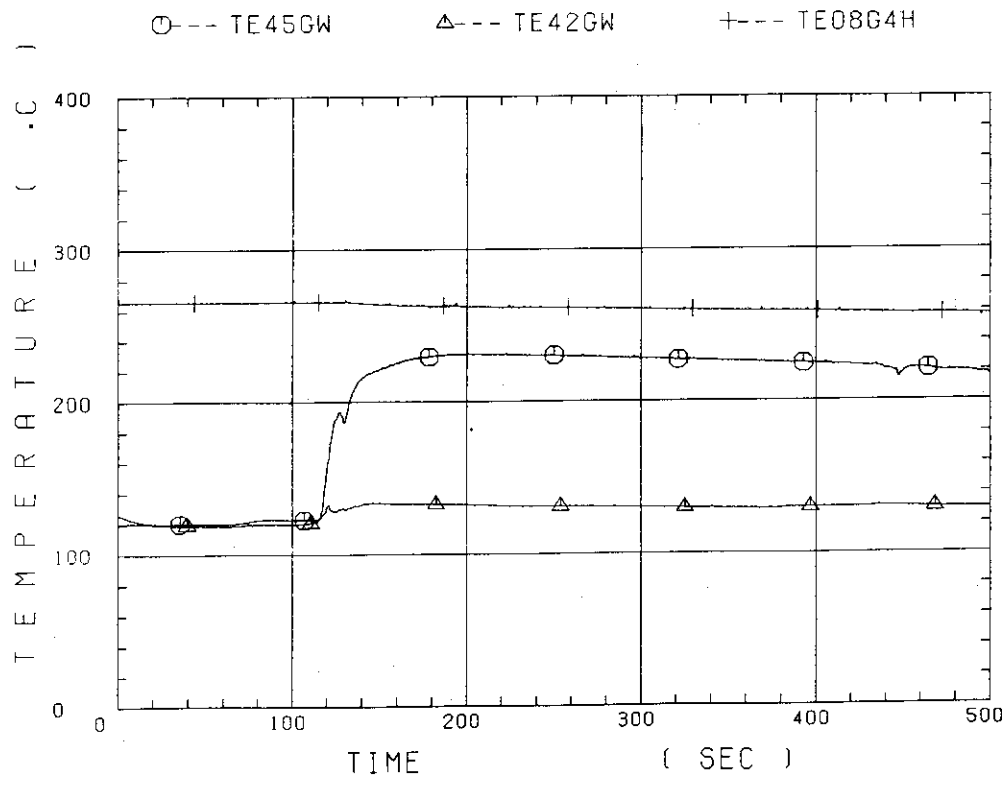

Fig. B-33 Fluid temperature in inlet plenum, output plenum, and secondary of steam generator 2

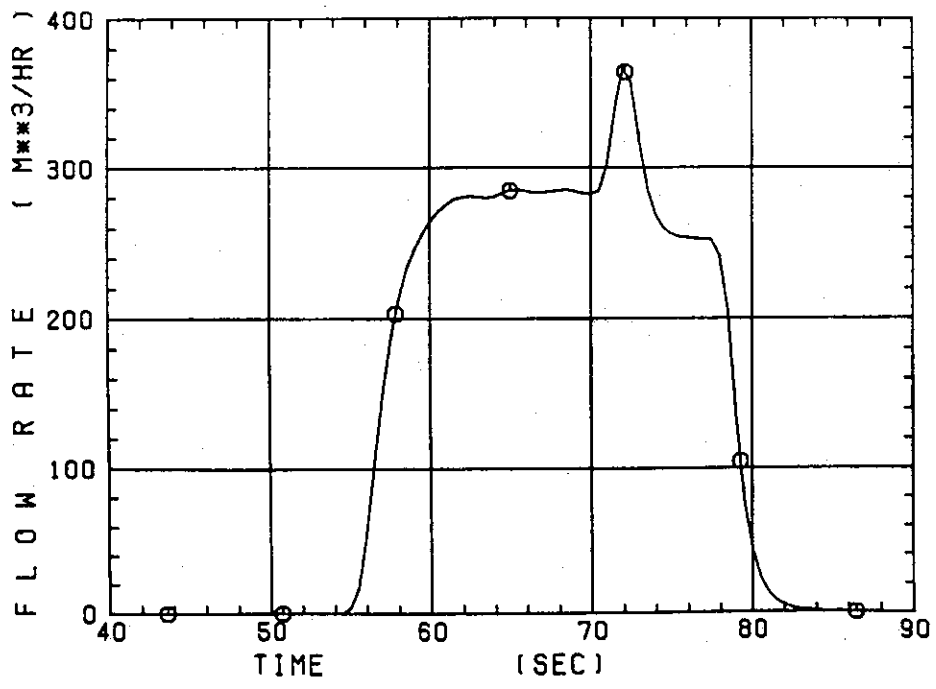

Fig. B-34 Total accumulator injection rate

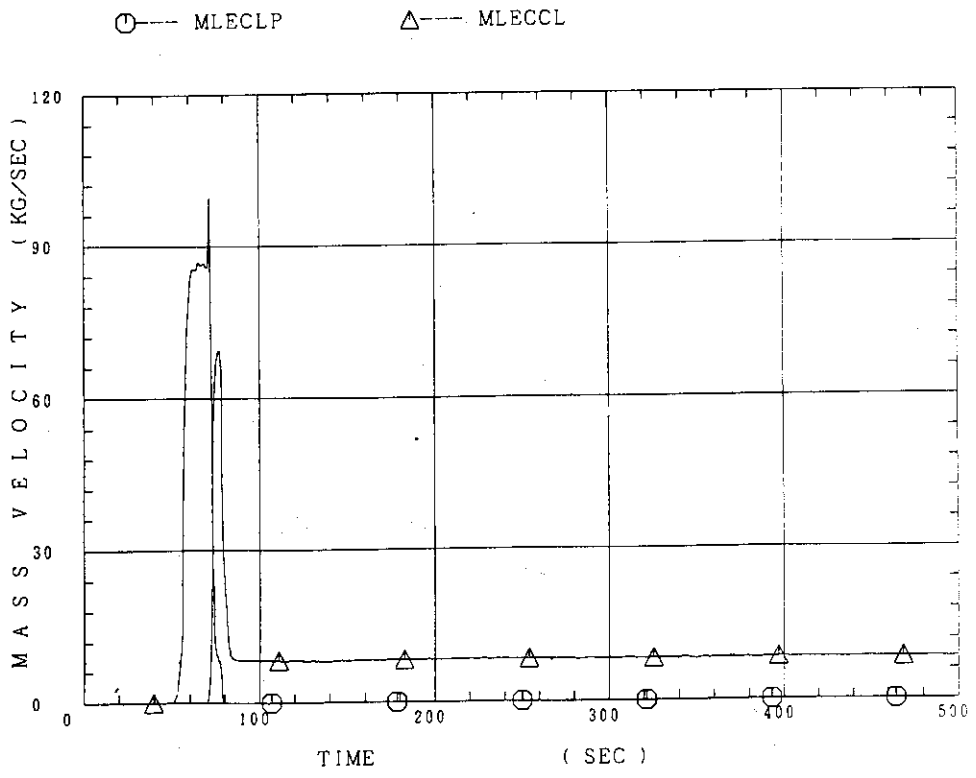

Fig. B-35 ECC water injection rates to lower plenum and to cold legs

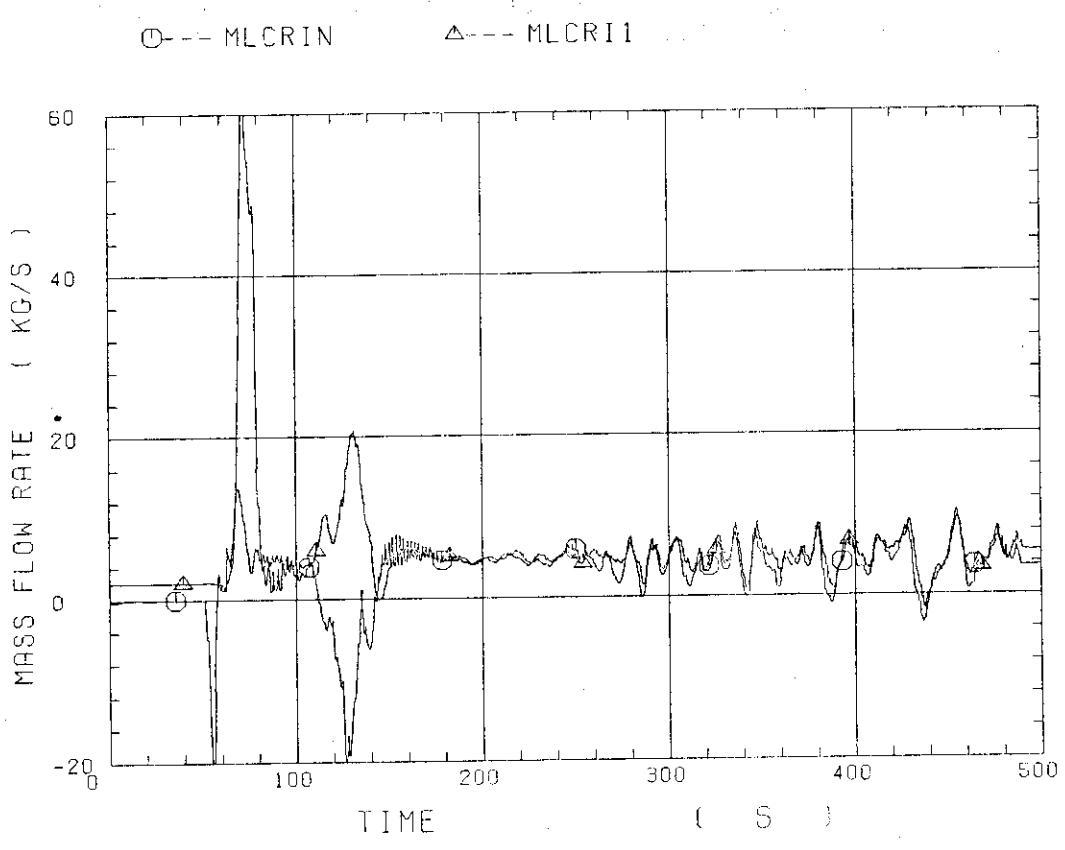

Fig. B-36 Core inlet mass flow rates estimated by mass balance downstream and upstread of core inlet

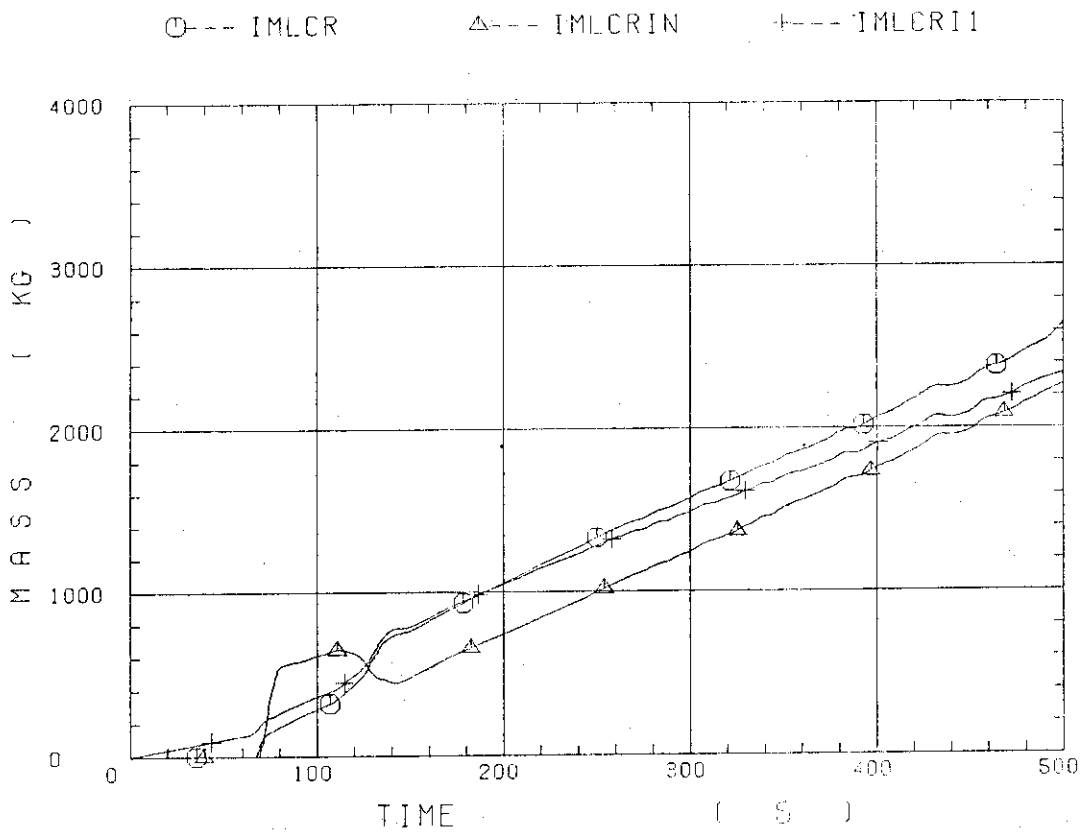

Fig. B-37 Comparison of injected mass into core among two estimation methods and evaluated mass

Appendix C

Main results of Test C1-8 (Run 17)

Table and Figure List

Table C-1 Summary of test conditions

1. TEST TYPE : LOOP SEAL WATER FILLING TEST
2. TEST NUMBER : RUN 017 3. DATE : Nov.29, 1979
4. POWER : A: TOTAL: 9.37 MW; B:LINEAR: 1.4 KW/M
5. RELATIVE RADIAL POWER SHAPE :

   A: ZONE: A B C

   B: RATIO: 1.07 : 1.0 : 0.82
6. AXIAL POWER SHAPE : CHOPPED COSINE
7. PRESSURE (KG/CM^2A) :

   A: SYSTEM: 2.08, B: CONTAINMENT 2.09,

   C: STEAM GENERATOR SECONDARY: 51
8. TEMPERATURE (DEG.C) :

   A: DOWNCOMER WALL 183, B: VESSEL INTERNALS 110,

   C: PRIMARY PIPING WALL 120, D: LOWER PELNUM LIQUID 111,

   E: ECC LIQUID 37, F: STEAM GENERATOR SECONDARY 264,

   G: CORE TEMPERATURE AT ECC INITIATION 516
9. ECC INJECTION TYPE: C

   A: COLD LEG, B: LOWER PLENUM, C: LOWER PLENUM + COLD LEG
10. PUMP K-FACTOR : ∿15
11. ECC FLOW RATES AND DURATION :

    A: ACCUMULATOR 279 M^3/HR FROM 0 TO 24 SECONDS

    B: LPCI 30.9 M^3/HR FROM 24 TO 355 SECONDS

    C: ECC INJECTION TO LOWER PLENUM : FROM 0 TO 17.5 SECONDS

    (VALVE OPENING AND CLOSING TIMES ARE INCLUDED IN THE INJECTION DURATION)
12. INITIAL WATER LEVEL IN LOWER PLENUM : 0.87 M.
13. POWER CONTROL : ANS x 1.2 + ACTINIDE (30 SEC AFTER SCRAM)
14. EXPECTED BOCREC TIME FROM ECC INITIATION 12 SEC
15. EXPECTED PEAK TEMPERATURE AT BOCREC 600 C

Table C-2 Chronology of events

EVENT	TIME (sec)
Test Initiated (Heater Rods Power on) (Data Recording Initiated)	0.0
Accumulator Injection Initiated	53
Power Decay Initiated (Bottom of Core Recovery)	65
Accumulator Injection Switched from Lower Plenum to Cold Leg	70.5
Accumulator Injection Ended and LPCI Injection Initiated	77
Power zone M5 reduced 20%	129.5
Power off	134
All heater rods quenched	287
LPCI injection ended	408
Test C1-8 ended (Data recording ended)	500

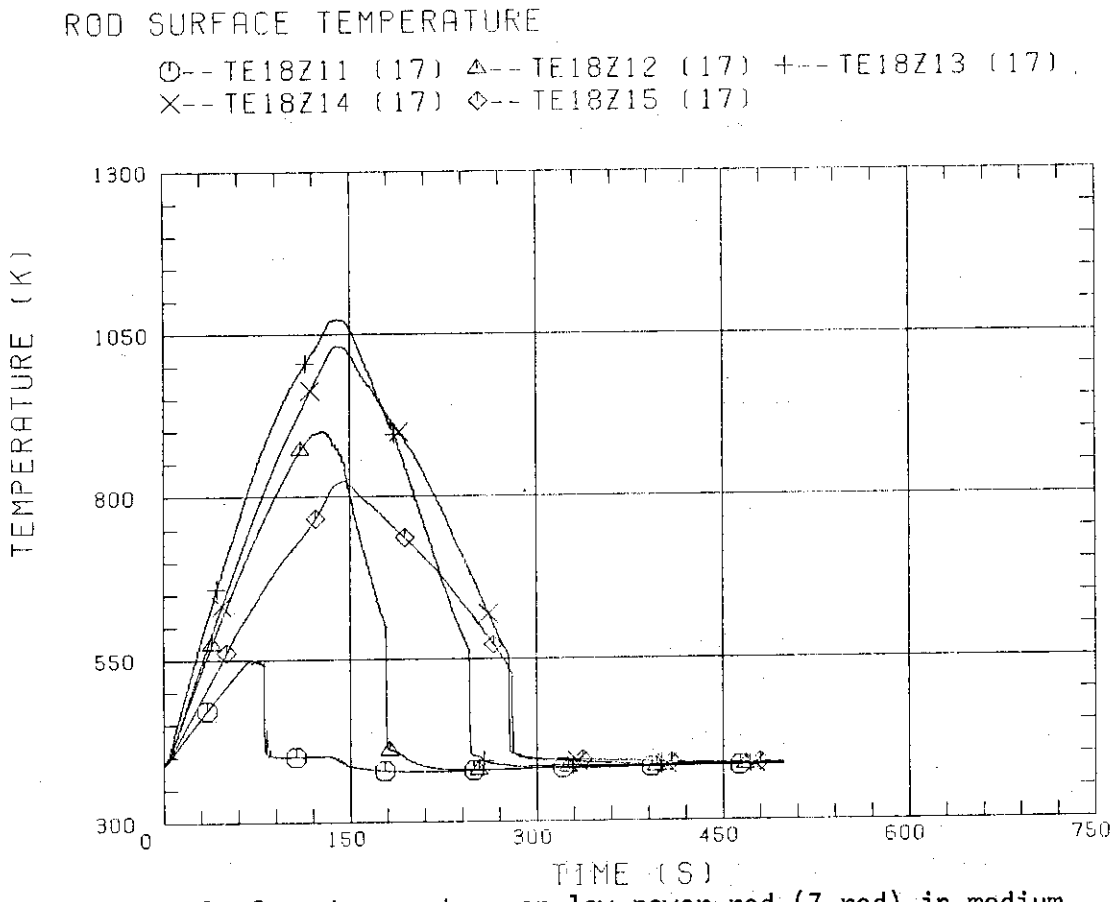

Fig. C-1 Surface temperature on low power rod (Z-rod) in medium power region (B region) (average power rod)

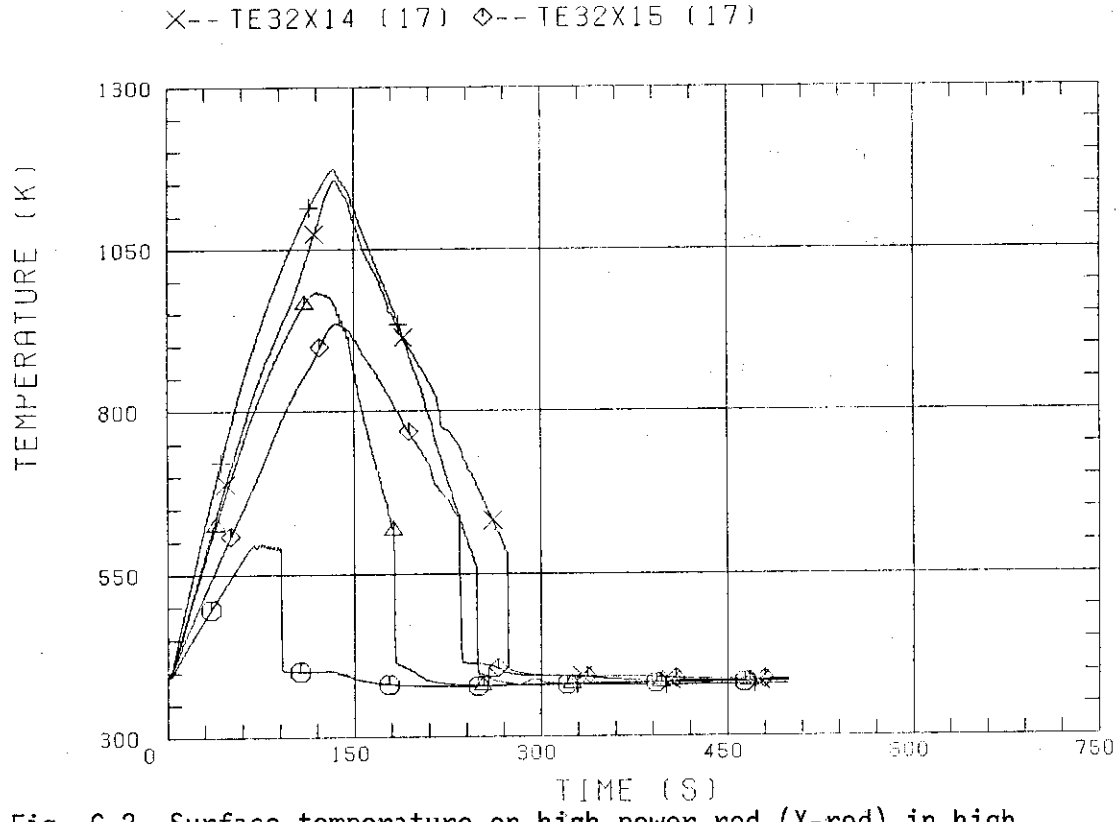

Fig. C-2 Surface temperature on high power rod (X-rod) in high power region (A region) (peak power rod)

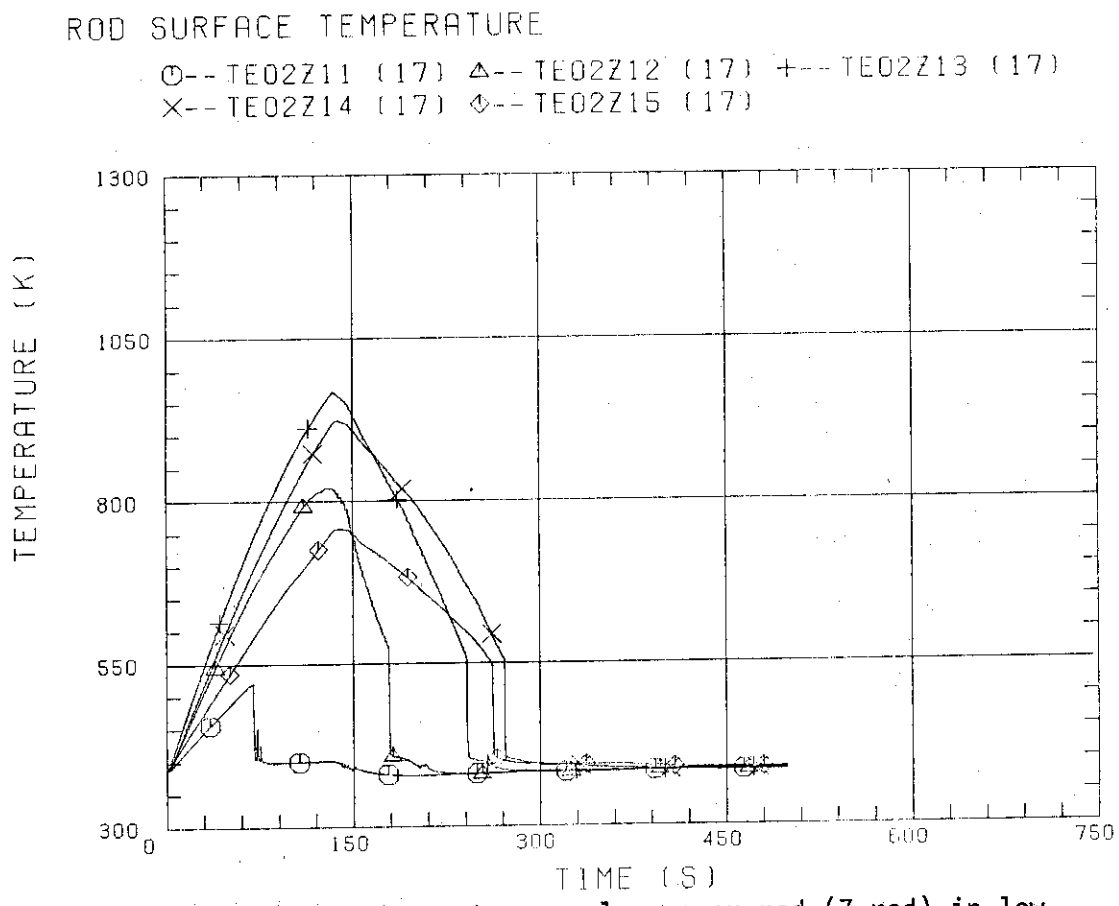

Fig. C-3 Surface temperature on low power rod (Z-rod) in low power region (C region) (lowest power rod)

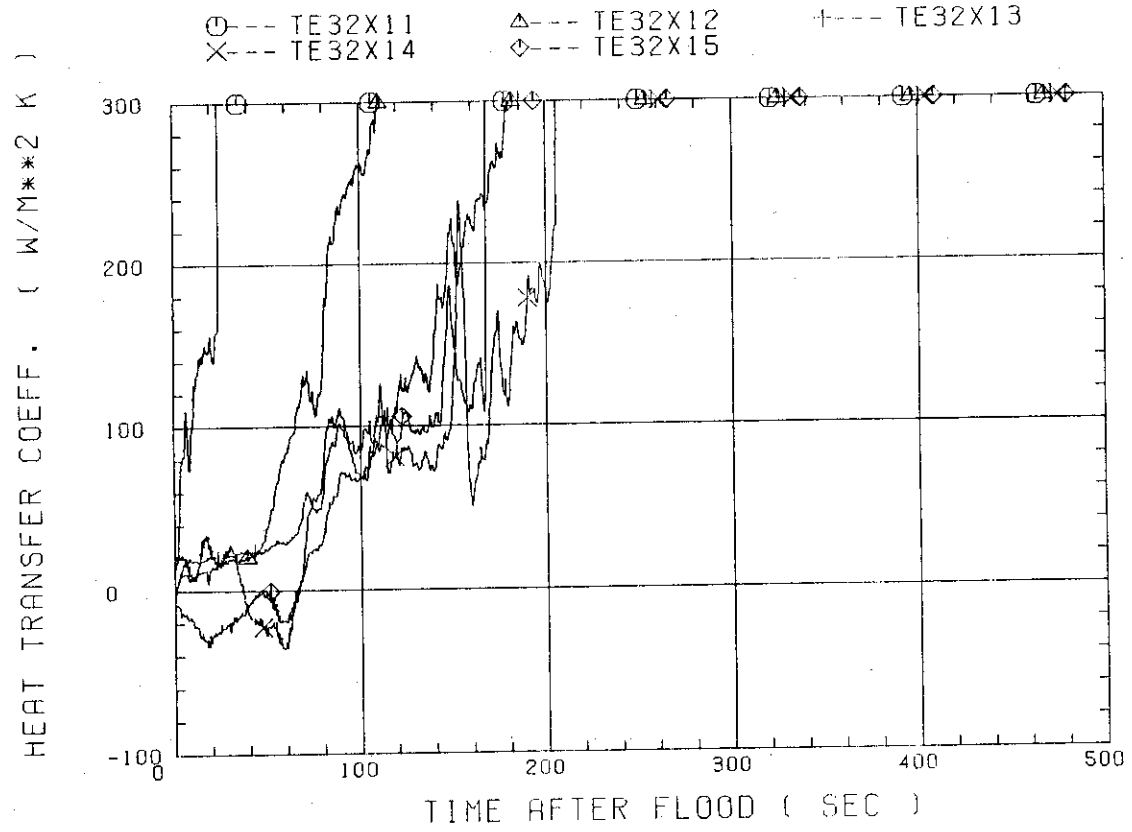

Fig. C-4 Heat transfer coefficient at midplane of low power rod (Z-rod) in medium power region (B region) (average power rod)

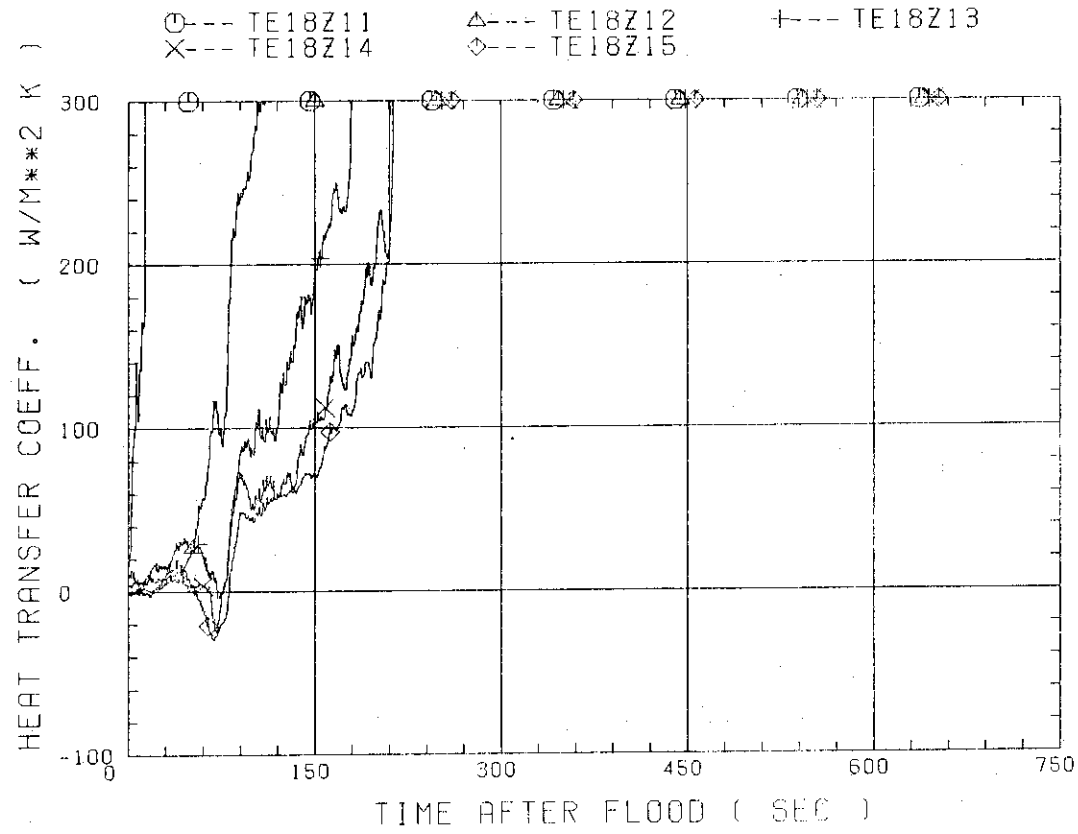

Fig. C-5 Heat transfer coefficient at midplane of high power rod (X-rod) in high power region (A region) (peak power rod)

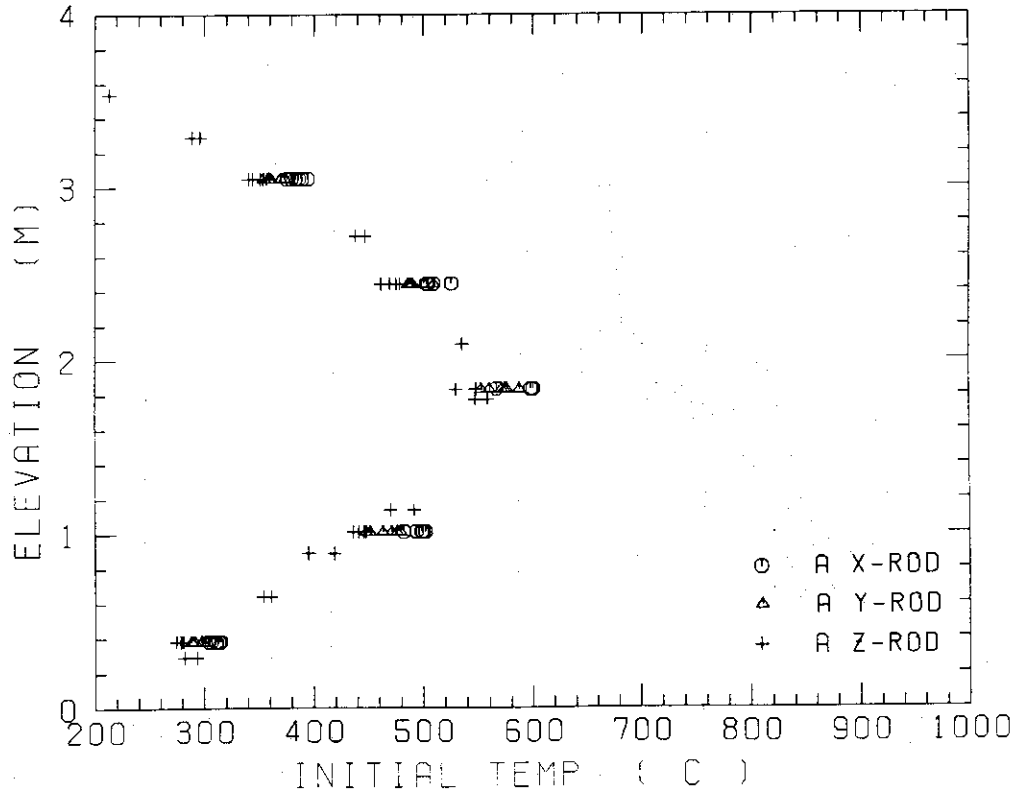

Fig. C-6 Initial rod surface temperature in high power region (A region)

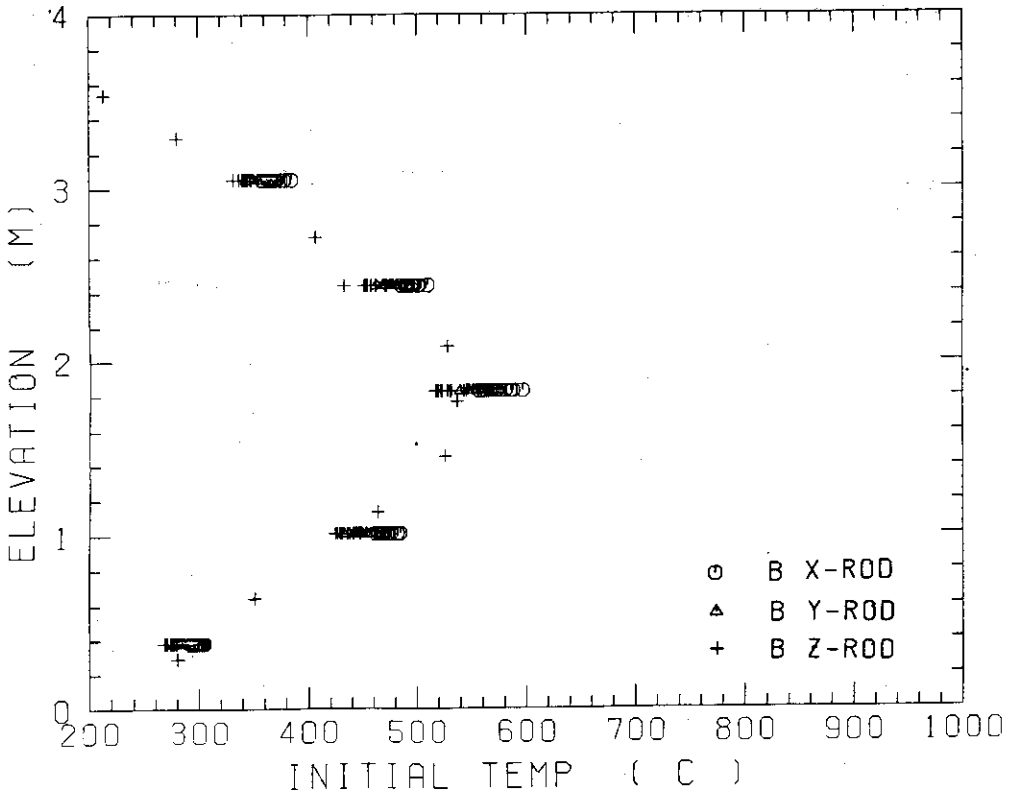

Fig. C-7 Initial rod surface temperature in medium power region (B region)

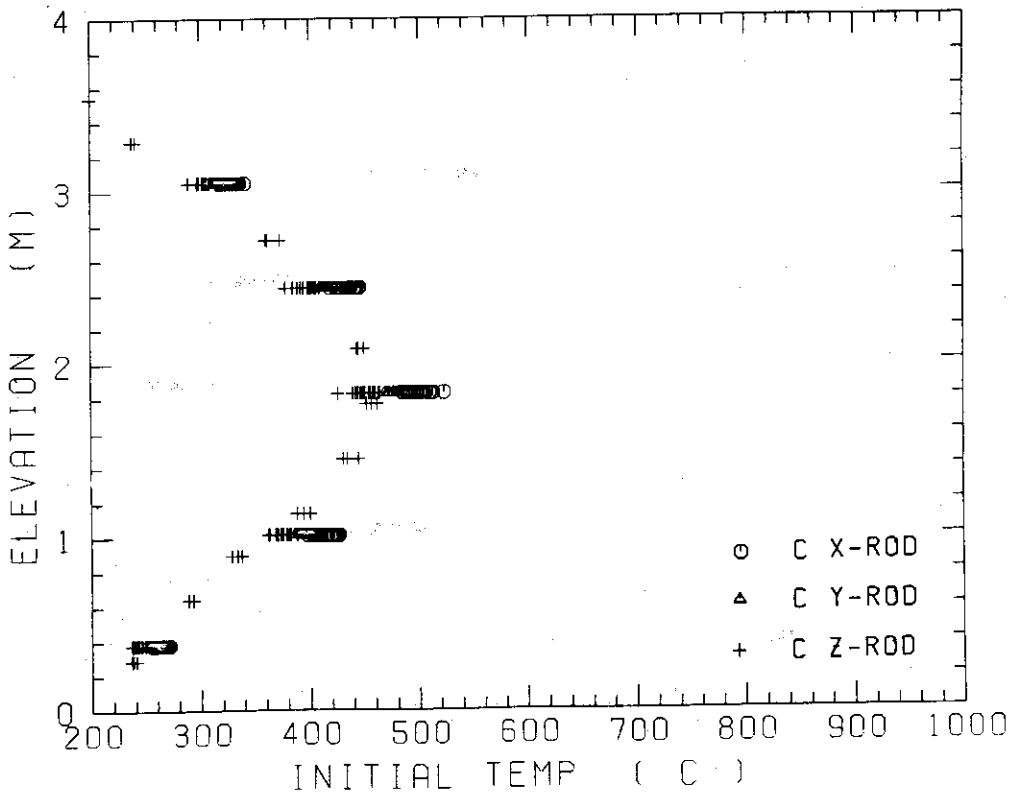

Fig. C-8 Initial rod surface temperature in low power region (C region)

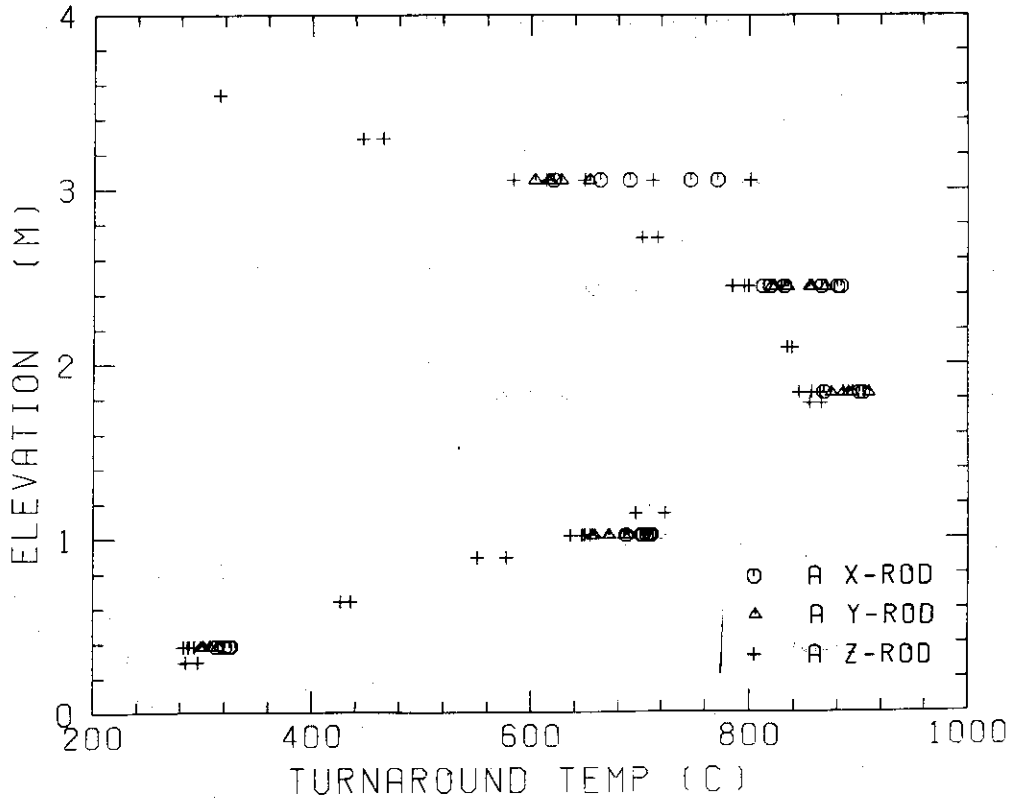

Fig. C-9 Turnaround temperature in high power region (A region)

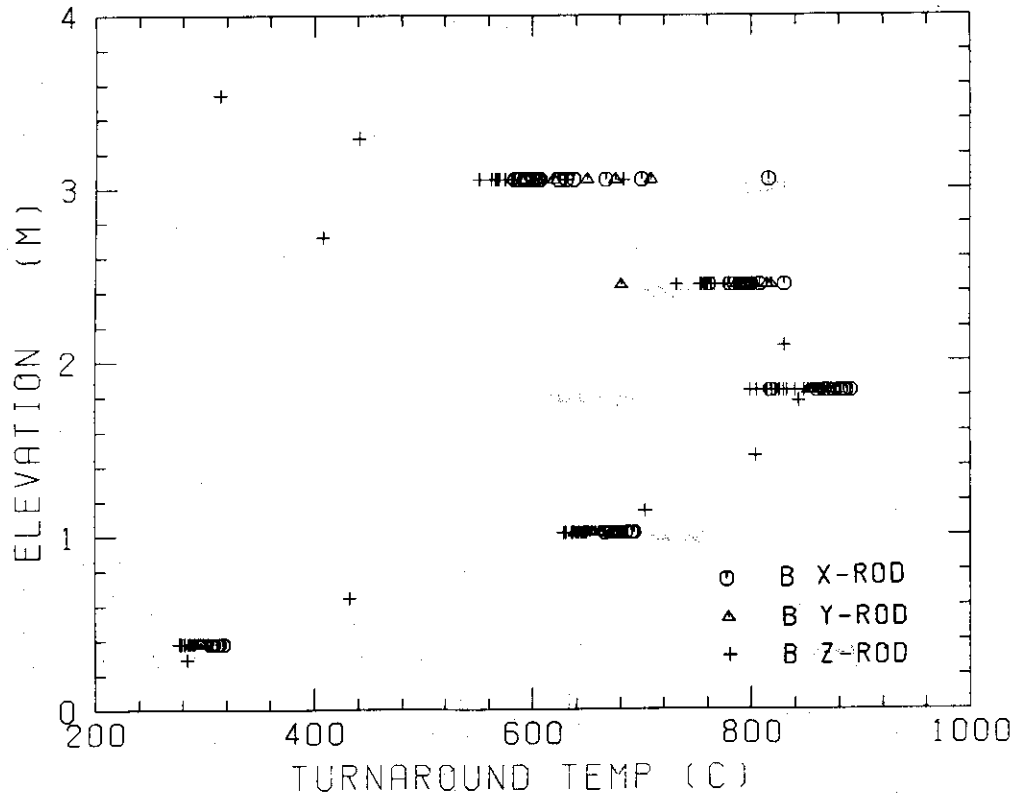

Fig. C-10 Turnaround temperature in medium power region (B region)

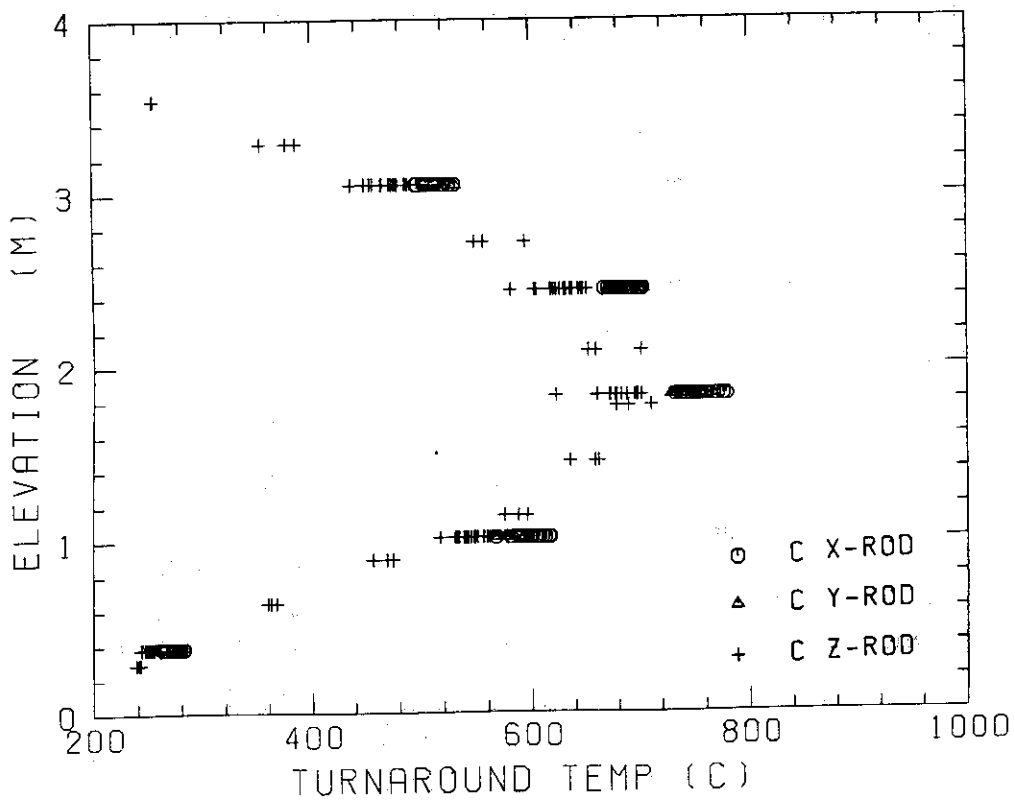

Fig. C-11 Turnaround temperature in low power region (C region)

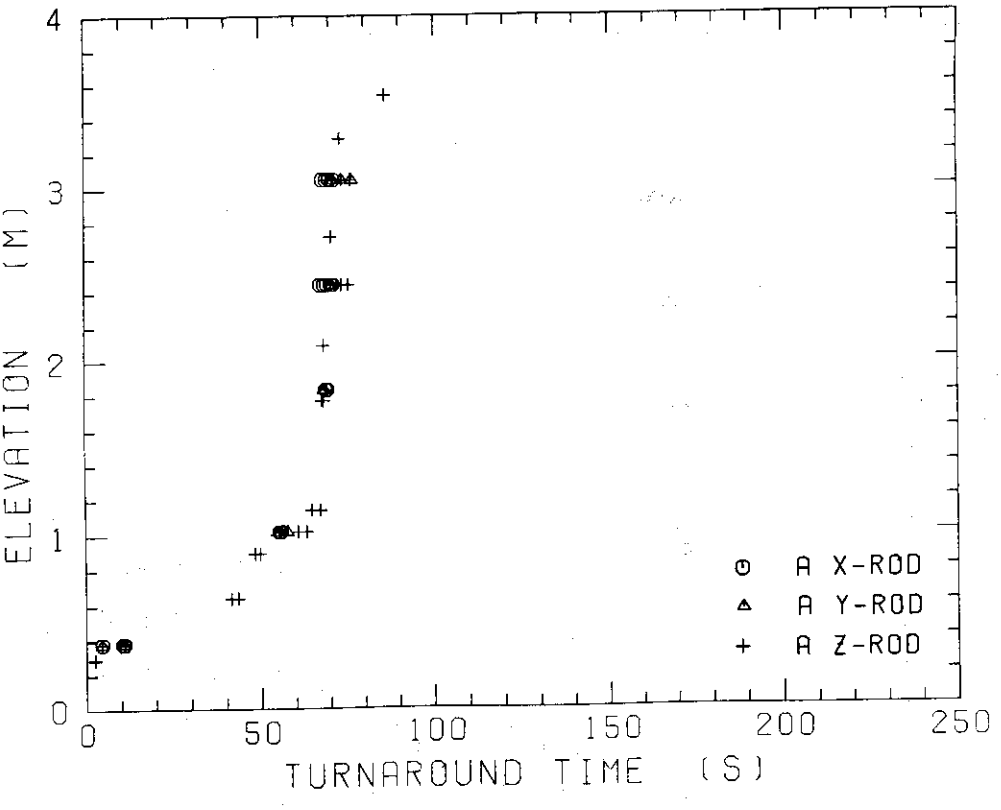

Fig. C-12 Turnaround time in high power region (A region)

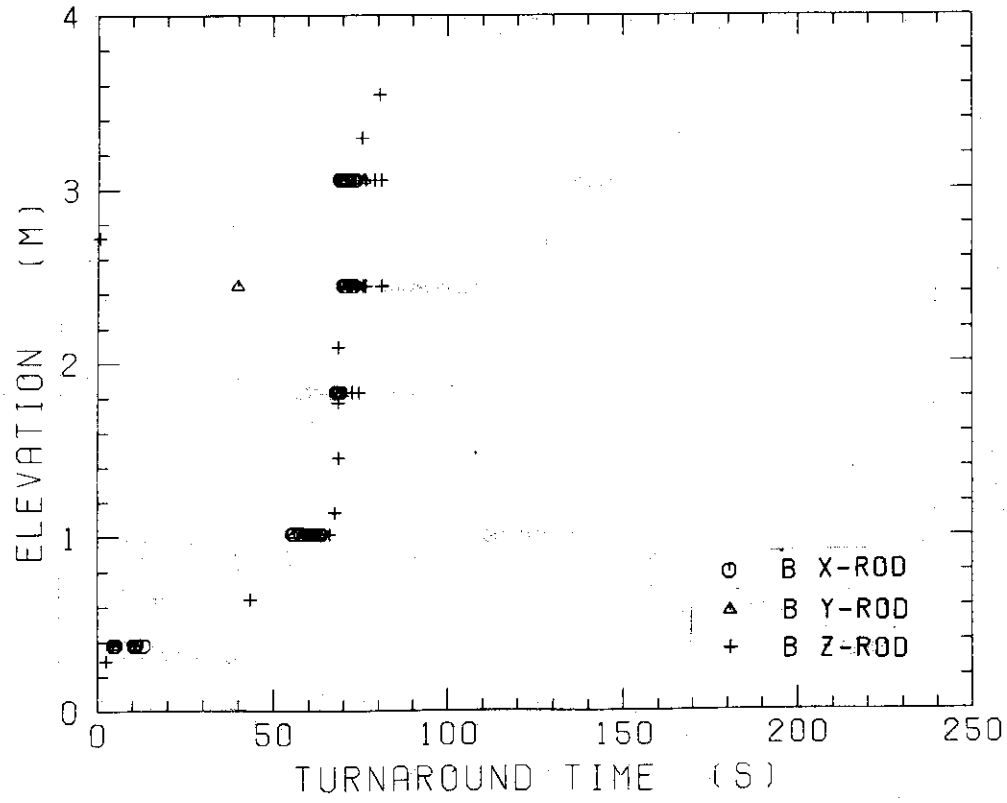

Fig. C-13 Turnaround time in medium power region (B region)

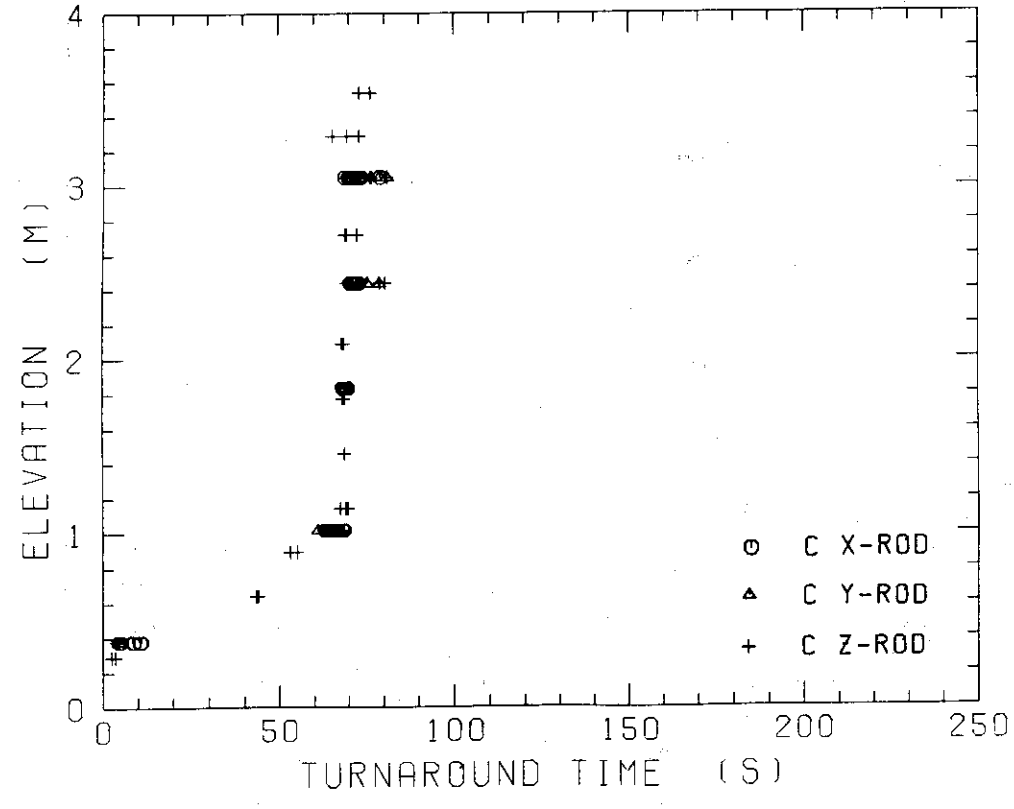

Fig. C-14 Turnaround time in low power region (C region)

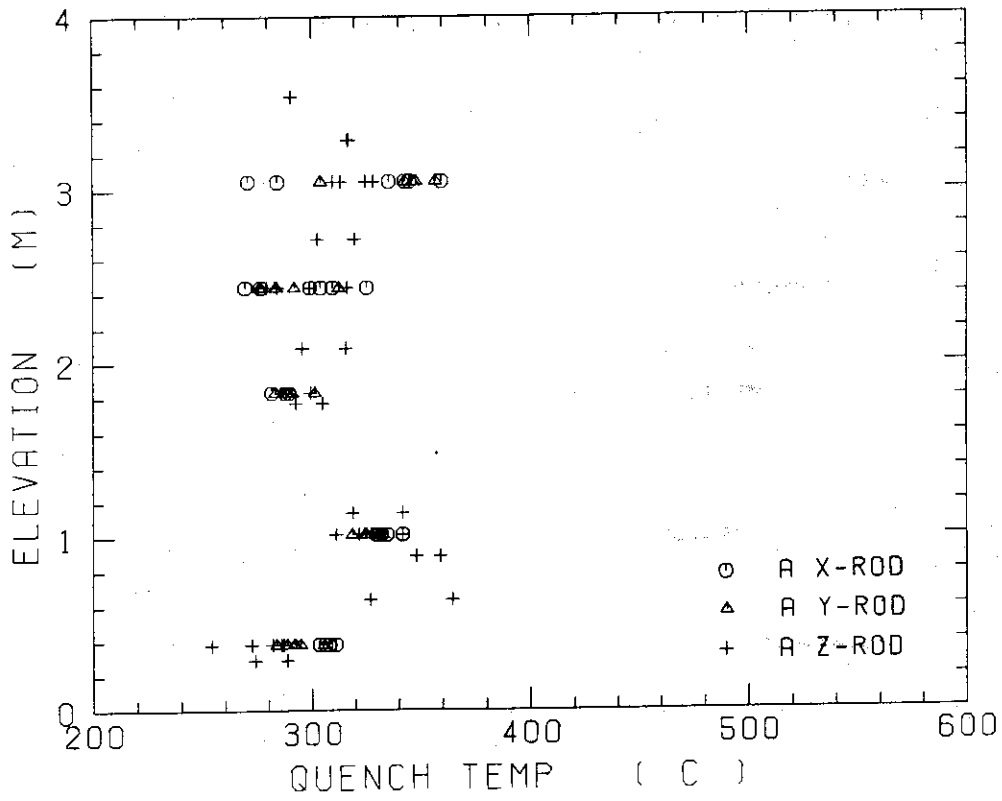

Fig. C-15 Quench temperature in high power region (A region)

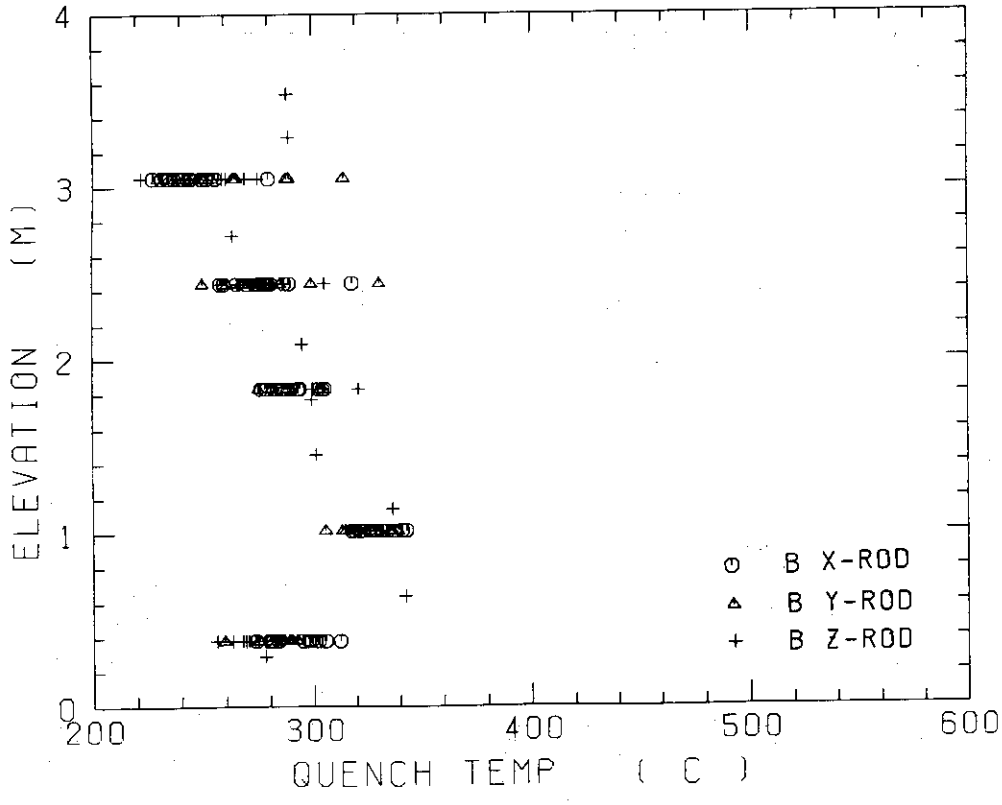

Fig. C-16 Quench temperature in medium power region (B region)

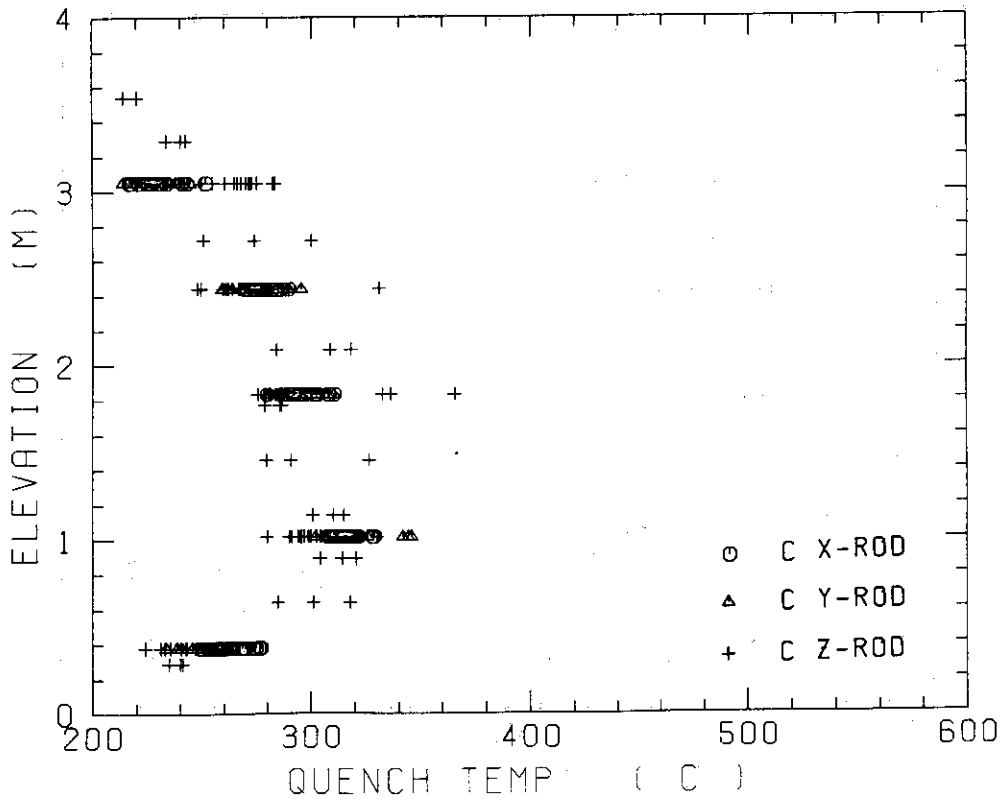

Fig. C-17 Quench temperature in low power region (C region)

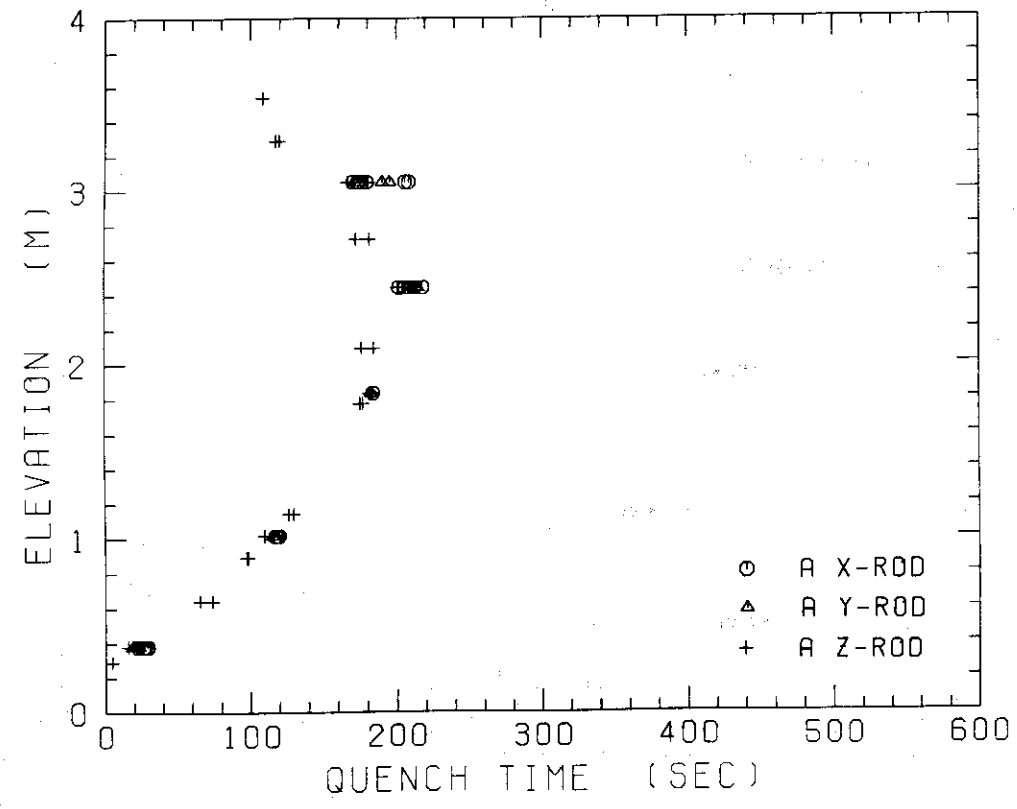

Fig. C-18 Quench time in high power region (A region)

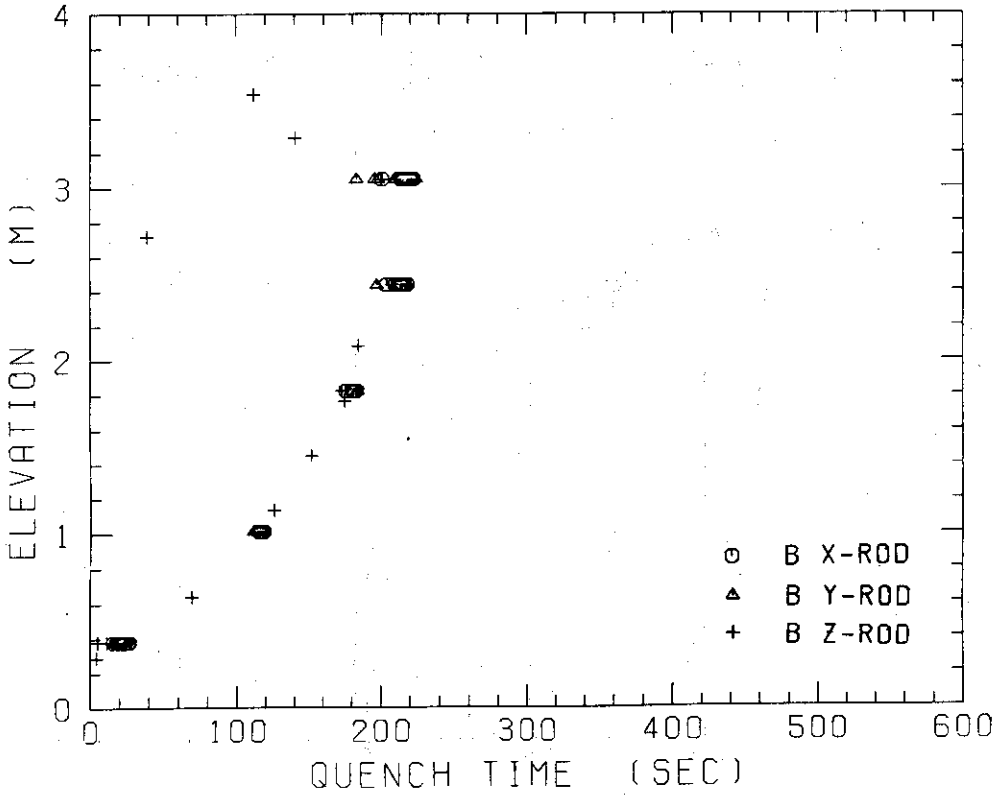

Fig. C-19 Quench time in medium power region (B region)

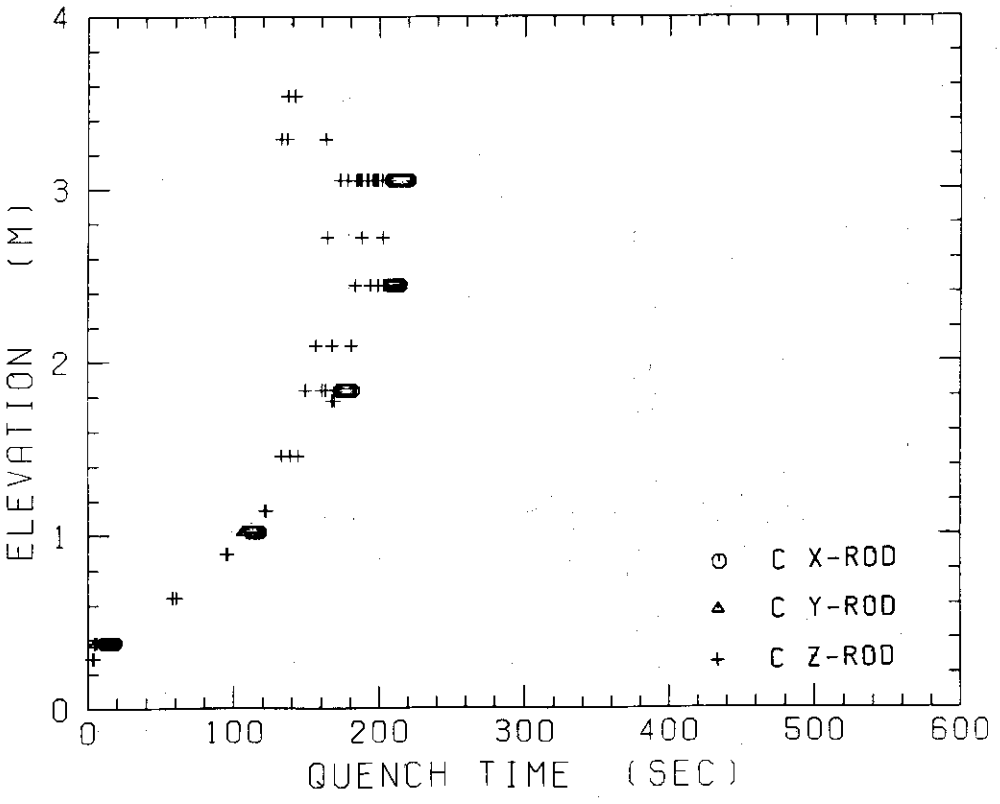

Fig. C-20 Quench time in low power region (C region)

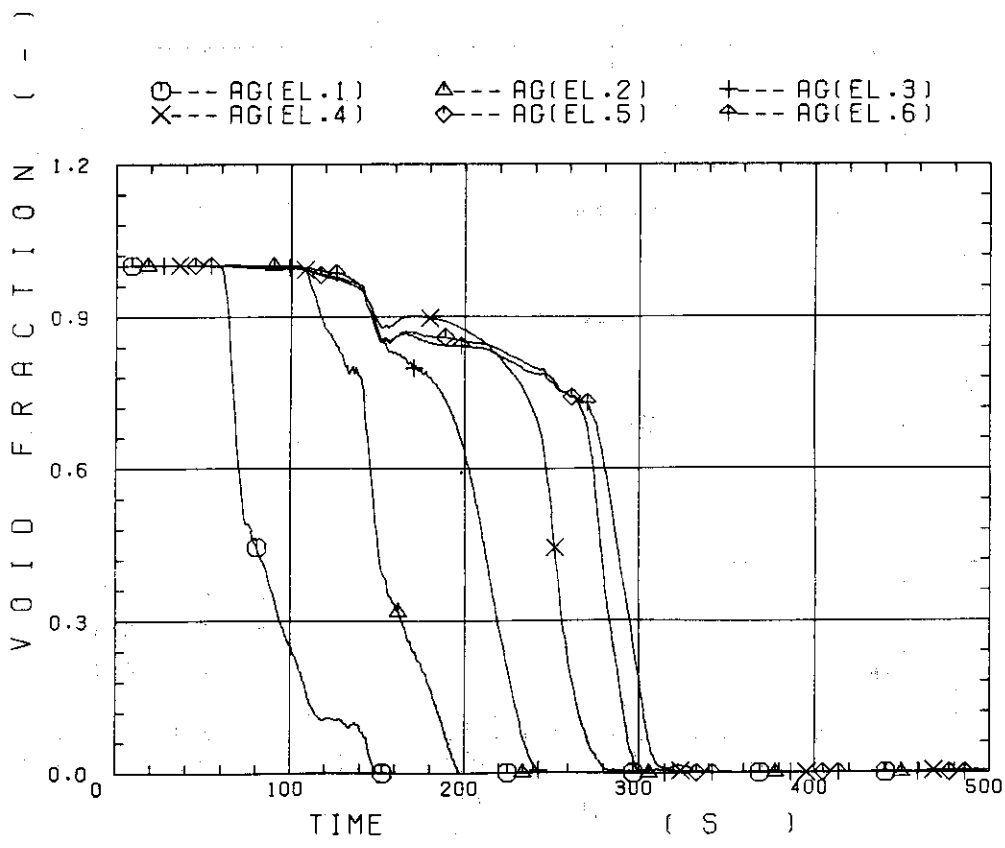

Fig. C-21 Void fraction in core

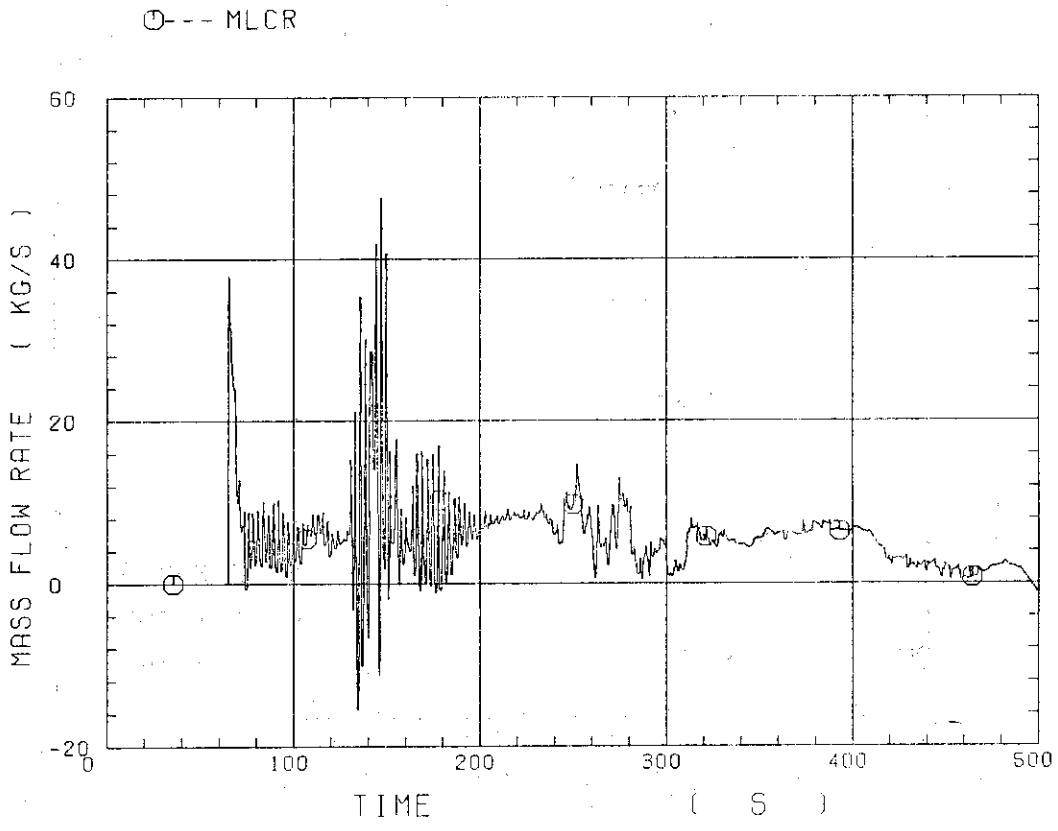

Fig. C-22 Core inlet mass flow rate

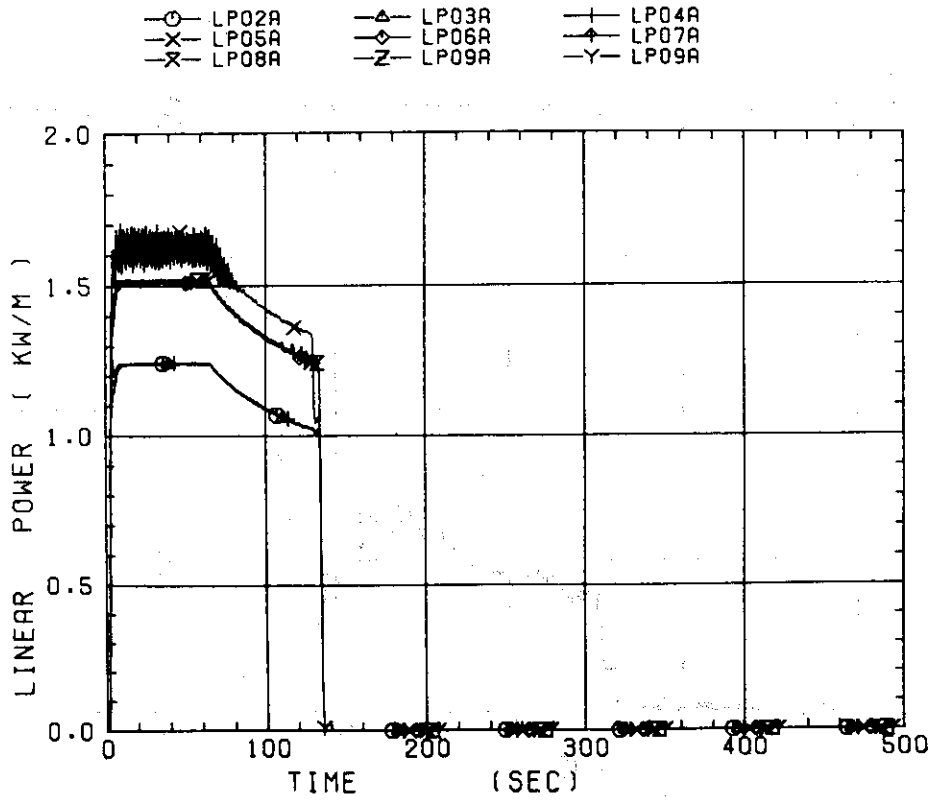

Fig. C-23 Average linear power of heater rod in each power unit zone

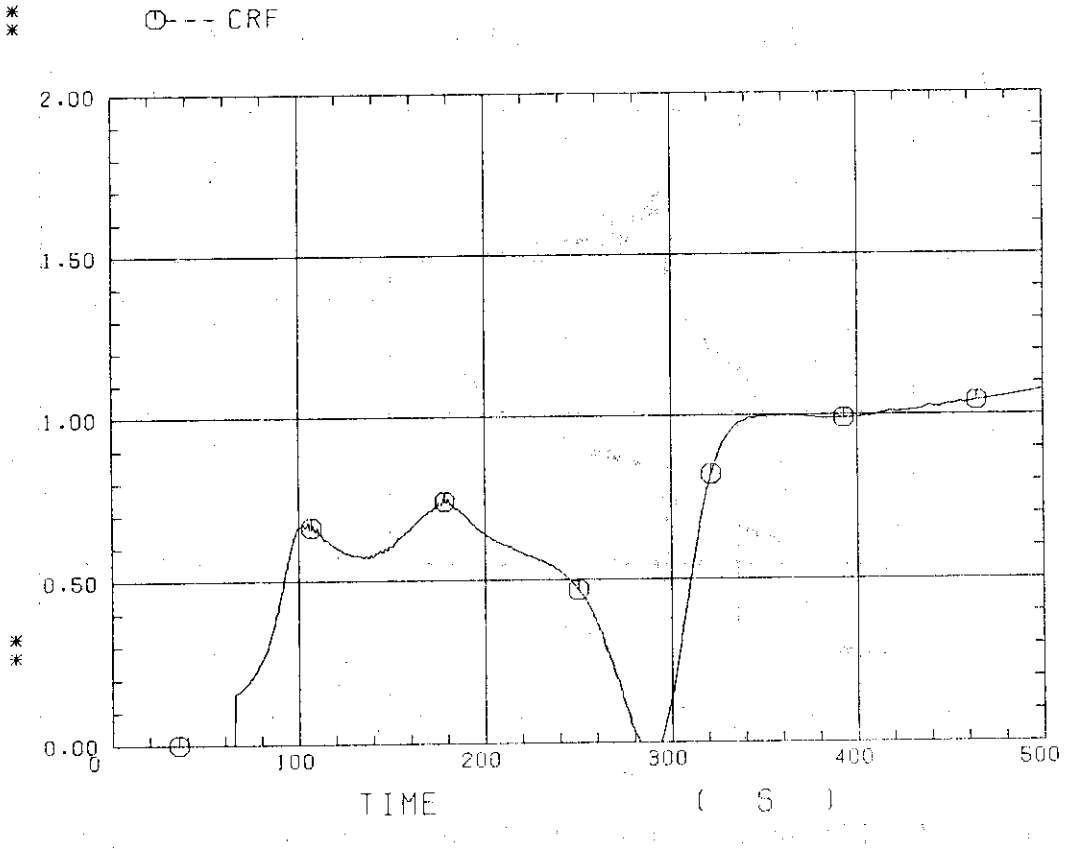

Fig. C-24 Carry-over rate fraction

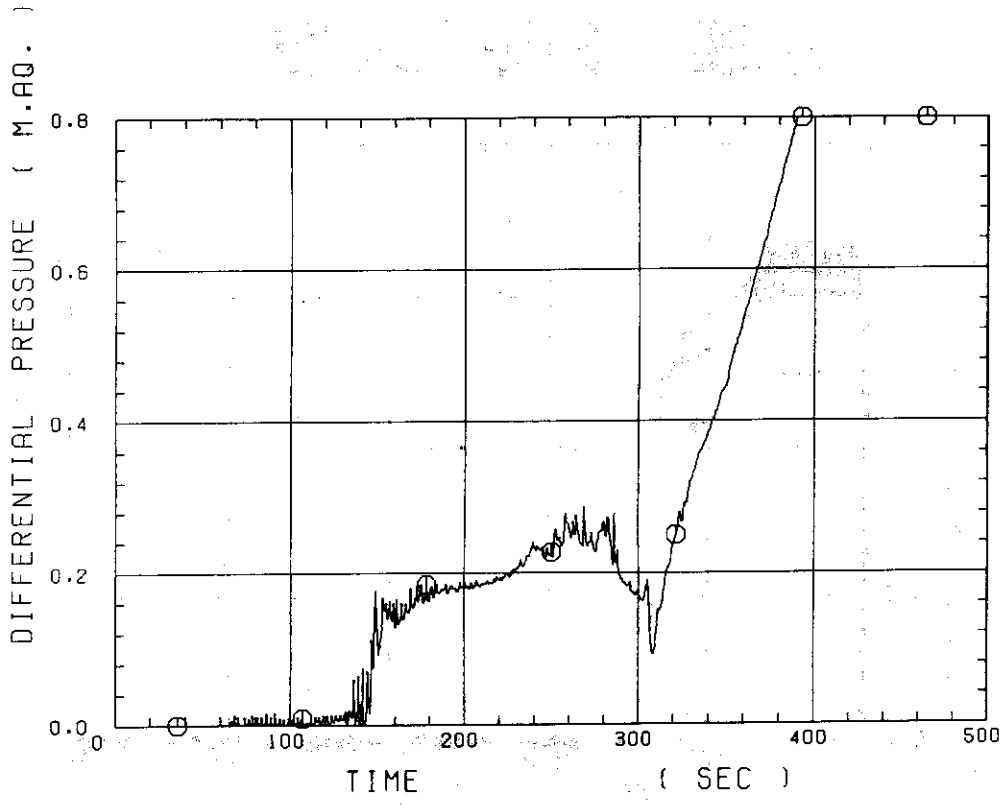

Fig. C-25 Differential pressure through upper plenum

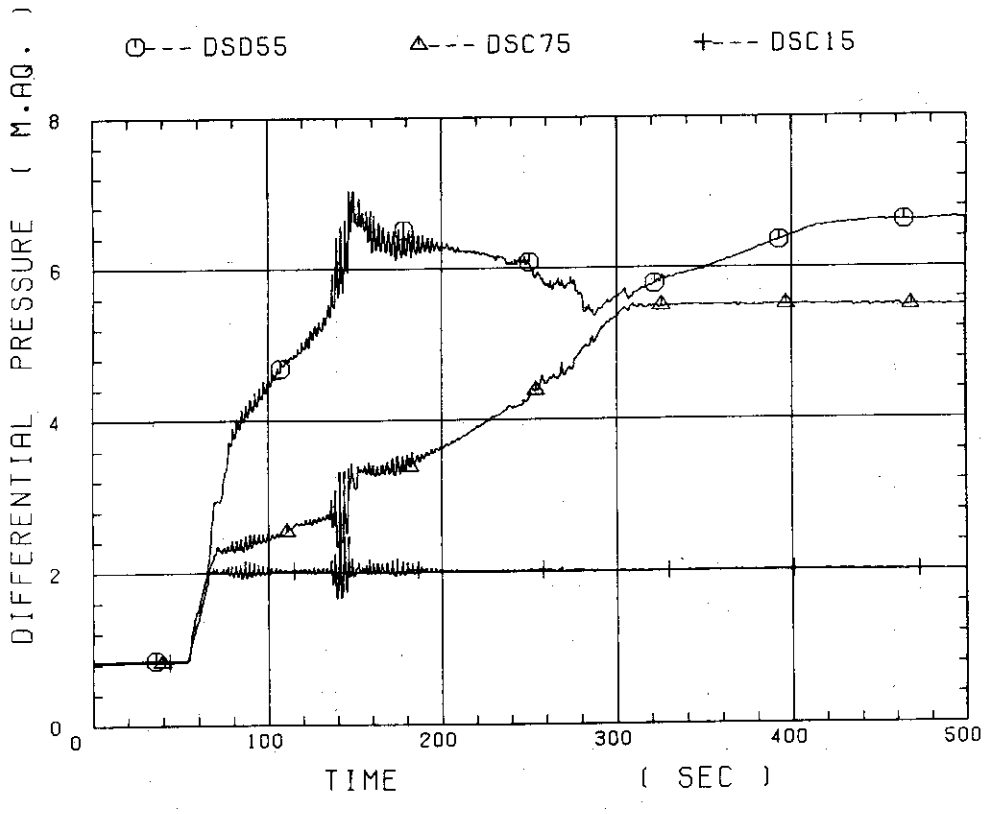

Fig. C-26 Differential pressure through downcomer, core, and lower plenum

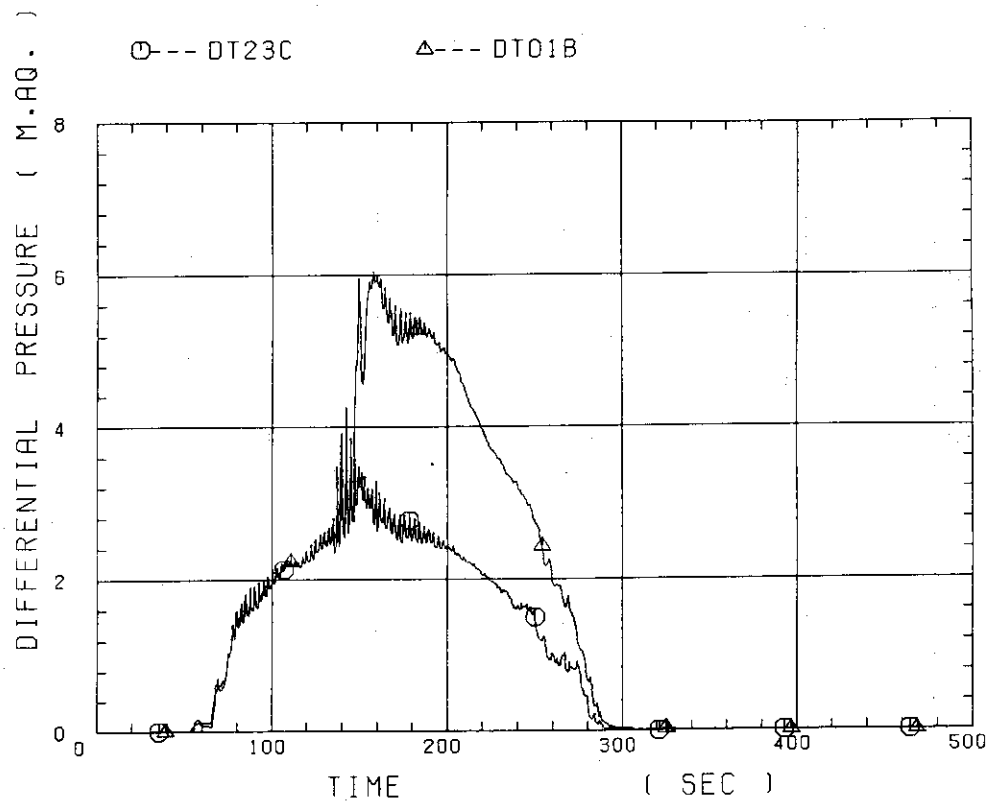

Fig. C-27 Differential pressure through intact and broken loops

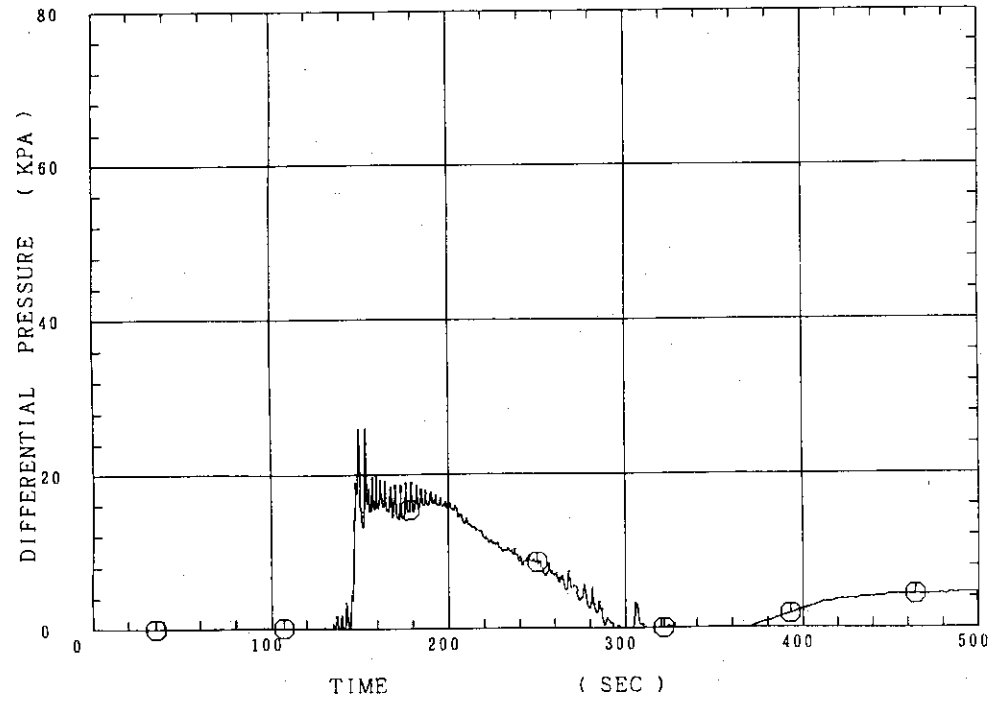

Fig. C-28 Differential pressure through broken cold leg nozzle

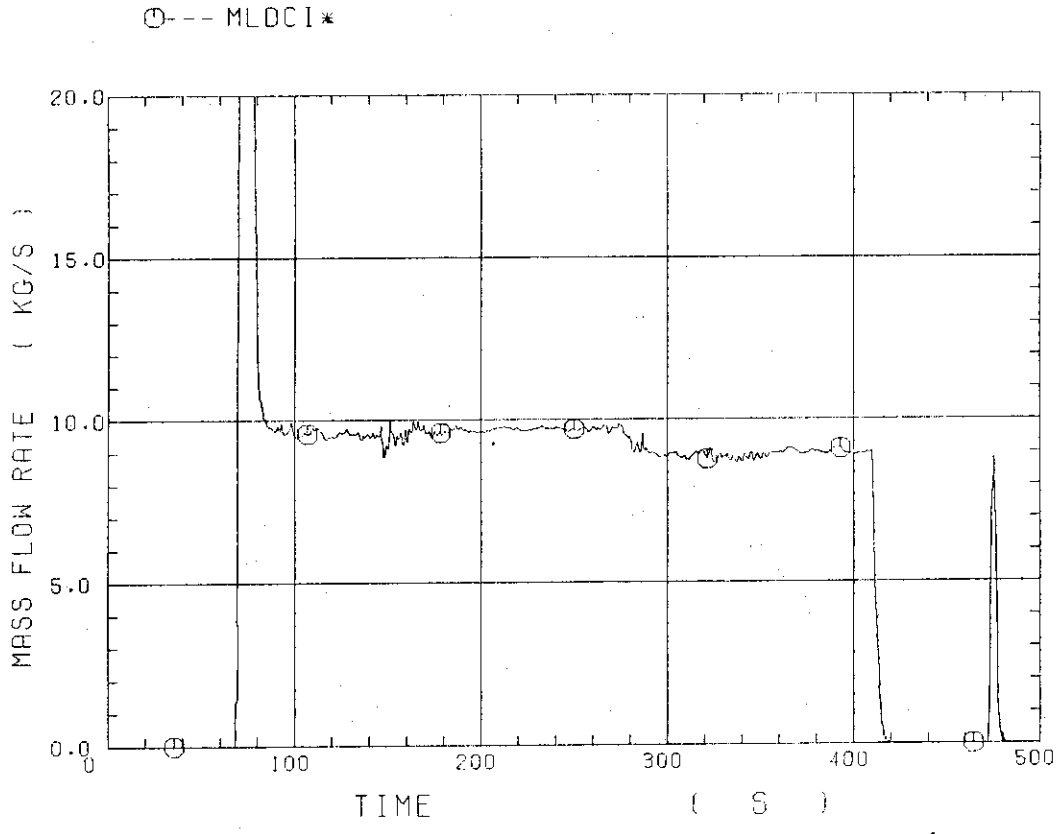

Fig. C-29 Total water mass flow rate from intact loops to downcomer

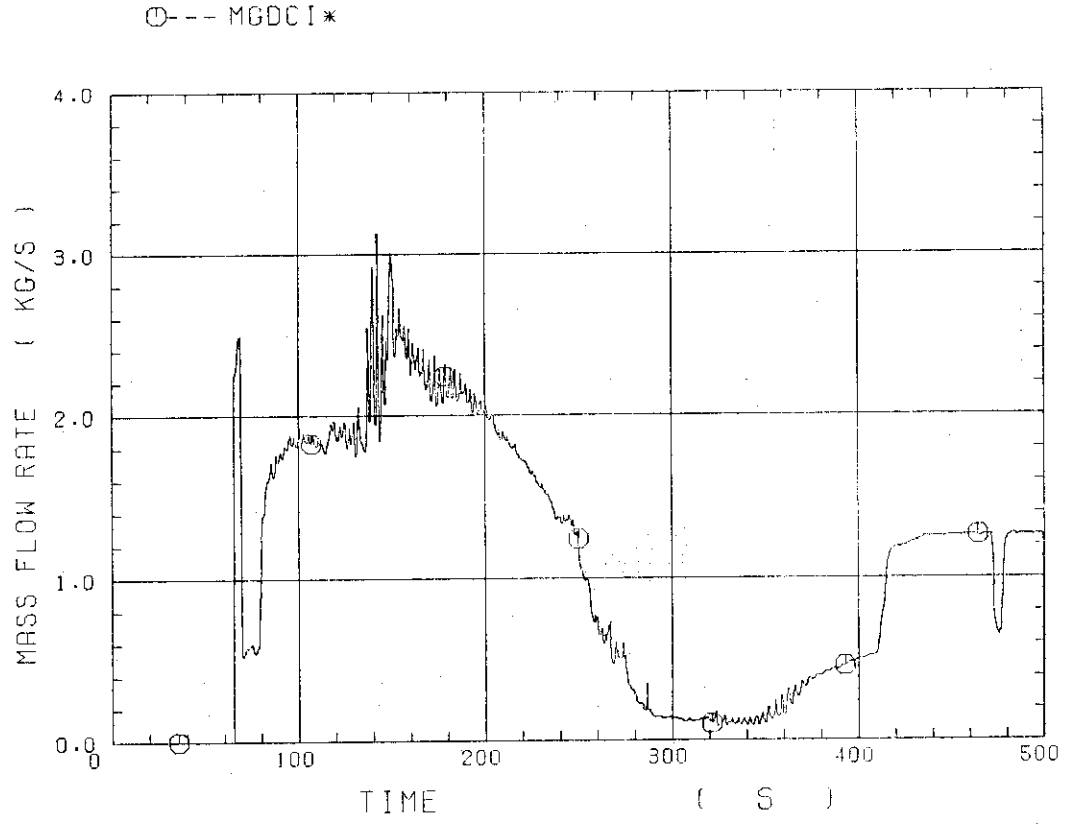

Fig. C-30 Total steam mass flow rate from intact loops to downcomer

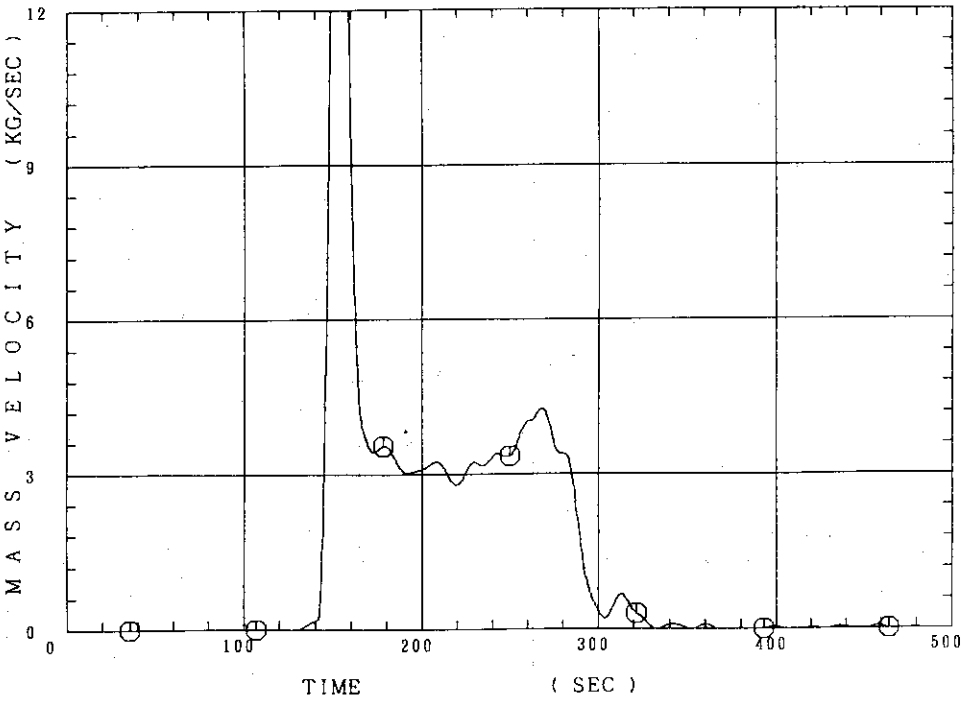

Fig. C-31 Water mass flow rate through broken cold leg nozzle

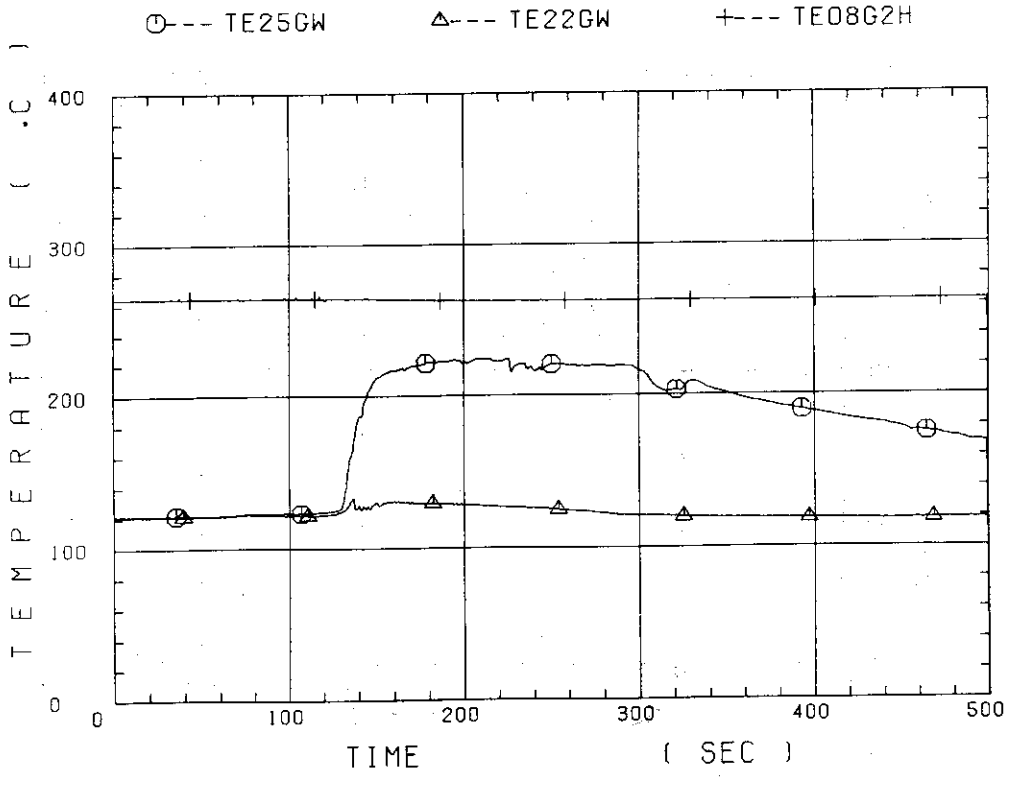

Fig. C-32 Fluid temperature in inlet plenum, outlet plenum, and secondary of steam generator 1

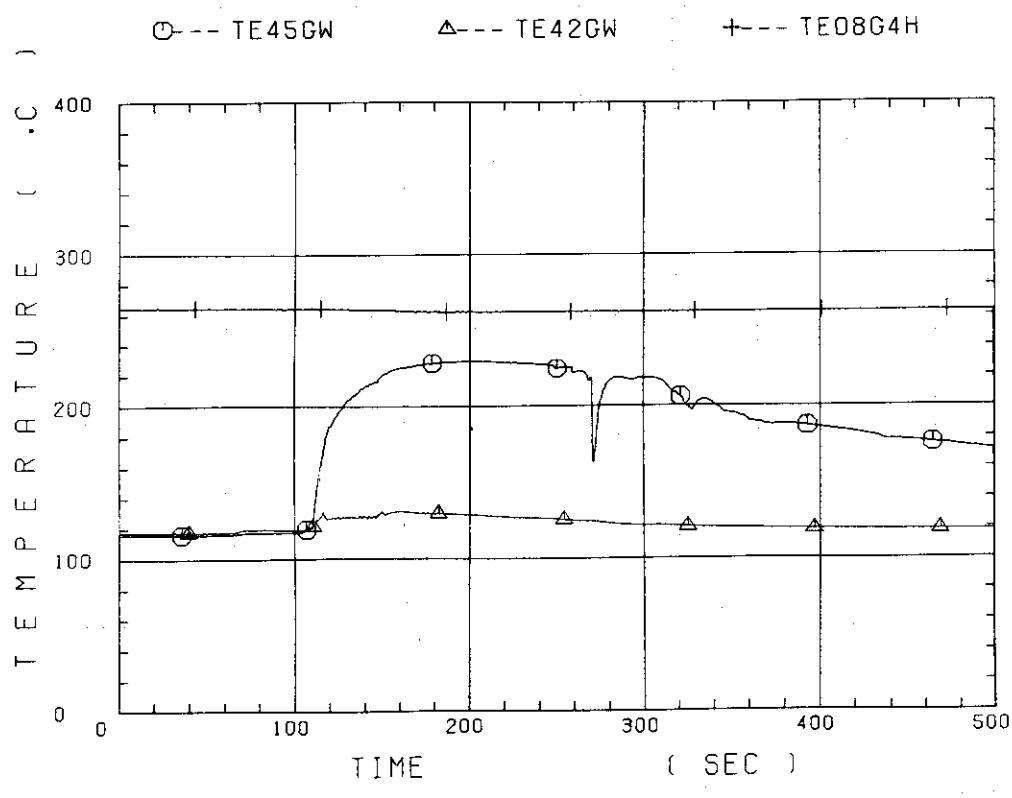

Fig. C-33 Fluid temperature in inlet plenum, output plenum, and secondary of steam generator 2

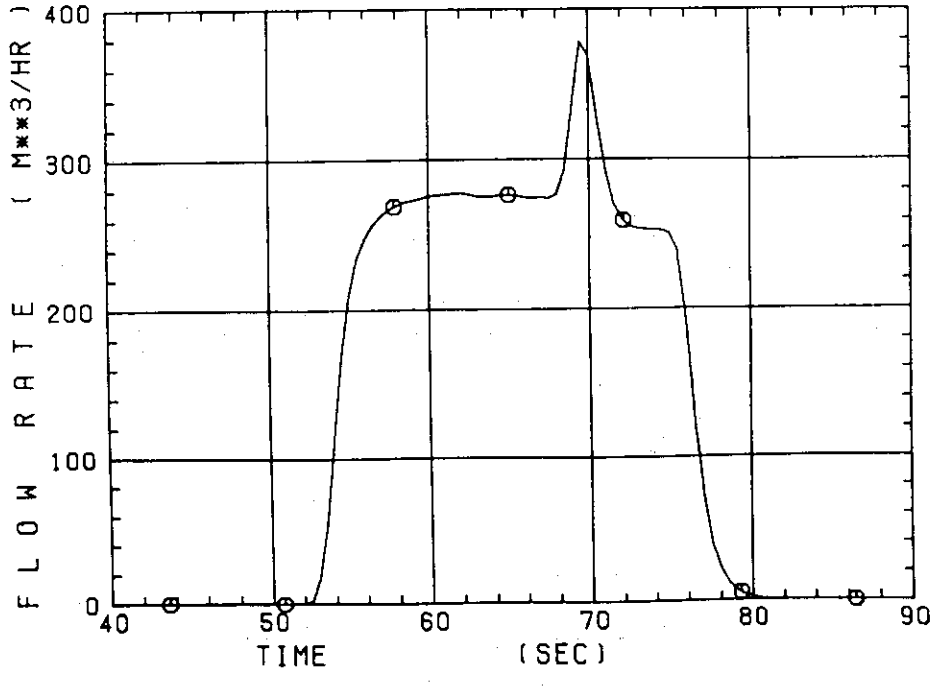

Fig. C-34 Total accumulator injection rate

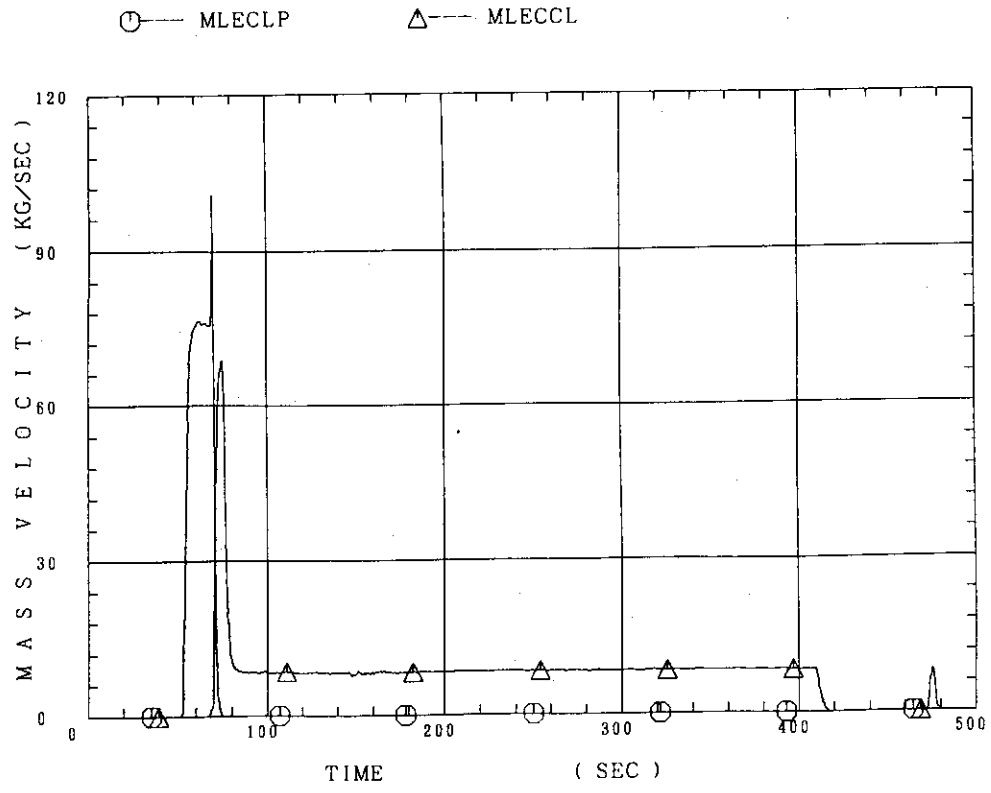

Fig. C-35 ECC water injection rates to lower plenum and to cold legs

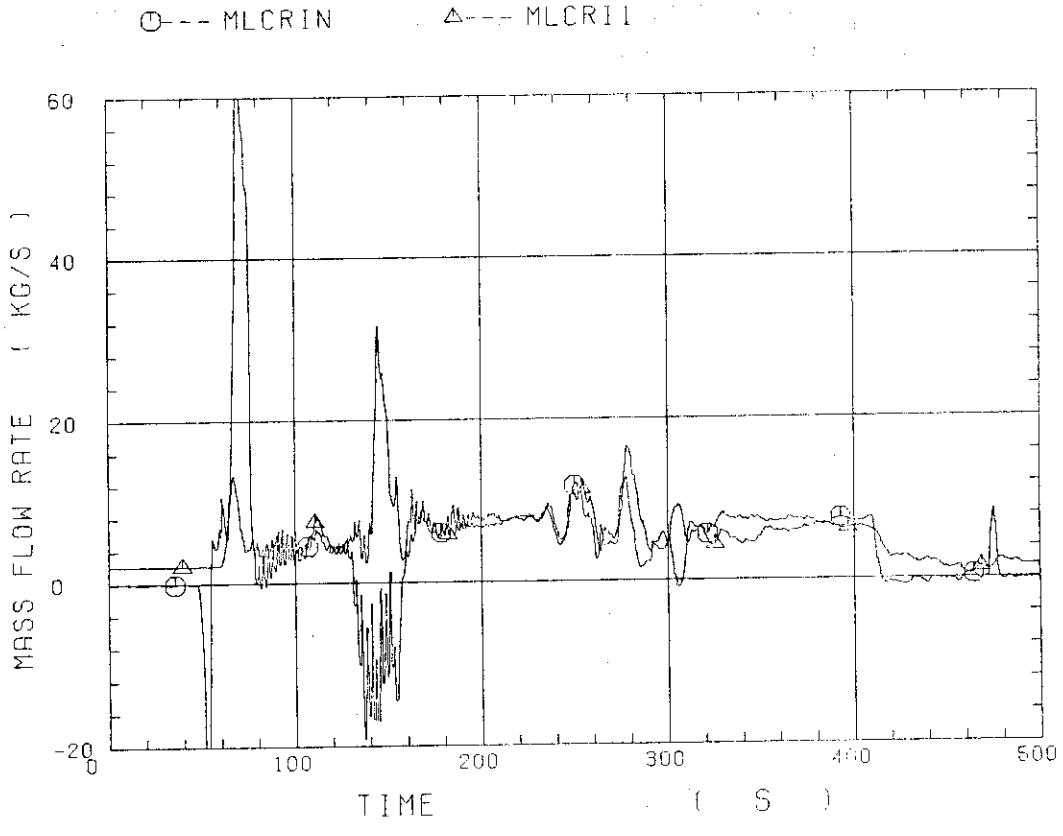

Fig. C-36 Core inlet mass flow rates estimated by mass balance downstream and upstream of core inlet

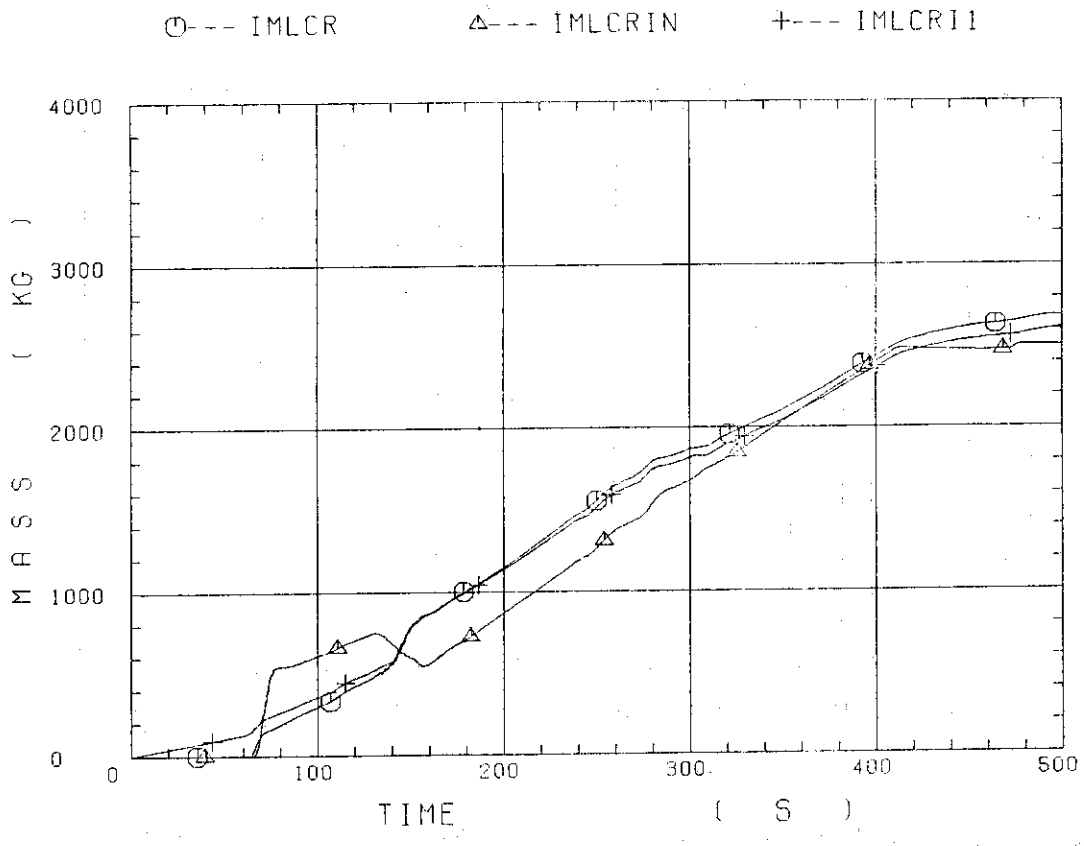

Fig. C-37 Comparison of injected mass into core among two estimation methods and evaluated mass